STATISTICAL RETURN PERIODS OF EXTREME WEATHER EVENTS

by

Aytaç Paçal

B.S., Physics, Boğaziçi University, 2015

Submitted to the Institute for Graduate Studies in
Science and Engineering in partial fulfillment of
the requirements for the degree of
Master of Science

Graduate Program in Computational Science and Engineering

Boğaziçi University

2019

STATISTICAL RETURN PERIODS OF EXTREME WEATHER EVENTS

APPROVED BY:

Prof. M. Levent Kurnaz ..... (Thesis Supervisor)

Prof. Arda Yurdakul .....

Asst. Prof. Tuğba Öztürk .....

DATE OF APPROVAL: 09.10.2019

ACKNOWLEDGEMENTS

I would like to express my profound thanks to my thesis advisor Prof. M. Levent Kurnaz for his patience, guidance and literally talking me out of leaving the university. He established an environment to learn about the discipline and many other things, and provided amazing opportunities to improve myself. I owe him a debt of gratitude.

I would like to thank Prof. V. Erkcan Özcan. He showed me what it means to think like a scientist. I will happily remember our small projects. I am honoured -with his own words- to be his colleague, not his student.

I would like to thank iklimBU family, especially Nazan An, Tuğba Öztürk and M. Tufan Turp, for their support and our long discussions about politics and life.

I have met lots of amazing people in Boğaziçi. I am lucky to have them in my life. I would like to thank all my friends for being a source of joy.

My family, Ilgın Paçal, Tayfun Paçal and Serpil Gül Paçal, always supported all my decisions and encouraged me to make my dreams come true. I cannot thank them enough for their never-ending unconditional support.

ABSTRACT

STATISTICAL RETURN PERIODS OF EXTREME WEATHER EVENTS

The Middle East & North Africa (MENA) region is one of the most populated areas on Earth in terms of city population. There are 643 cities in MENA region with population of urban agglomerations with 300,000 or more in 2018 according to United Nations.

In this thesis, return periods of extreme temperature events are calculated using the probability density functions. For this purpose, Global Climate Model (GCM) outputs of Max Plank Institute Earth System Model Mixed Resolution (MPI-ESM-MR) and Hadley Global Environment Model 2 - Earth System (HadGEM2-ES) are dynamically downscaled to 50 km for the MENA region by using the Regional Climate Model v4.4 (RegCM4.4) for 2 different Representative Concentration Pathways scenarios, namely RCP 4.5 and RCP 8.5. Elevation correction is applied to each point for sea level. Temperatures at city centers are calculated from the nearest 4 grid points using inverse distance squared interpolation method. Daily maximum temperatures histograms are plotted for each city and future predictions of return periods are compared with the reference period of 1971-2000 using the means and standard deviations obtained from Gaussian Mixture Model.

The results show that the frequency of extreme events increases for all cities between 2070 and 2099. Peaks in temperature distribution are diverging from each other which will cause more severe extreme events. This divergence would cause cities to have shorter transition seasons and their climate would transform into only 2 seasons.

ÖZET

AŞIRI HAVA OLAYLARININ İSTATİSTİKSEL GERİ DÖNÜŞ PERİYODLARI

MENA (Middle East & North Africa) bölgesi Dünya'daki en kalabalık şehirlere sahip yerleşim alanlarındandır. Dünya Bankası verilerine göre 2018 yılında MENA bölgesinde nüfusu 300.000'den yüksek olan 643 şehir bulunmaktadır.

Bu çalışmada, MENA bölgesindeki aşırı hava olaylarının geri dönüş periyodları, olasılık dağılım fonksiyonları kullanılarak hesaplandı. Bu amaçla, MPI-ESM-MR (Max Plank Institute Earth System Model Mixed Resolution) ve HadGEM2-ES (Hadley Global Environment Model 2 - Earth System) küresel iklim modeli, Bölgesel İklim Modeli v4.4 (RegCM4.4) kullanılarak RCP 4.5 ve RCP 8.5 (Representative Concentration Pathways) senaryoları için 50km çözünürlüğe dinamik olarak düşürüldü. Karelajlamanın her bir noktası deniz seviyesine indirgendi. Şehir merkezlerindeki sıcaklıklar, bu noktalara en yakın 4 karelaj noktasından ters mesafenin karesi ağırlıklı enterpolasyon yöntemi kullanarak hesaplandı. Günlük maksimum sıcaklıkların histogramları çizdirildi ve uygun Gauss Karışım Modeliyle elde edilen ortalama ve standart sapmalar kullanılarak, aşırı hava olaylarının gelecekteki geri dönüş periyotları, referans yıllar olan 1971-2000 ile karşılaştırıldı.

Aşırı hava olaylarının 2070 ve 2099 yılları arasında tüm şehirlerde artacağı bulundu. Sıcaklık dağılım grafiğindeki tepelerin birbirinden uzaklaştığı gözlemlendi. Bu açılma hem şehirlerde daha sert hava olaylarının, hem de daha kısa geçiş mevsimlerine neden olarak şehirlerin ikliminin 2 mevsime dönüşmesine neden olacağı bulundu.

TABLE OF CONTENTS

LIST OF FIGURES

LIST OF TABLES

LIST OF SYMBOLS

f_n^{past}	Frequency of extreme event in past
f_n^{future}	Frequency of extreme event in future
$\mathcal{N}(\mu, \sigma)$	Normal distribution with mean μ and standard deviation σ
$\lvert\mathcal{N}(\mu_{hot}^{past}, \sigma_{hot}^{past})\rvert$	Number of days in the Gaussian distribution of hot period in past
$\lvert\mathcal{N}(\mu_{hot}^{future}, \sigma_{hot}^{future})\rvert$	Number of days in the Gaussian distribution of hot period in future
$\Delta\mu^{future}$	Peak temperature difference in future
$\Delta\mu^{past}$	Peak temperature difference in past
$\Delta\mu^{future} - \Delta\mu^{past}$	Change in peak temperature differences
μ_{hot}^{past}	Mean of the past hot side distribution
μ_{cold}^{past}	Mean of the past cold side distribution
μ_{hot}^{future}	Mean of the future hot side distribution
μ_{cold}^{future}	Mean of the future cold side distribution
σ_{hot}^{past}	Standard deviation of the past hot side distribution
σ_{cold}^{past}	Standard deviation of the past cold side distribution
σ_{hot}^{future}	Standard deviation of the future hot side distribution
σ_{cold}^{future}	Standard deviation of the future cold side distribution
$\dot{\sigma}$	Vertical sigma coordinates in the RegCM

LIST OF ACRONYMS/ABBREVIATIONS

1D	One-Dimensional
2D	Two-Dimensional
3D	Three-Dimensional
AOGCM	Atmosphere-Ocean GCM
AR4	IPCC Fourth Assessment Report, 2007
AR5	IPCC Fifth Assessment Report, 2014
CDO	Climate Data Operators
CO_2	Carbon Dioxide
CORDEX	Coordinated Regional Climate Downscaling Experiment
GCM	General Circulation Model *or* Global Climate Model
GMM	Gaussian Mixture Models
ICBC	Initial Conditions and Boundary Conditions
ICTP	The Abdus Salam International Centre for Theoretical Physics
IPCC	Intergovernmental Panel on Climate Change
MENA	Middle East & North Africa
MPI	Max Planck Institute
MPI-ESM-MR	Max Planck Institute Earth System Model Mixed Resolution
HadGEM2-ES	Hadley Global Environment Model 2 - Earth System
NetCDF	Network Common Data Form
ppm	Parts-per-million
RCM	Regional Climate Modelling or Dynamical Downscaling
RCP	Representative Concentration Pathways
RegCM4.4	The Regional Climate Model version 4.4
SRES	the Special Report on Emission Scenarios
SRCCL	Climate Change and Land, an IPCC special report.
tasmax	Daily Maximum Near-Surface Air Temperature

1. INTRODUCTION

Climate change is the most important man-made problem the humanity has ever faced. Usage of fossil fuels and deforestation are the main reasons that increase the greenhouse gases in the atmosphere. Average temperatures have increased by about 1.0°C with respect to pre-industrial levels and will reach 1.5°C between 2030 and 2052 [1]. With the increasing energy in the atmosphere, effects of climate change become clearer. Frequency, intensity and duration of extreme events increase with the climate change [2]. Statistically, daily temperatures are shaped similar to a Gaussian curve. Increase in means causes more extreme hot and less extreme cold days. However, climate change also induces an increase in variance which causes more extreme hot and more extreme cold days as shown in Figure 1.1. These effects cause more severe events in places already experiencing extreme events. In addition to this, extreme events are introduced in some new locations. Most importantly, increase in extreme events pose great risks to human health.

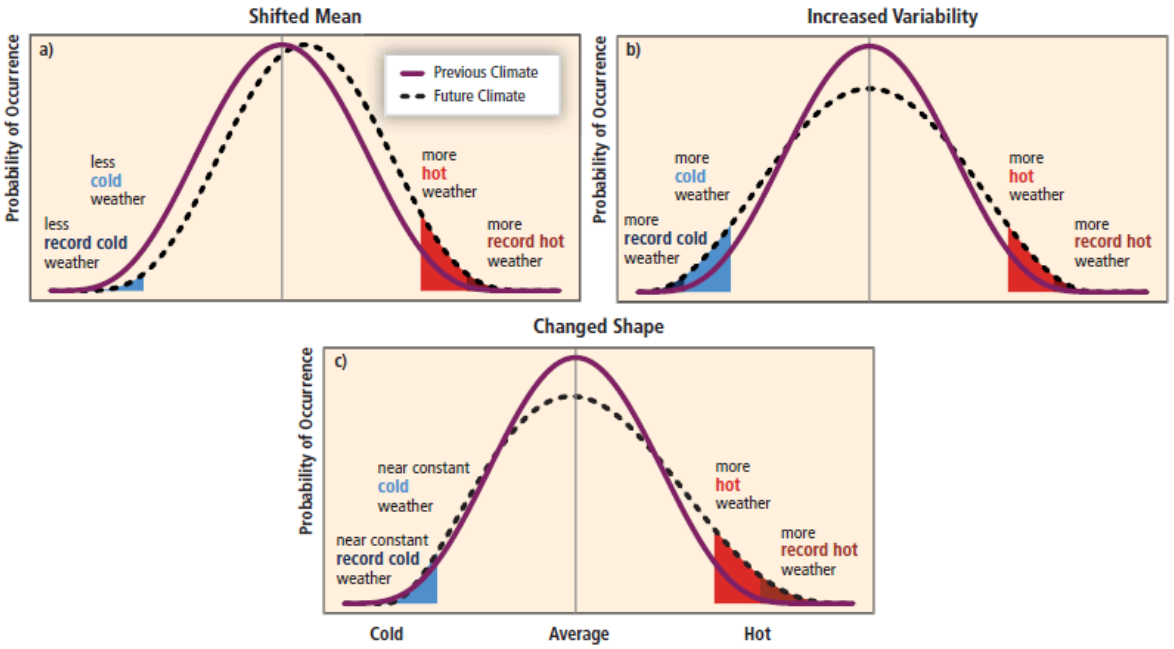

Figure 1.1. Probability density function of daily temperature [2]

According to some estimations, more than 1,300 deaths per year are caused by extreme heat in the United States [3]. In summer 2003, more than 70,000 additional deaths were due to extreme heat in Europe [4]. More frequent and prolonged extreme temperatures produce environmental and social results. Extreme temperatures pose health risks for people with chronic illnesses, cardiovascular diseases, respiratory diseases and diabetes-related diseases. Urban heat island effect further increases the health risks. Therefore, estimating the change in the frequency of extreme events in the future is very important for human health.

In this study, 643 cities with population more than 300,000 in MENA region are analysed [5]. The MPI-ESM-MR and HadGEM2-ES general circulation model outputs are dynamically downscaled to 50 km resolution using Regional Climate Model v4.4(RegCM4.4) of the Abdus Salam International Centre for Theoretical Physics (ICTP) for Representative Concentration Pathway Scenarios. Thereafter, the histograms of daily maximum temperatures for 30-year periods are plotted for the periods 1971-2000 and 2070-2099. Means and standard deviations are calculated for each Gaussian component contributed in bimodal distribution using Scikit-learn Machine Learning package in Python. Change in return periods of extreme weather events (1-year, 10-year, 30-year, 50-year and 100-year events) are calculated using empirical rule. 16 of the largest cities in the MENA region are presented in this thesis.

2. CLIMATE CHANGE

2.1. The Industrial Revolution

In the 18th century, high growth in the population created a high demand on food and new resources. In order to supply the needs of the population, new efficient methods of production were required. Steam engines were in use for a long time, but the critical improvements made by James Watt that improved the efficiency of steam engines further accelerated the growth. Steam-powered engines allowed more coal extraction from the Earth's crust. Heat generated by the steam engines were used to process iron ore which led to a boom in iron industry and resulted in more demand of resources. Steam engines were used in factories and replaced the old systems such as sails and horses in transportation. Agricultural land expansion sped up.

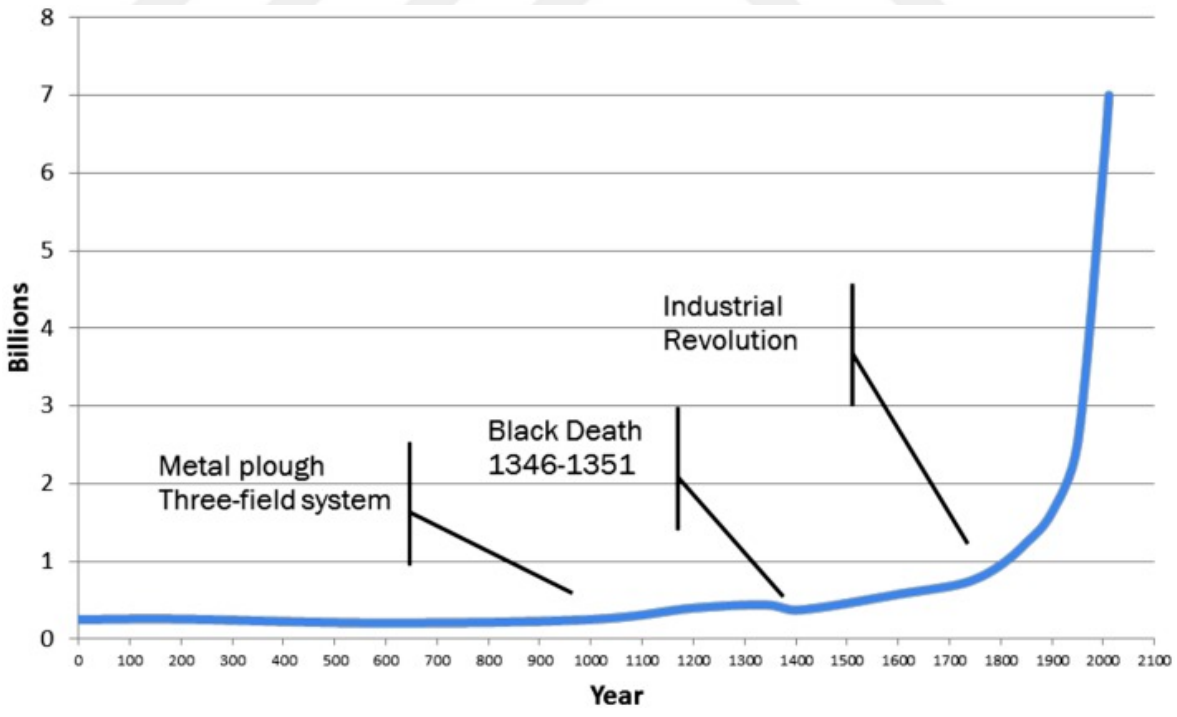

Figure 2.1. Historical growth of the world population since year 0 [6]

In those days, coal and fossil fuels, which are the nature's way of carbon capturing in billions of years, were the main energy sources for steam engines. With deforestation and use of fossil fuels, this captured carbon dioxide re-released and increased the CO_2 amount in the atmosphere, and this situation continues to date.

French scientist Joseph Fourier (1824) proposed that the Earth's atmosphere behaves like a greenhouse and provides moderate climatic conditions that support life. There is a known physical process called black-body radiation. All objects emit invisible infrared radiation and loose energy. Without an atmosphere, Earth would be -18°C due to its "albedo" which is the measure of reflection of sunlight by an astronomical body [7]. The atmosphere insulates the Earth like a blanket and creates the natural Greenhouse Effect, but Fourier did not know how the atmosphere trapped the heat. In the following years, Irish physicist John Tyndall showed how different molecules absorb infrared radiation and re-emit according to their molecular structure [8]. Thus, the Earth's atmosphere could store the heat to keep the planet warm at about 14°C (1951-1980 average).

2.2. The First Estimation

The first calculation of how the CO_2 emissions from fossil fuels could affect the global temperatures was made by Arrhenius in 1896 [9]. In this pioneering study, he used an energy budget model that includes the solar and terrestrial radiation, and relation between them. He concluded that doubling the amount of CO_2 in the atmosphere would cause the temperatures rise by about 6°C. Similarly, a decrease in the amount of CO_2 would lower the temperature and that was the cause of ice ages. We would argue that this study was the first numerical modelling of atmosphere and the beginning of many more studies, such as this thesis, to predict the future temperature anomalies.

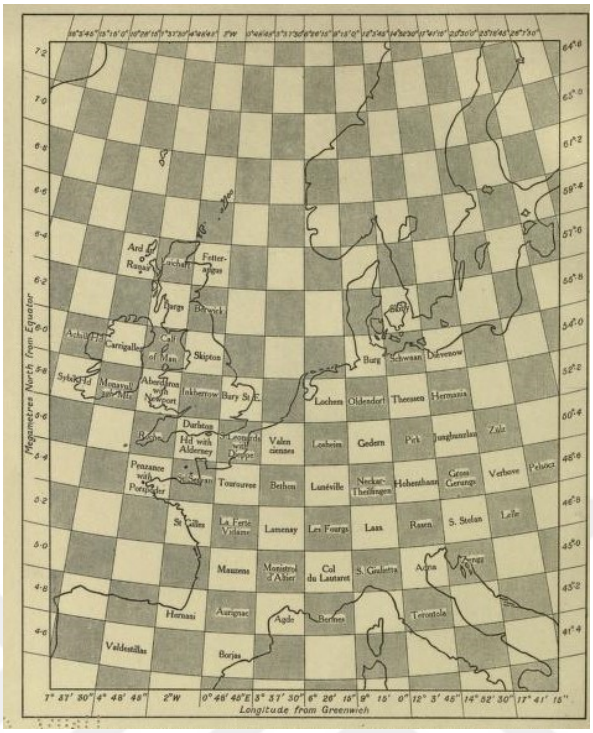

Figure 2.2. A page from Richardson's book showing the gridded cells.

Building upon these studies, English mathematician and meteorologist Lewis Fry Richardson (1922) presented a new method in his book to predict future climates by dividing the atmosphere into gridded cells (See Figure 2.2) [10]. Unfortunately, his efforts to produce a forecast by hand were in vain as it took six weeks for an 8-hour forecast without computers. This gridded cell method is still used in climate modelling.

In the mid-20$^{\text{th}}$ century, Serbian geophysicist and astronomer Milutin Milankovich (1920) worked out how the climate changes on Earth due to its orbit around sun [11]. The eccentricity of Earth's orbit changes in every 100,000 years and this periodicity causes the glacial and interglacial periods. When orbital cycles put Earth in ice ages, Earth's albedo increases as its surface is covered with ice and reflects more incoming radiation. Therefore, more CO_2 is solved in oceans as the solubility of gases in liquids increases with decreasing temperature. When orbital cycles put Earth in warm interglacial periods, warmed oceans emit more CO_2 to the atmosphere and further amplify the warming effect.

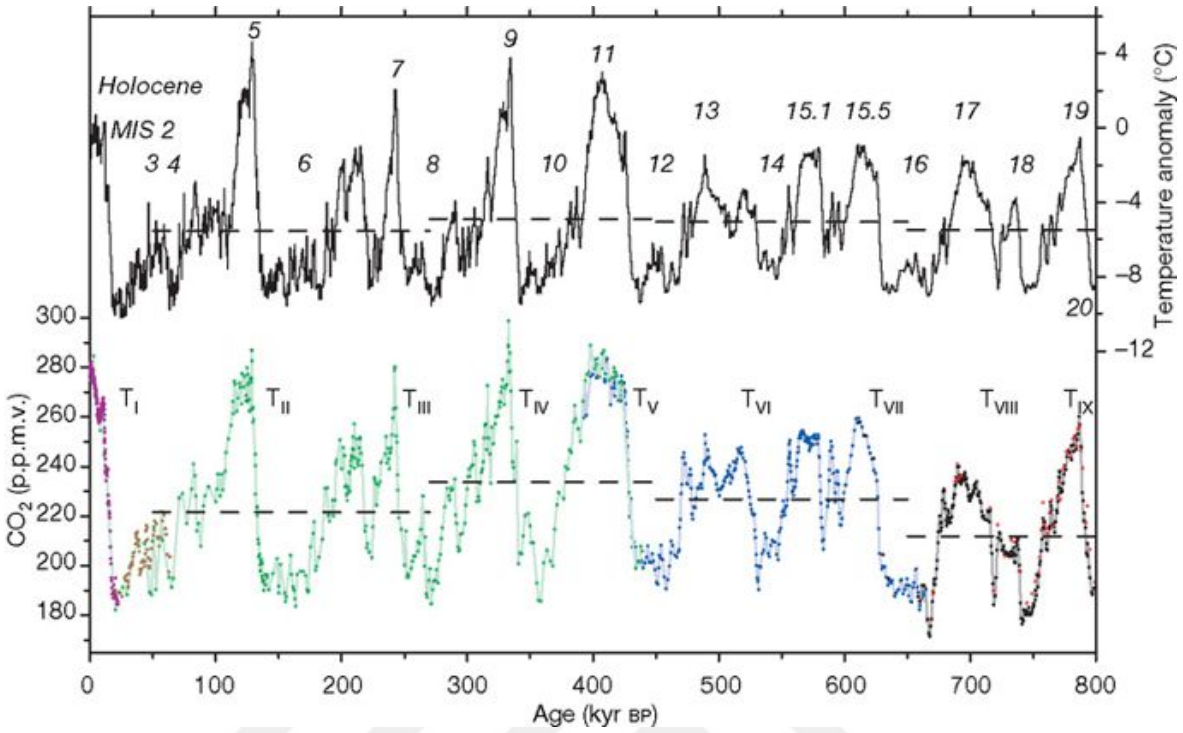

Figure 2.3. CO_2 records and temperature anomaly over the past 800,000 years [12]

This oscillation between temperature anomalies and the amount of CO_2 can be seen in Figure 2.3. The key importance of this graph is that the CO_2 levels change between 180-280 ppm over the course of 800,000 years. The amount of CO_2 in the atmosphere was about 180 ppm during ice ages and about 280 ppm during warm interglacial periods. During the glacial periods, Earth's average temperature dropped by about 6°C. These results were parallel with the ideas of Arrhenius.

Guy Stewart Callendar (1938) estimated that the amount of CO_2 in the atmosphere was 290 ppm and there was an increase of 6% from 1900 to 1936 [13]. He indicated that "The temperature observations at 200 meteorological stations were used to show that world temperatures had actually increased at an average rate of 0.005°C per year during the past half century". He showed the correlation between the rising amount of anthropogenic CO_2 and global temperatures, known as Callendar Effect. Although, he thought that the combustion of fossil fuels and consequently increasing temperatures were beneficial to mankind as it provided both power and also delayed

the return of the deadly glaciers.

2.2.1. Continuous Measurement of CO_2 Concentration

In the beginning of 20^{th} century, the reliability of CO_2 measurements was disputed with the growing interest in increasing temperatures due to fossil fuel combustion. In 1953, Charles Keeling started to take precise CO_2 measurements for his doctoral study. He took measurements near Monterey and he soon realised a diurnal pattern with steady values of about 310 ppm. He repeated these measurements at different part of the world and obtained the same result: strong diurnal behaviour with steady values of about 310 ppm in the afternoon. His measurements drew the attention and in March 1958, continuous measurements at Mauna Loa, Hawaii had started. These long-term measurements showed that the CO_2 reached a maximum value in May and declined to a minimum value in October. Keeling explained this fact as "We were witnessing for the first-time nature's withdrawing CO_2 from the air for plant growth during summer and returning it each succeeding winter." Another discovery these measurements provided was the fact that average CO_2 concentration was gradually increasing. These annual fluctuations and increase in averages can be seen in Figure 2.4 which is now called as "Keeling Curve". CO_2 concentrations have already exceeded 410 ppm in this day and age.

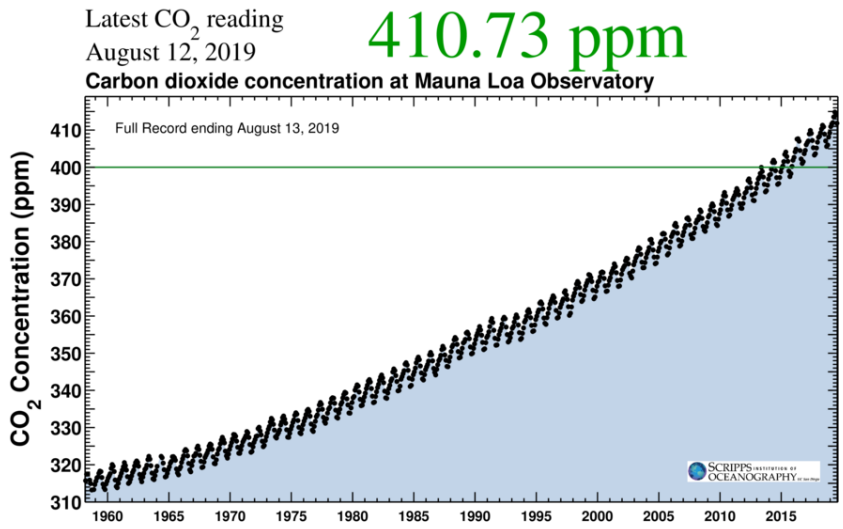

Figure 2.4. Full record of measurements at Mauna Loa Observatory

Now, we can place the measurements from Mauna Loa to 800,000 years of CO_2 measurements obtained from ice cores (See Figure 2.3). Current CO_2 levels are approximately 50% higher than the maximum value of 280 ppm seen during warm interglacial periods.

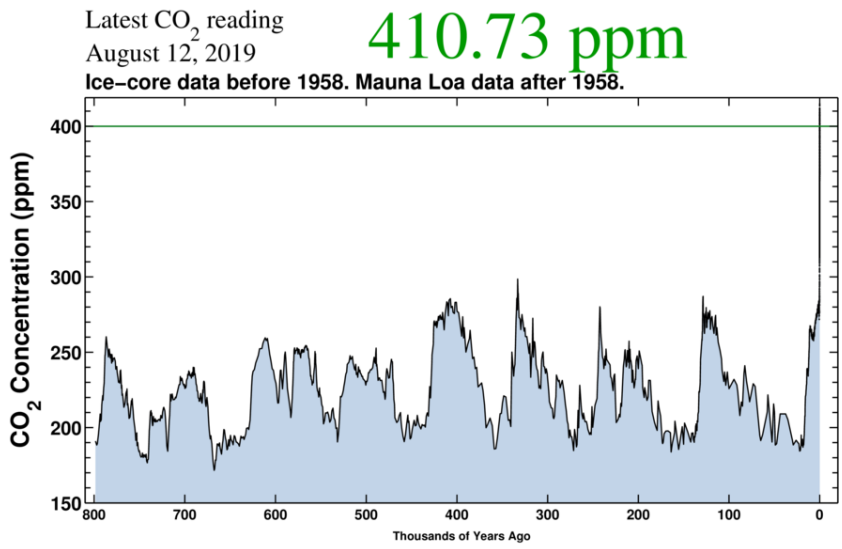

Figure 2.5. 800,000 years of CO_2 levels.

2.3. Computerised Forecasts

The World's first electronic, large scale, general-purpose digital computer ENIAC was proposed by John von Neumann to be used in numerical weather forecasting at Princeton. In 1950s, ENIAC was used to compute forecasts with 2D gridded atmospheric model in a similar way Richardson had proposed. In the later years, Norman Philips created the first general circulation model (GCM) to forecast atmospheric dynamics. His model was successful in predicting seasonal patterns and jet streams [14].

Interest in numerical modelling of climate increasingly continued in those years parallel with the developments in computers. However, in 1963, Müller showed that calculations showing an increase in temperatures due to CO_2 were highly susceptible to the model assumptions. This result made CO_2 based warming theories very questionable [15].

A study made by Manabe and Wetherald (1967) worked things out. In their paper, they proposed the first sound climate model using a 1D radiative-convective model. They found out the influence of clouds and water vapour on CO_2 based warming and concluded a 2.4°C warming due to doubling CO_2 [16]. Their findings still hold to this day well within the limits of current predictions. Thanks to their results, more realistic climate simulations can be carried out.

With the emerging consciousness about environment and climate change, the first Earth Day was celebrated on 22 April 1970. Twenty million participants around the country joined to the largest demonstration in American history. Later that year, the Clean Air Act, a comprehensive air quality law, passed in the Senate.

The early climate models were not considering the atmospheric and oceanic interactions. In reality, the climate system consists of several components. Manabe *et al.* (1975) constructed a coupled ocean-atmosphere model which takes into account the individual components and used a realistic topography rather than idealized one [17]. Their work was the first exemplary of coupled ocean-atmosphere GCM(AOGCM).

Though, the resolution was coarse with grid sizes of 500 km as shown in Figure 2.6.

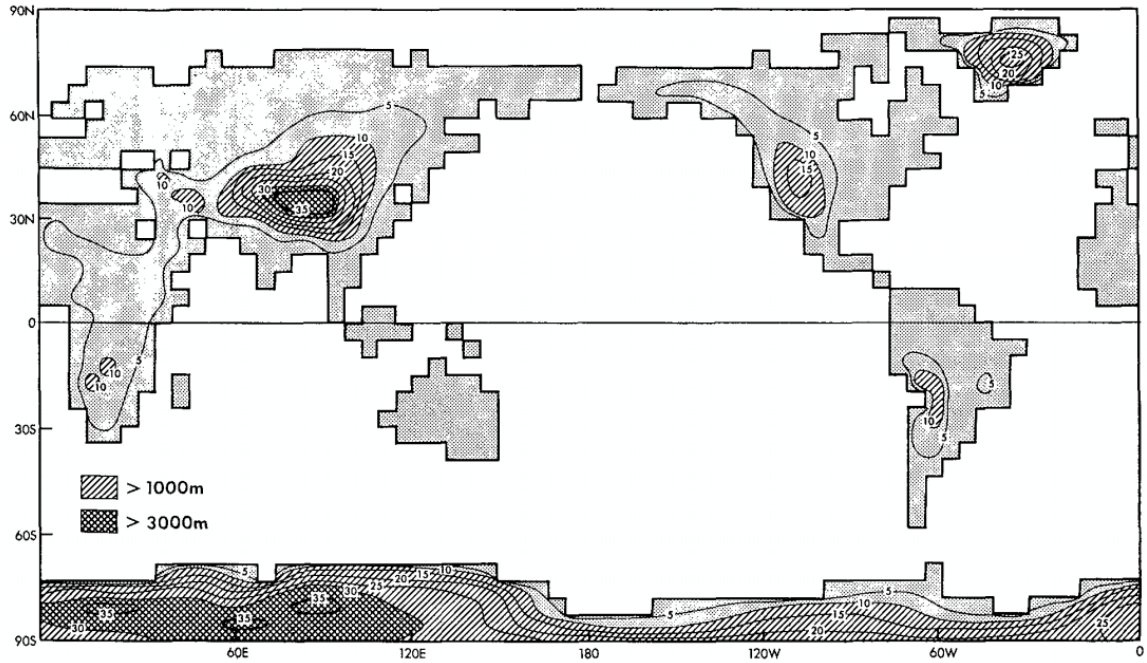

Figure 2.6. Topography of Earth surface used in the first coupled GCM [17]

2.4. IPCC

The Intergovernmental Panel on Climate Change (IPCC) was established in 1988 to provide an objective and scientific assessment of current studies on climate change and its effects. The IPCC is an intergovernmental body of the United Nations and an internationally accepted authority on climate change.

The first IPCC report published in 1990 stated that under the IPCC Business-as-Usual emissions of greenhouse gases, a rate of increase of global-mean temperature during the next century of about 0.3°C per decade. The report also predicted a 6 cm rise in sea-levels. The IPCC's fifth assessment report published in 2013 predicted an increase in temperatures with lower limit of 1.5°C [2].

In 2000, IPCC's special report presented future greenhouse gas emission scenarios. Future emissions depend on socio-economic development, demographic development

and technological change. As their future is uncertain, emission scenarios are used in climate change analysis and future climate modelling. The Special Report on Emissions Scenarios (SRES) followed four different schemes to describe the relationships between emission driving forces and their evolution. The SRES storylines were divided into 4 types; A1, A2, B1 and B2. These scenarios were characterized to project the future greenhouse gas pollution, economic developments, land-use and other driving forces [18]. These scenarios were later replaced by "Representative Concentration Pathway" scenarios, which were also used in this thesis.

IPCC's Special Report on Global Warming of 1.5°C published in 2018 stated that approximately 1.0°C increase in temperatures since pre-industrial period are caused by anthropogenic emissions. It is expected that this increase is to reach 1.5°C between 2030 and 2052. The report stated that climate-related risks to health, food security, water supply, human security, economic growth increase as the global warming increases but impact of these risks depend on not only rate of warming but also geographic location, levels of development and vulnerability, and climate adaptation and mitigation [1].

2.5. Extreme Events

2003 heatwave caused 15,000 deaths in France. Multiple all-time maximum temperature records were broken in different European cities. The United Nations Environment Program estimated a death toll more than 30,000 people. Elderly people were the most affected group. During the heatwave multiple nuclear reactors had to shut-down due to either the water levels were dropped, or water temperatures exceeded safety limits. Increased demand of electricity as people turned on the air conditioning and refrigerators together with the insufficient electricity generation due to shutdowns caused electric cut-outs in Europe, which further increased heat related deaths [19]. Robine *et al.* discovered that there were 70,000 additional deaths in Europe during the summer of 2003 [4].

Kuglitsch *et al.* (2010) found that about 7 times increase in the mean heatwave intensity, length and frequency had occurred between 1960 and 2006 in the eastern Mediterranean using data from 246 stations [20]. Lieveld *et al.* (2012) proposed that rare hot summer conditions might be norm for the Balkan Peninsula and Turkey by the end of the 21st century [21]. Leliveld *et al.* (2016) found that the extreme events in MENA were stronger in summers rather than winters as shown in other areas and heat extremes are projected to gradually increase in the future [22]. Öztürk *et al.* (2015) found a shift and flattening in the probability distribution functions of temperatures in the future with respect to reference period. They proposed that the frequency of extreme heat events will increase in the future [23]. Sillmann *et al.* (2013) found that changes in temperature and precipitation are most apparent in RCP8.5 scenario [24]. Efthymiadis *et al.* (2011) found that trends in Mediterranean temperature extremes are consistent with the global trends with decreases in cold extremes and increases in hot extremes [25]. Sheerwood *et al.* (2010) stated that the current wet-bulb temperatures, the lowest temperature for air to be cooled by the evaporation of water, are similar across different climates and never exceed 31°C. If wet-bulb temperatures reach 35°C in the future for extended periods with global mean temperature increase of about 7°C as seen in climate projections, this will induce hyperthermia in humans as it would be impossible to dissipate metabolic heat by perspiration [26].

Several studies presented the impacts of extreme events on human health, environment, water resources and economy. Therefore, knowing how the frequency of extreme events will change in the future is very important to take precaution against climate-related disasters in the future.

3. METHODOLOGY

3.1. The Climate System

The Earth's climate system consists of five major components: the atmosphere (air), the hydrosphere (water), the cryosphere (ice and permafrost), the land surface and the biosphere. In addition to these, external climate forcing is also responsible for change in climate such as incoming sunlight, volcanism, plate tectonics and greenhouse gases due to human activity.

The atmosphere is the most unstable, rapidly changing and most effective part of Earth's climate. Even though the large part of the gases in the atmosphere, i.e. nitrogen (78.1% N_2), oxygen (20.9% O_2) and argon (0.93% Ar), have only limited interaction with the incoming solar radiation and does not absorb and emit the infrared radiation emitted by Earth. On the other hand, carbon dioxide (CO_2), methane (CH_4), nitrous oxide (N_2O) and ozone (O_3) are called greenhouse gases and they play an essential role in the Earth's energy budget by absorbing and emitting infrared radiation. Besides, aerosols and clouds are also influential in climate.

The hydrosphere comprises all liquid surface and subterranean water. 75% of Earth surface is covered with water. The oceans are important regulators on Earth's climate due to their ability to store and transport large amount of energy and carbon storage. The cryosphere consists of ice sheets and glaciers, and effective on climate system due to its albedo. Also, water stored in glaciers is a potential of sea level rise. Land surfaces affect how the wind blows over topography and aerosolizes the dust from the surface, and how the energy absorbed by the earth and changes the soil moisture which brings water vapour back to the atmosphere [27].

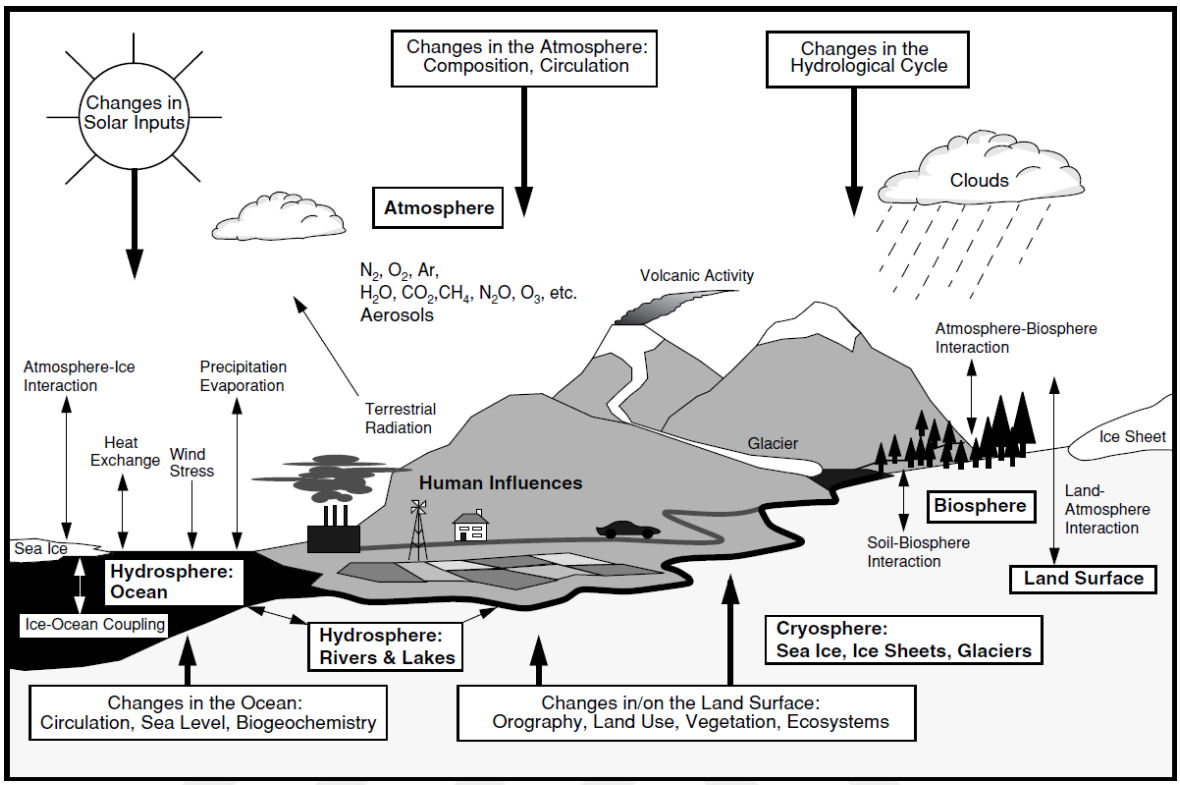

Figure 3.1. Schematic view of the components of the global climate system (bold), their processes and interactions (thin arrows) and some aspects that may change (bold arrows) [27]

3.2. General Circulation Model GCM

General Circulation or Global Climate models (GCMs) are primary tools used to project the Earth's climate in the future using mathematical equations that describe the movement of energy (first law of thermodynamics) and momentum (Newton's second law of motion), along with the conservation of mass (continuity equation) and water vapour (ideal gas law) that simulate atmospheric and oceanic processes, interactions and feedbacks [28]. GCMs use 3D grids over the globe with horizontal and vertical levels. In each cell, atmospheric interactions, radiation, precipitation, snow cover, sea ice, heat and moisture are computed. Grid resolutions are generally quite course with a range of 100 to 500 kilometers in horizontal and 10 to 20 layers in vertical.

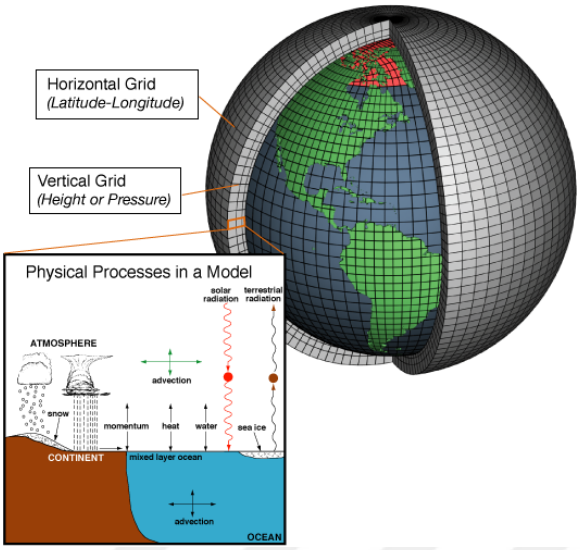

Figure 3.2. Climate models are systems of differential equations based on the basic laws of physics, fluid motion, and chemistry. Atmospheric models calculate winds, heat transfer, radiation, relative humidity, and surface hydrology within each grid and evaluate interactions with neighbouring points [29]

In GCMs, many physical processes cannot be properly modelled as they occur at smaller scales. Their known properties must be averaged over the larger scales and this is a source of uncertainty in future climate models. Also, various feedback mechanisms such as water vapour and warming, clouds and radiation, ocean circulation and albedo are other sources of uncertainty. Therefore, GCMs may project different responses depending on how processes and feedbacks are modelled.

3.3. The Max-Planck-Institute Earth System Model

The Max-Planck-Institute Earth System Model Mixed Resolution (MPI-ESM-MR) is one of the models used in this study. The mixed resolution (MR) version of MPI-ESM (MPI-ESM-MR) has higher vertical resolution in the atmosphere and higher horizontal resolution in the ocean. The MR configuration doubles the number of levels in the atmosphere and decreases the horizontal grid spacing of the ocean, compared to the low resolution (LR) configuration.

MPI-ESM couples the atmosphere, ocean and land surface through the exchange of energy, momentum, water and carbon dioxide. The model consists of the coupled general circulation models ECHAM6 for the atmosphere, MPIOM for the ocean, JSBACH for terrestrial biosphere and HAMOCC for the marine biogeochemistry as shown in Figure 3.3. Included carbon cycle to the model is the largest conceptual difference compared to predecessors. In addition to these, geographic distribution of vegetation has been improved by a climate-consistent development. Anthropogenic land-cover change, and the surface albedo scheme have been also improved [30].

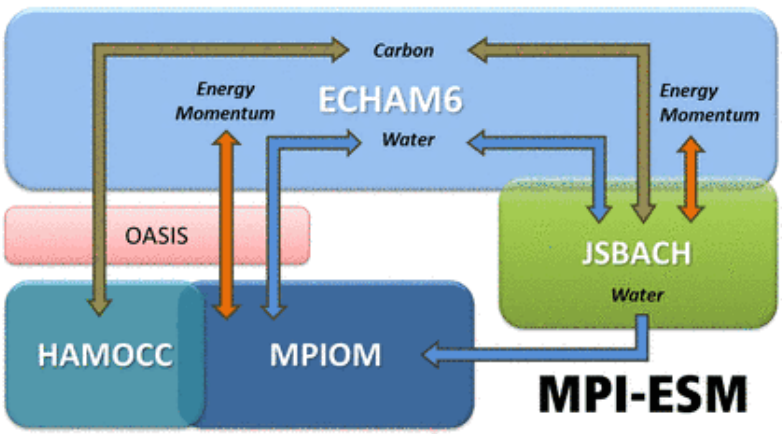

Figure 3.3. Schematic view of MPI-ESM [30]

3.4. Hadley Centre Global Environment Model version 2

The Hadley Centre Global Environment Model version 2 Earth System (HadGEM2-ES) is another model used in this study. The HadGEM2 model includes atmosphere, ocean and sea-ice components. Dynamic vegetation, ocean biology and atmospheric chemistry are included in the Earth-system configuration.

The standard atmospheric component has 38 levels extending to 40km height, with a horizontal resolution of 1.25 degrees of latitude by 1.875 degrees of longitude, which produces a global grid of 192 x 145 grid cells. This is equivalent to a surface resolution of about 208 km x 139 km at the Equator, reducing to 120 km x 139 km

at 55 degrees of latitude. A vertically extended version, with 60 levels extending to 85km height, is also used for investigating stratospheric processes and their influence on global climate. The HadGEM model takes all months as 30 days [31].

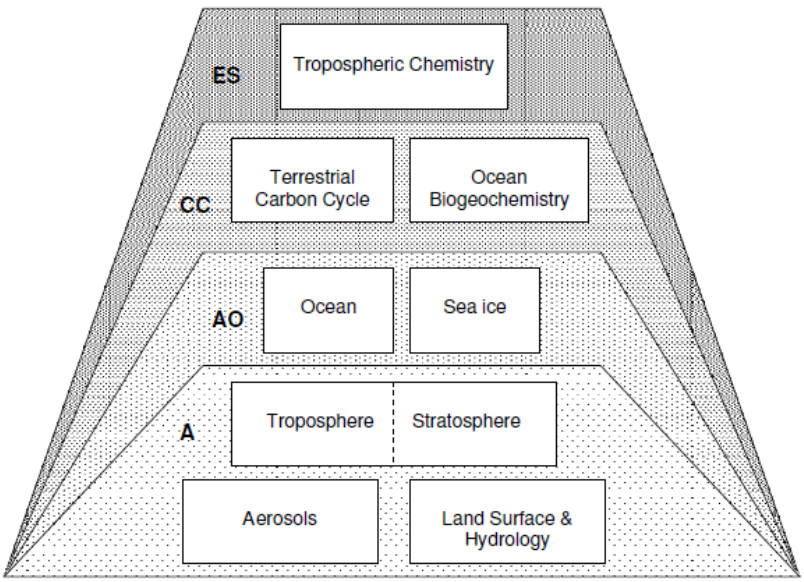

Figure 3.4. Processes included in the HadGEM2 model family [31]

3.5. Regional Climate Model RegCM

GCMs are valuable but due to their coarse resolution, they are not useful for high-resolution regional climate variability analyses. Geographical features of a region affect its climate and local atmospheric interactions. To assess the effects of climate change on fine-scale processes such as crop production, hydrology and such, high-resolution climate models are needed at scales of 10-50 kilometres.

Regional Climate Models (RCM) use GCM output as input and incorporate more complex topography, the land-sea distribution and surface features in order to generate realistic climate outputs at higher spatial resolution. The concept of downscaling is shown in Figure 3.5.

In this study, the RegCM is used for generating regional climate model outputs for MENA region. The RegCM has started to be developed since 80s starting with the

version 1 and today has reached the version 4. It is designed and developed by a varied community and distributed as an open source and portable code. The distribution and maintenance are coordinated by the Earth System Physics section of the Abdus Salam International Centre for Theoretical Physics (ICTP).

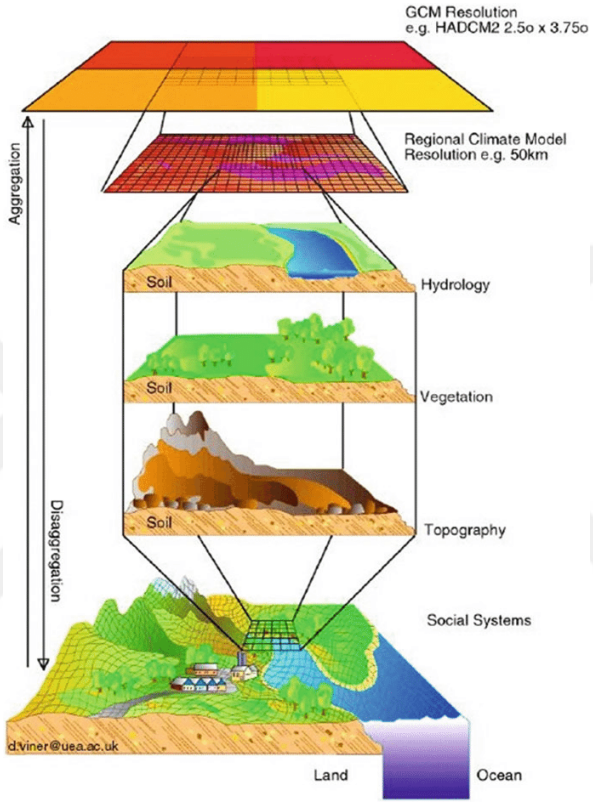

Figure 3.5. The concept of downscaling. (Source: David Viner, Climatic Research Unit, University of East Anglia, UK)

3.5.1. Model components

The RegCM uses four components: Terrain, ICBC (Initial Conditions Boundary Conditions), RegCM and Post-processor. Elevation, land use, sea surface temperature and 3D isobaric meteorological data are horizontally interpolated using Terrain and ICBC preprocessors from a coordinate mesh to high-resolution domain on either a Rotated (and Normal) Mercator, Lambert Conformal, or Polar Stereographic projection.

Sigma coordinate system, $\dot{\sigma}$, which is a vertical coordinate system used in computational models defined as the ratio of the pressure at a given point in the atmosphere to the pressure on the surface of the earth underneath it, is used for vertical interpolation from pressure levels to the $\dot{\sigma}$ coordinates. The $\dot{\sigma}$ surfaces near the ground closely follow the terrain as shown in Figure 3.6 [32].

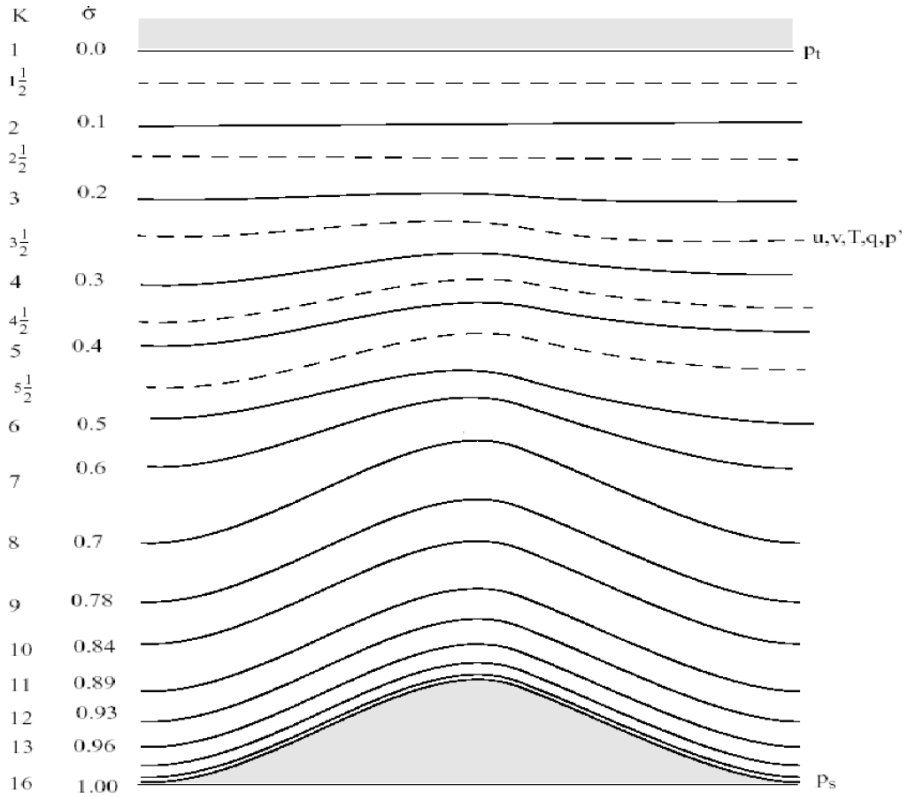

Figure 3.6. Schematic representation of the vertical structure of the model [32]

3.5.2. The RegCM Model Horizontal and Vertical Grid

Data is generated on pressure surfaces and then interpolated to model's vertical coordinates before input to model. The vertical coordinates follow the terrain as getting closer to surface and flattens at higher levels. The model levels are defined by the Hydrostatic solver using a dimensionless $\dot{\sigma}$ coordinate where p is the pressure, p_t is a specified constant top pressure and p_s is the surface pressure,

$$\dot{\sigma} = \frac{(p - p_t)}{(p_s - p_t)} \tag{3.1}$$

where we can define:

$$p^*(x, y) = p_s(x, y) - p_t \tag{3.2}$$

For the Non-hydrostatic solver, a similar dimensionless coordinate is used, but it is defined entirely from the reference pressure. Given a reference atmospheric profile the values:

$$p(x, y, z, t) = p_0(z) + p'(x, y, z, t) \tag{3.3}$$

$$T(x, y, z, t) = T_0(z) + T'(x, y, z, t) \tag{3.4}$$

$$\rho(x, y, z, t) = \rho_0(z) + \rho'(x, y, z, t) \tag{3.5}$$

are changing on the vertical axis where (p', T',ρ') are the perturbations of the reference atmospheric profile, the vertical sigma coordinate is defined as:

$$\dot{\sigma} = \frac{(p_0 - p_t)}{(p_s - p_t)} \tag{3.6}$$

where ρ is the air density, T is the temperature, p_s is the surface pressure, p_t is a specified constant top pressure and p_0 is the reference pressure profile. The total pressure at each grid point is thus given as:

$$p = p^* \dot{\sigma} + p_t + p' \tag{3.7}$$

with p^* defined as in the hydrostatic solver. It can be seen from the Equation 3.6 and Figure 3.6 that $\dot{\sigma}$ is 0 at the top and 1 at the surface, and each model level is defined by a value of $\dot{\sigma}$, which do not necessarily have to be evenly spaced.

The horizontal grids use the Arakawa grid system, specifically Arakawa-B staggering, to define the scalars at the center of the grid box and to evaluate the eastward and northward velocity components at the grid corners as shown in Figure 3.7. The

center points of grid squares are referred to as cross points, and the corner points are dot points. Necessary interpolations are made by the preprocessors to assure consistency with the grid.

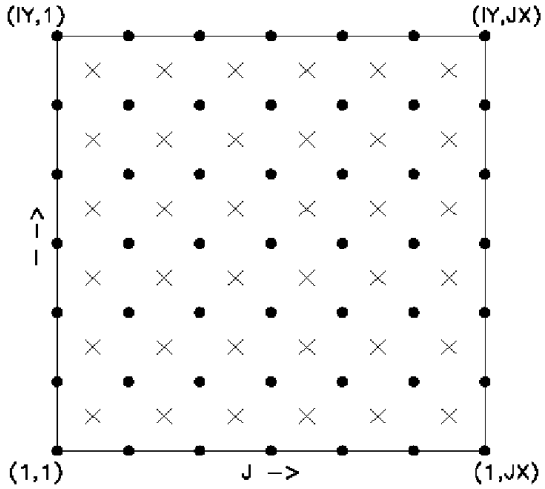

Figure 3.7. Schematic representation showing the horizontal Arakawa B-grid staggering of the dot and cross grid points.

3.6. Representative Concentration Pathways (RCP)

Climate models are used to predict the changes in climate in the future. As the effects of climate change depends on socio-economic and emission scenarios, plausible descriptions of how the future may evolve is needed. For this purpose, different scenarios with a range of variables including socio-economic change, technological change, energy and land use, and emissions of greenhouse gases and air pollutants were defined to be used as input for climate model runs. Representative Concentration Pathways (RCP) are defined to provide possible development trajectories for the main drivers of climate change.

The RCPs describe possible climate situations in the future which emphasize how much greenhouse gases are emitted and how socio-economic factors are changed. The four RCP scenarios, namely RCP2.6, RCP4.5, RCP6 and RCP8.5; are defined by their target radiative forcing values for 2100 in the range between, 2.6 to 8.5 W/m^2. Description of scenarios and corresponding studies are shown in Table 3.1.

Table 3.1. Overview of representative concentration pathways (RCPs) [33].

	Description	Publication
RCP8.5	Rising radiative forcing pathway leading to 8.5 W/m^2 (∼1370 ppm CO_2 eq) by 2100.	Riahi *et al.* (2007) [34]
RCP6	Stabilization without overshoot pathway to 6 W/m^2 (∼850 ppm CO_2 eq) at stabilization after 2100	Fujino *et al.* (2006) [35] Hijioka *et al.* (2008) [36]
RCP4.5	Stabilization without overshoot pathway to 4.5 W/m^2 (∼650 ppm CO_2 eq) at stabilization after 2100	Clarke *et al.* (2007) [37] Smith and Wigley (2006) [38] Wise *et al.* (2009) [39]
RCP2.6	Peak in radiative forcing at ∼3 W/m^2 (∼490 ppm CO_2 eq) before 2100 and then decline (the selected pathway declines to 2.6 W/m^2 by 2100).	Van Vuuren *et al.* (2006) [40] Van Vuuren *et al.* (2007) [41]

In this study, RCP 4.5 and RCP 8.5 scenarios are used. RCP4.5 and RCP8.5 scenarios lead to a radiative forcing of 4.5 W/m^2 and 650 ppm CO_2 eq., and 8.5 W/m^2 and 1370 ppm CO_2 eq., respectively. RCP 2.6 scenario is the best case scenario for limiting the anthropogenic climate change and keeping the temperatures below 2°C above pre-industrial levels. RCP 4.5 is a stabilization scenario with emissions peak around mid-century and then decline. This scenario is between RCP2.6 best case and RCP8.5 worst-case scenarios and predicts 2.4°C increase and 0.47 m sea level rise at the end of the century. RCP 8.5 is also referred as business-as-usual scenario as it does not include any specific climate mitigation target. This scenario predicts 4.3°C increase at the end of the century, 0.63 m sea level rise and large increase in extreme

weather events.

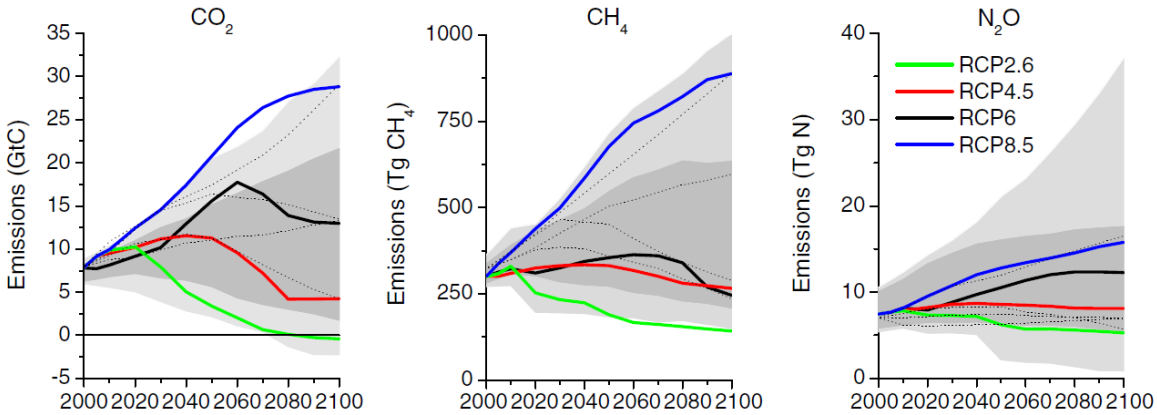

Figure 3.8. Greenhouse Gases emissions of RCP scenarios [33]

3.7. The Coordinated Regional Climate Downscaling Experiment (CORDEX)

The CORDEX is an international coordinated framework established by World Climate Research Programme (WCRP) to organize, evaluate and improve regional climate modelling techniques. CORDEX aims to bridge the gap between the climate modelling community and end users of climate information.

The grid resolutions are set to 0.44° by 0.44° for the RCMs using a rotated pole system where the model operates over an equatorial domain with a quasi-uniform resolution of approximately 50km. The globe is divided into 14 domains where the regional downscaling takes place:

- Region 1: South America
- Region 2: Central America
- Region 3: North America
- Region 4: Africa
- Region 5: Europe (EURO)
- Region 6: South Asia

- Region 7: East Asia
- Region 8: Central Asia
- Region 9: Australasia
- Region 10: Antarctica
- Region 11: Arctic
- Region 12: Mediterranean (MED)
- Region 13: Middle East North Africa (MENA)
- Region 14: South-East Asia (SEA)

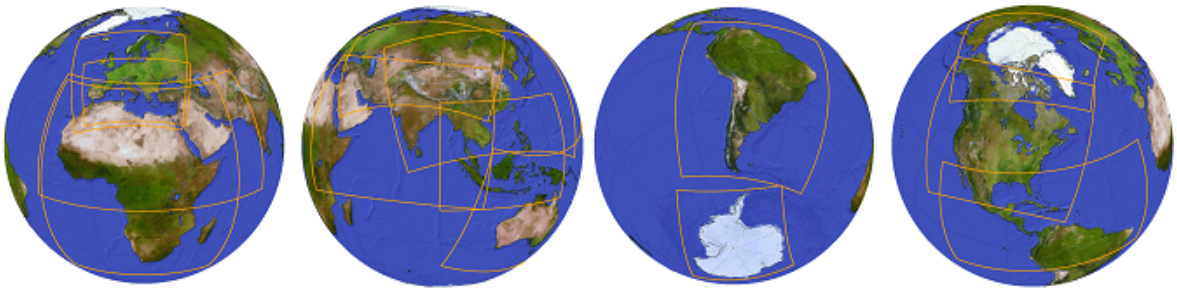

Figure 3.9. CORDEX Domains [42]

In this study, Region 13: Middle East & North Africa (MENA) is used. The GCM outputs of MPI-ESM-MR and HadGEM2 models are dynamically downscaled to 50×50 km grid for MENA region.

3.7.1. Region 13: MENA

The CORDEX MENA region used in this study spans an extensive area bordered by the Europe to the north, Democratic Republic of the Congo to the south, Atlantic Ocean to the west and India to the east. CORDEX MENA region is showed in Figure 3.10. Total population of 643 cities with population higher than 300,000 used in this study is approximately 550 million [5]. Total population of 16 cities presented in this thesis is about 100 million. Therefore, a change in extreme events in this region would potentially affect approximately 10% of the World's population.

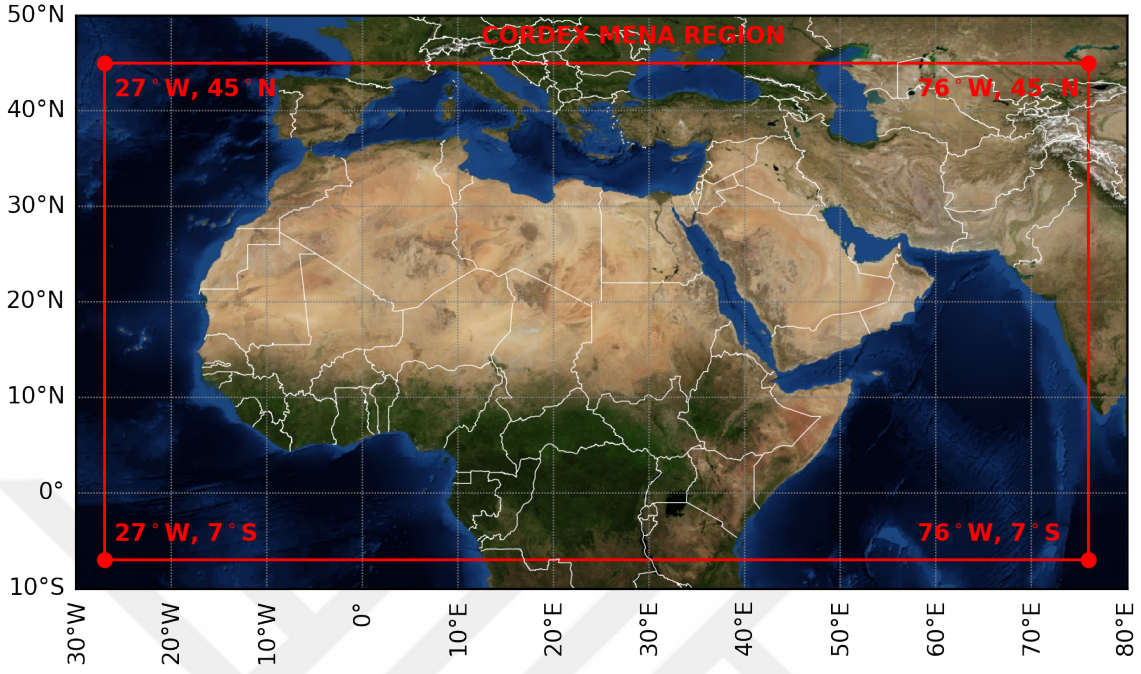

Figure 3.10. CORDEX Region 13: Middle East North Africa (MENA)

The Köppen-Geiger climate classification is widely used in climate systems. Climate is divided into 5 main climate groups with certain temperature and precipitation patterns. Each group is represented by a letter, namely A (tropical), B (arid), C (temperate), D (continental), and E (polar). As it can be seen in Figure 3.11, most of the MENA region falls into tropical(A), arid(B) and temperate(C) climates. Among 643 cities with population higher than 300,000 in MENA region, 16 cities with population higher than 1 million from different countries are chosen to be presented in this thesis. These cities are shown in Figure 3.11.

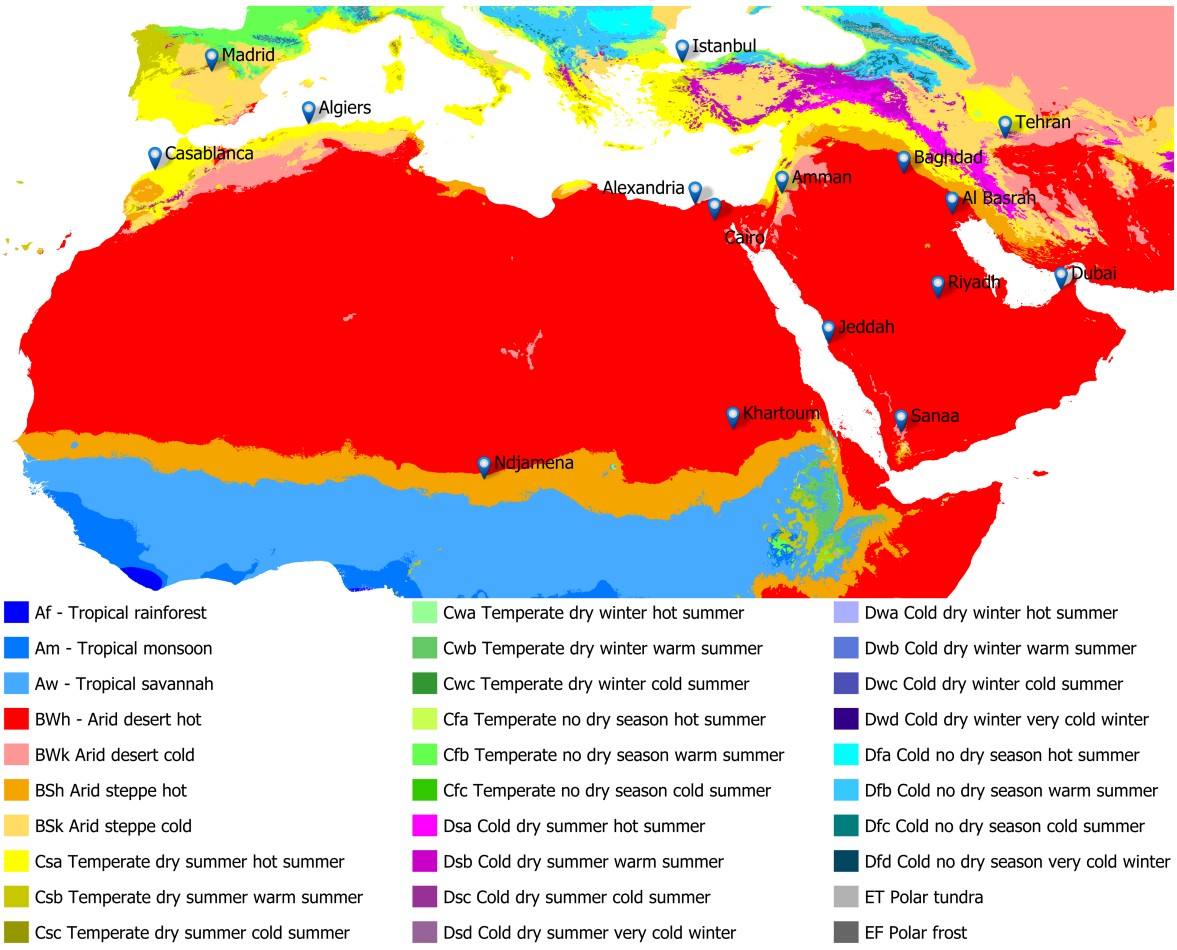

Figure 3.11. Köppen-Geiger Classification [43]

3.8. Data Preparation

Daily city maximum temperature data are obtained from the RegCM outputs of MPI-ESM-MR and HadGEM2 model for RCP4.5 and RCP8.5 scenarios for MENA region. First, as the raw data changes with topography and is in 50-by-50 km grid format, elevation correction to sea level is applied to all dataset using temperature lapse rate of 6.5°C/km to get rid of the effects of sudden changes in elevation due to coarse grid resolution at city scale [44].

$$T_{sea\ level} = (T_i - 273.15) + 0.0065H \tag{3.8}$$

where $T_{sea\ level}$ is the temperature of the grid point reduced to sea level, T_i is the initial temperature of the grid point and H is the elevation of that grid point. In the parenthesis, unit of temperature is changed from Kelvin to Celsius scale. Then, daily temperatures at city centers are calculated using inverse distance squared weighted interpolation method from the nearest 4 grid points:

$$T(\mathbf{x}) = \frac{\sum_{1}^{4} \frac{T(x_i)}{d(\mathbf{x}, x_i)^2}}{\sum_{1}^{4} \frac{1}{d(\mathbf{x}, x_i)^2}} \tag{3.9}$$

where $T(\mathbf{x})$ is the interpolated temperature at city center, $T(x_i)$ is the temperature at i^{th} nearest grid point and $d(\mathbf{x}, x_i)^2$ is the square of the distance between the city center and the i^{th} nearest grid point. Daily temperature histograms for each city center are plotted using this elevation corrected data.

3.9. Scikit-learn Machine Learning Library for Python

Scikit-learn is a Python library that provides many supervised and unsupervised learning algorithms such as regression, classification, clustering, model selection and preprocessing. For this study, Gaussian mixture model is used for analysis [45].

When the city histograms are plotted, the prominent feature was that the daily temperatures follow a bimodal distribution, a continuous distribution with two different modes, i.e. two peaks. Therefore, a unimodal (one 'peak') fit on a multi-modal distribution gives a poor fit. A Gaussian distribution is defined by two parameters, mean μ and standard deviation σ. To analyse the return periods of extreme temperature events, mean and standard deviation of each Gaussian component in daily city temperature histograms should be known. Thus, Gaussian mixture model is used to find the means and standard deviation for each Gaussian component in multimodal distribution.

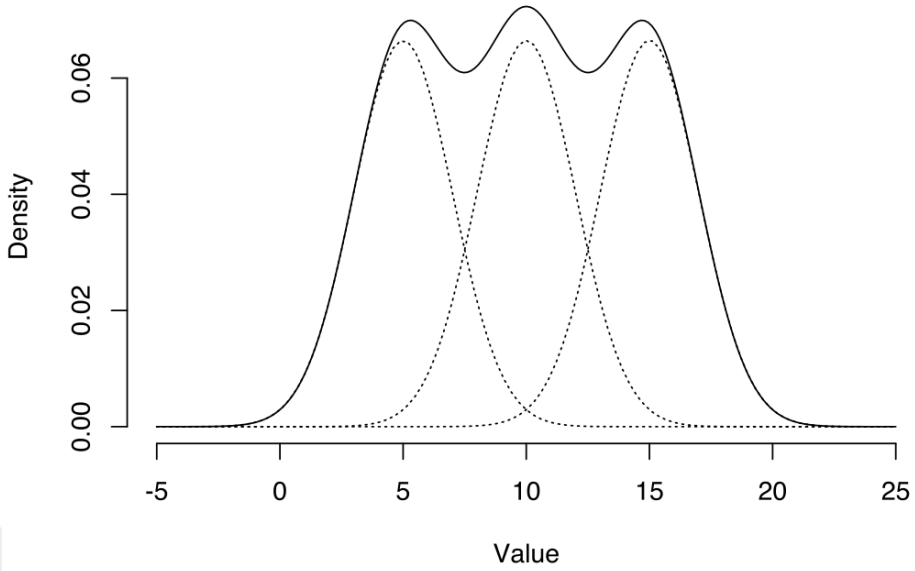

Figure 3.12. A Gaussian mixture of three normal distributions [46]

3.9.1. Gaussian Mixture Model

A Gaussian mixture model is a probabilistic model that assumes all the data points are generated from a mixture of a finite number of Gaussian distributions with unknown parameters. Mixture models do not require knowing subpopulation and learn the population automatically in a form of unsupervised learning [46].

For a Gaussian mixture model with K components, the k^{th} component has a mean of μ_k and variance of σ_k^2 for the unimodal case and a mean of $\vec{\mu}_k$ and covariance matrix of Σ_k for multimodal case. The mixture component weights are defined as ϕ_k such that the total probability distribution normalizes to 1.

Unimodal case:

$$p(x) = \sum_{i=1}^{K} \phi_i \mathcal{N}(x \mid \mu_i, \sigma_i) \tag{3.10}$$

$$\mathcal{N}(x \mid \mu_i, \sigma_i) = \frac{1}{\sigma_i \sqrt{2\pi}} exp\bigg(- \frac{(x-\mu_i)^2}{2\sigma_i^2} \bigg) \tag{3.11}$$

$$\sum_{i=1}^{K} \phi_i = 1 \tag{3.12}$$

where $p(x)$ is the probability function, $\mathcal{N}(x \mid \mu, \sigma)$ is the normal distribution of x with mean μ and variance σ^2 and ϕ is the component weights.

Multimodal case:

$$p(\vec{x}) = \sum_{i=1}^{K} \phi_i \mathcal{N}(\vec{x} \mid \vec{\mu}_i, \Sigma_i) \tag{3.13}$$

$$\mathcal{N}(\vec{x} \mid \vec{\mu}_i, \Sigma_i) = \frac{1}{\sqrt{(2\pi)^K |\Sigma_i|}} exp\bigg(- \frac{1}{2} (\vec{x} - \vec{\mu}_i)^T \Sigma_i^{-1} (\vec{x} - \vec{\mu}_i) \bigg) \tag{3.14}$$

$$\sum_{i=1}^{K} \phi_i = 1 \tag{3.15}$$

where $\vec{\mu}$ is a d dimensional vector denoting the mean of distribution, K is the number of Gaussian components and Σ is the $d \times d$ covariance matrix.

For known number of components K, for this study K=2, expectation-maximization (EM) algorithm is used to predict the mixture model's parameters. The main difficulty in learning Gaussian mixture models is that which points have come from which latent component is unknown. Expectation-maximization algorithm gets around this problem by an iterative process. At the first step, expectation step, random Gaussian components with random model parameters μ, Σ and ϕ are used to calculate for each point the probability of being generated by each component. Then, in the second step, maximization step, model parameters are adjusted to maximize the likelihood of a point being generated by these components. This process repeats until the algorithm converges.

3.10. Empirical Rule of Normal Distribution

The empirical rule is a statistical method used to determine how many σ away a value is from the mean in a normal distribution. The expected percentage of population inside $\mu \pm x\sigma$ range is defined as:

$$E(\mu \pm x\sigma) = \text{erf}\left(\frac{x}{\sqrt{2}}\right) \tag{3.16}$$

Figure 3.13 shows the approximate percentage of population that falls into 1σ, 2σ, 3σ away from the mean.

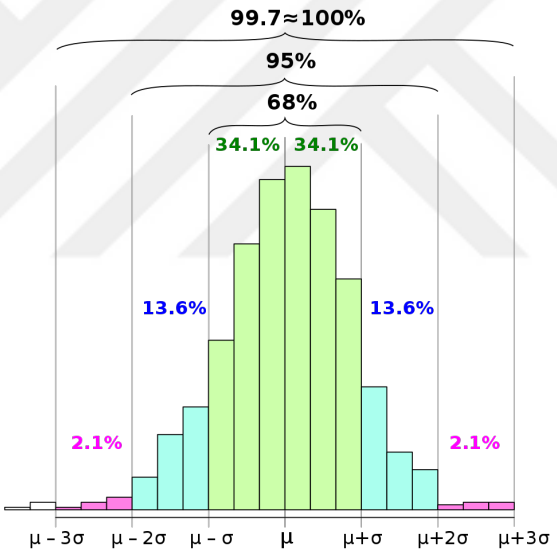

Figure 3.13. 68-95-99.7 Rule

The return period of an event is determined by the frequency of event that falls outside of $\mu \pm x\sigma$ range. The approximate expected frequency outside range is defined as:

$$1 \; in \; \frac{1}{1 - \text{erf}\left(\frac{x}{\sqrt{2}}\right)} \tag{3.17}$$

In this study, 1-year, 10-year, 30-year, 50-year and 100-year events are calculated. The mean and standard deviation of each Gaussian component of bimodal daily temperature histogram for the past and the future are found. 2 Gaussian components in bimodal distribution for the past and the future are defined as $\mathcal{N}(\mu_{cold}^{past}, \sigma_{cold}^{past})$ and $\mathcal{N}(\mu_{hot}^{past}, \sigma_{hot}^{past})$, $\mathcal{N}(\mu_{cold}^{future}, \sigma_{cold}^{future})$ and $\mathcal{N}(\mu_{hot}^{future}, \sigma_{hot}^{future})$, respectively. The data are of daily temperatures for 30 years, thus the number of days falls into a period in a year is needed for calculating the return periods. Using Equation 3.16, the number of days with temperatures higher than $\mu - \sigma$ is found to be approximately 83.14% of the total population as shown in Figure 3.14.

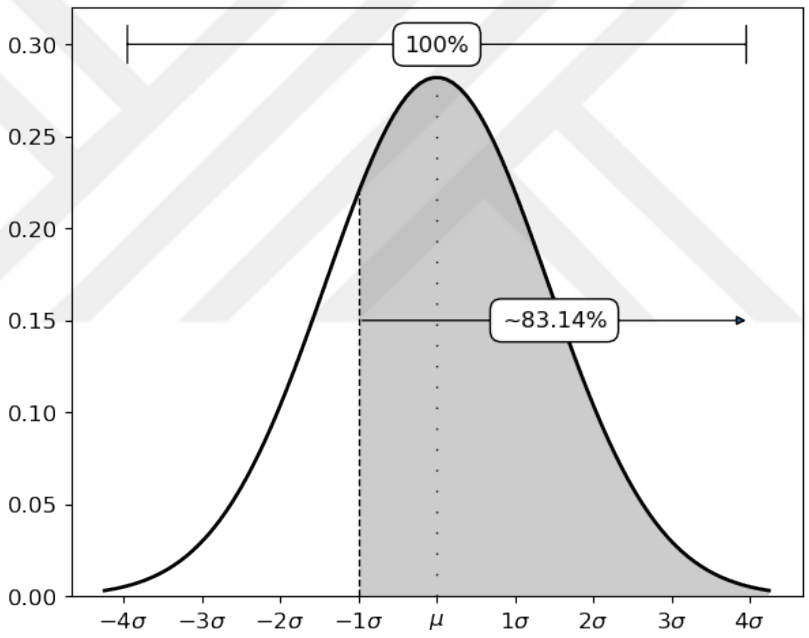

Figure 3.14. The population higher than $\mu - 1\sigma$ is ∼83.14% of total population

Then, total population of hot period in a year can be found. Let T is the set of days hotter than $\mu_{hot}^{past} - \sigma_{hot}^{past}$,

$$T = \{t : \ \forall t \geq \mu_{hot}^{past} - \sigma_{hot}^{past}\} \tag{3.18}$$

where t is the temperature of a day. T consists 30-year data.

Thus, the number of days in the normal distribution of hot period for a year is found as:

$$|\mathcal{N}(\mu_{hot}^{past}, \sigma_{hot}^{past})| = \frac{|T|}{15\left(1 + \text{erf}\left(\frac{1}{\sqrt{2}}\right)\right)} \tag{3.19}$$

where $|\mathcal{N}(\mu_{hot}^{past}, \sigma_{hot}^{past})|$ is the cardinality of the normal distribution for the past hot period in a year, $|T|$ is the cardinality of the set of days hotter than $\mu_{hot}^{past} - \sigma_{hot}^{past}$. In other words, length of a year is defined by $|\mathcal{N}(\mu_{hot}^{past}, \sigma_{hot}^{past})|$.

Then, expected frequency of n-year events, where the number of days in a year is defined as $|\mathcal{N}(\mu_{hot}^{past}, \sigma_{hot}^{past})|$, is calculated.

$$f_n^{past} = n \times |\mathcal{N}(\mu_{hot}^{past}, \sigma_{hot}^{past})| \tag{3.20}$$

where f_n^{past} is the expected frequency outside range and n is the number of year. For example, a city with $|\mathcal{N}(\mu_{hot}^{past}, \sigma_{hot}^{past})| = 170$ will have a frequency of 1-in-17,000 for a 100-year event. Then, Equation 3.17 is solved for the σ range of that event.

$$x^{past} = \text{erf}^{-1}\left(1 - \frac{1}{f_n}\right)\sqrt{2} \tag{3.21}$$

The temperature limit τ of n-year event can be calculated as,

$$\tau = \mu_{hot}^{past} + x^{past}\sigma_{hot}^{past} \tag{3.22}$$

Now, the change in n-year event in the future can be found by solving Equation 3.22, 3.21 and 3.20 backward using μ_{hot}^{future} and σ_{hot}^{future} for x^{future}, $f_{\dot{n}}^{future}$ and $\dot{n}$, respectively.

$$x^{future} = \frac{\tau - \mu_{hot}^{future}}{\sigma_{hot}^{future}} \tag{3.23}$$

$$f_{\dot{n}}^{future} = \frac{1}{1 - \text{erf}\left(\frac{x^{future}}{\sqrt{2}}\right)} \tag{3.24}$$

$$\dot{n} = \frac{f_{\dot{n}}^{future}}{|\mathcal{N}(\mu_{hot}^{future}, \sigma_{hot}^{future})|} \tag{3.25}$$

where $\dot{n}$ is the changed value of n-year event.

4. RESULTS

4.1. Alexandria

Alexandria is the second largest city in Egypt with a population of 5,086,000 in 2018 [5]. It is located on the Mediterranean coast where the Nile flows into the sea. Its location near water masses causes the city to be vulnerable against sea level rise due to its low elevation. Alexandria has an arid desert hot climate BWh according to Köppen-Geiger climate classification as shown in Figure 3.11. Also, the Mediterranean Sea affects the city's climate by moderating its temperatures and causing rainy winters. Alexandria's daily maximum temperature histogram shows a bimodal distribution in 1971-2000 and 2070-2099 periods for both MPI-ESM-MR and HadGEM2-ES dataset for both RCP4.5 and RCP8.5 scenarios.

For MPI-ESM-MR RCP4.5 dataset, parameters of the Gaussians are $\mu_{cold}^{past} = 18.08°C$, $\sigma_{cold}^{past} = 3.4°C$ for the cold side, $\mu_{hot}^{past} = 29.58°C$, $\sigma_{hot}^{past} = 3.43°C$ for the hot side in 1971-2000 curve. Between 2070-2099, parameters are $\mu_{cold}^{future} = 20.02°C$, $\sigma_{cold}^{future} = 3.47°C$ for the cold side, $\mu_{hot}^{future} = 31.62°C$, $\sigma_{hot}^{future} = 3.48°C$ for the hot side. The peaks will diverge about 0.09°C from each other in the future with respect to 1971-2000 as shown in Figure 4.1, which will further increase the occurrence of extreme events. The hot period has 199.2 days in the past as shown in Table 4.1 and taken as the length of a year. Then, 1-year, 10-year, 30-year, 50-year and 100-year temperature events are calculated for the future that they would be seen in every 0.179, 1.181, 2.957, 4.545 and 8.167 years, respectively. This means that a 1-year temperature would be seen once in every month, a 10-year temperature would be seen once in every year, a 30-year temperature would be seen once in every 3 years, a 50-year temperature would be seen once in every 5 years, and a 100-year temperature would be seen once in every 8 years. Additional variables are given in Table 4.1.

For HADGEM2-ES RCP4.5 dataset, parameters of the Gaussians are $\mu_{cold}^{past} = 17.84°C$, $\sigma_{cold}^{past} = 3.43°C$ for the cold side, $\mu_{hot}^{past} = 29.85°C$, $\sigma_{hot}^{past} = 3.68°C$ for the hot

side in 1971-2000 curve. For 2070-2099, parameters are $\mu_{cold}^{future} = 20.5°C$, $\sigma_{cold}^{future} = 3.55°C$ for the cold side, $\mu_{hot}^{future} = 33.41°C$, $\sigma_{hot}^{future} = 3.91°C$ for the hot side. Also, the peaks will diverge about 0.89°C from each other in the future with respect to 1971-2000 as shown in Figure 4.1, which will further increase the occurrence of extreme events. The hot period has 192.9 days in the past as shown in Table 4.5 and taken as the length of a year. Then, 1-year, 10-year, 30-year, 50-year and 100-year temperature events are calculated for the future that they would be seen in every 0.062, 0.285, 0.606, 0.864 and 1.404 years, respectively. This means that a 1-year temperature would be seen once in every 11.8 days, a 10-year temperature would be seen once in every 2 months, a 30-year temperature would be seen twice in every year, a 50-year temperature would be seen once in every years and a 100-year temperature would be seen twice in every 3 years. Additional variables are given in Table 4.5.

For MPI-ESM-MR RCP8.5 dataset, parameters of the Gaussians are $\mu_{cold}^{past} = 18.08°C$, $\sigma_{cold}^{past} = 3.4°C$ for the cold side, $\mu_{hot}^{past} = 29.58°C$, $\sigma_{hot}^{past} = 3.44°C$ for the hot side in 1971-2000 curve. Between 2070-2099, parameters are $\mu_{cold}^{future} = 21.44°C$, $\sigma_{cold}^{future} = 3.79°C$ for the cold side, $\mu_{hot}^{future} = 33.61°C$, $\sigma_{hot}^{future} = 3.74°C$ for the hot side. Also, the peaks will diverge about 0.67°C from each other in the future with respect to 1971-2000 as shown in Figure 4.1, which will further increase the occurrence of extreme events. The hot period has 199.3 days in the past as shown in Table 4.3 and taken as the length of a year. Then, 1-year, 10-year, 30-year, 50-year and 100-year temperature events are calculated for the future that they would be seen in every 0.039, 0.151, 0.298, 0.411 and 0.636 years, respectively. This means that a 1-year temperature would be seen once in every week, a 10-year temperature would be seen once in every month, a 30-year temperature would be seen once in every 2 months, a 50-year temperature would be seen 3 times in every year, a 100-year temperature would be seen twice in every year. Additional variables are given in Table 4.3.

For HADGEM2-ES RCP8.5 dataset, parameters of the Gaussians are $\mu_{cold}^{past} = 17.85°C$, $\sigma_{cold}^{past} = 3.44°C$ for the cold side, $\mu_{hot}^{past} = 29.86°C$, $\sigma_{hot}^{past} = 3.68°C$ for the hot side in 1971-2000 curve. For 2070-2099, parameters are $\mu_{cold}^{future} = 24.73°C$, $\sigma_{cold}^{future} = 3.89°C$ for the cold side, $\mu_{hot}^{future} = 36.82°C$, $\sigma_{hot}^{future} = 3.75°C$ for the hot side. The peak

diverge is about 0.09°C from each other in the future with respect to 1971-2000. The hot period has 192.7 days in the past as shown in Table 4.7 and taken as the length of a year. Then, 1-year, 10-year, 30-year, 50-year and 100-year temperature events are calculated for the future that they would be seen in every 0.014, 0.043, 0.077, 0.102 and 0.151 years, respectively. This means that a 1-year temperature would be seen once in every 2.7 days, a 10-year temperature would be seen once in every week, a 30-year temperature would be seen once in every 2 weeks, a 50-year temperature would be seen once in every 19.5 days, a 100-year temperature would be seen once in every month. Additional variables are given in Table 4.7.

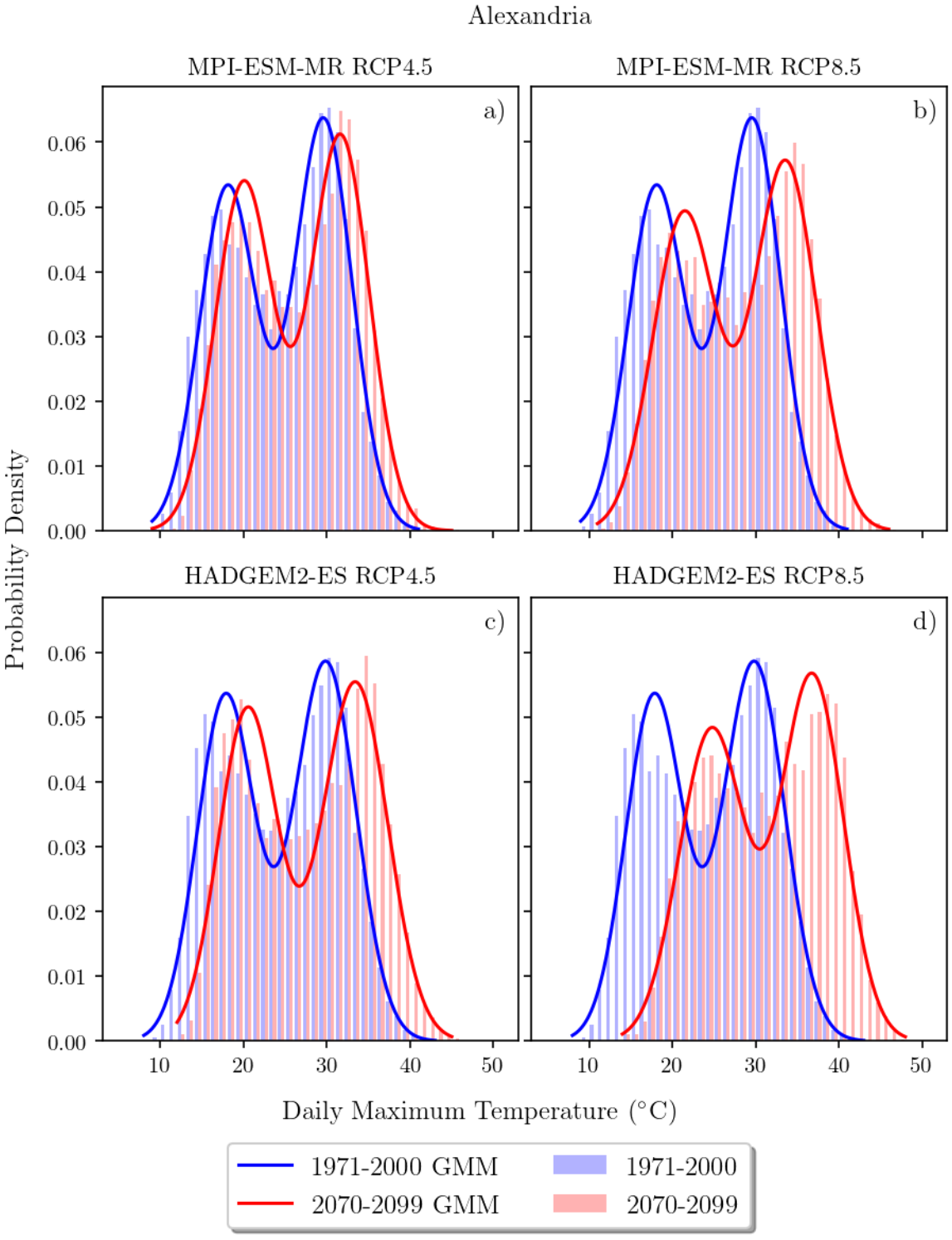

Figure 4.1. Alexandria Daily Maximum Temperatures histogram at sea level for 1971-2000 and 2070-2099 and corresponding Gaussian Mixture Model fits: (a) MPI-ESM-MR RCP4.5, (b) MPI-ESM-MR RCP8.5, (c)HadGEM2-ES RCP4.5, (d) HadGEM2-ES RCP8.5

4.2. Algiers

Algiers is the capital of Algeria. Its population of urban agglomeration is 2,694,000 in 2018 [5]. Algiers has a temperate dry hot summer *Csa* climate according to Köppen-Geiger classification 3.11. The city's climate is influenced by the Mediterranean Sea. This effects the city's climate and moderate its temperatures. Algires' daily maximum temperature histogram shows a bimodal distribution in 1971-2000 and 2070-2099 periods for both MPI-ESM-MR and HadGEM2-ES dataset for both RCP4.5 and RCP8.5 scenarios.

For MPI-ESM-MR RCP4.5 dataset, parameters of the Gaussians are $\mu_{cold}^{past} = 15.42°C$, $\sigma_{cold}^{past} = 3.4°C$ for the cold side, $\mu_{hot}^{past} = 27.4°C$, $\sigma_{hot}^{past} = 4.56°C$ for the hot side in 1971-2000 curve. Between 2070-2099, parameters are $\mu_{cold}^{future} = 17.15°C$, $\sigma_{cold}^{future} = 3.53°C$ for the cold side, $\mu_{hot}^{future} = 29.72°C$, $\sigma_{hot}^{future} = 4.65°C$ for the hot side. The peaks will diverge about 0.59°C from each other in the future with respect to 1971-2000 as seen in Figure 4.2 according to 1971-2000 base., which will further increase the occurrence of extreme events. The hot period has 168.6 days in the past as shown in Table 4.1 and taken as the length of a year. Then, 1-year, 10-year, 30-year, 50-year and 100-year temperature events are calculated for the length of future hot period that they would be seen in every 0.218, 1.486, 3.767, 5.821 and 10.531 years, respectively. This means that a 1-year temperature would be seen once in every month, a 10-year temperature would be seen twice in every 3 years, a 30-year temperature would be seen once in every 4 years, a 50-year temperature would be seen once in every 6 years, a 100-year temperature would be seen once in every 10 years. Additional variables are given in Table 4.1.

For HADGEM2-ES RCP4.5 dataset, parameters of the Gaussians are $\mu_{cold}^{past} = 15.21°C$, $\sigma_{cold}^{past} = 3.42°C$ for the cold side, $\mu_{hot}^{past} = 27.25°C$, $\sigma_{hot}^{past} = 3.93°C$ for the hot side in 1971-2000 curve. For 2070-2099, parameters are $\mu_{cold}^{future} = 17.7°C$, $\sigma_{cold}^{future} = 3.7°C$ for the cold side, $\mu_{hot}^{future} = 31.44°C$, $\sigma_{hot}^{future} = 4.35°C$ for the hot side. The peaks will diverge about 1.7°C from each other in the future with respect to 1971-2000 as shown in Figure 4.2, which will further increase the occurrence of extreme events.

The hot period has 147.1 days in the past as shown in Table 4.5 and taken as the length of a year. Then, 1-year, 10-year, 30-year, 50-year and 100-year temperature events are calculated for the length of future hot period that they would be seen in every 0.046, 0.184, 0.362, 0.499 and 0.773 years, respectively. This means that a 1-year temperature would be seen once in every week, a 10-year temperature would be seen once in every month, a 30-year temperature would be seen once in every 2 months, a 50-year temperature would be seen twice in every year, a 100-year temperature would be seen 3 times in every 2 years. Additional variables are given in Table 4.5.

For MPI-ESM-MR RCP8.5 dataset, parameters of the Gaussians are $\mu_{cold}^{past} = 15.42°C$, $\sigma_{cold}^{past} = 3.4°C$ for the cold side, $\mu_{hot}^{past} = 27.4°C$, $\sigma_{hot}^{past} = 4.57°C$ for the hot side in 1971-2000 curve. Between 2070-2099, parameters are $\mu_{cold}^{future} = 19.11°C$, $\sigma_{cold}^{future} = 3.82°C$ for the cold side, $\mu_{hot}^{future} = 32.21°C$, $\sigma_{hot}^{future} = 4.93°C$ for the hot side. The peaks will diverge about 1.11°C from each other in the future with respect to 1971-2000 as shown in Figure 4.2, which will further increase the occurrence of extreme events. The hot period has 168.6 days in the past as shown in Table 4.3 and taken as the length of a year. Then, 1-year, 10-year, 30-year, 50-year and 100-year temperature events are calculated for the length of future hot period that they would be seen in every 0.049, 0.207, 0.421, 0.588 and 0.93 years, respectively. This means that a 1-year temperature would be seen once in every 8.6 days, a 10-year temperature would be seen once in every month, a 30-year temperature would be seen twice in every year, a 50-year temperature would be seen 3 times in every 2 years, a 100-year temperature would be seen once in every year. Additional variables are given in Table 4.3.

For HADGEM2-ES RCP8.5 dataset, parameters of the Gaussians are $\mu_{cold}^{past} = 15.21°C$, $\sigma_{cold}^{past} = 3.42°C$ for the cold side, $\mu_{hot}^{past} = 27.25°C$, $\sigma_{hot}^{past} = 3.93°C$ for the hot side in 1971-2000 curve. For 2070-2099, parameters are $\mu_{cold}^{future} = 21.64°C$, $\sigma_{cold}^{future} = 4.24°C$ for the cold side, $\mu_{hot}^{future} = 36.3°C$, $\sigma_{hot}^{future} = 4.46°C$ for the hot side. The peaks will diverge about 2.62°C from each other in the future with respect to 1971-2000 as shown in Figure 4.2, which will further increase the occurrence of extreme events. The hot period has 147.1 days in the past as shown in Table 4.7 and taken as

the length of a year. Then, 1-year, 10-year, 30-year, 50-year and 100-year temperature events are calculated for the length of future hot period that they would be seen in every 0.009, 0.018, 0.028, 0.034 and 0.045 years, respectively. This means that a 1-year temperature would be seen twice in every 3 days, a 10-year temperature would be seen once in every 3 days, a 30-year temperature would be seen once in every 4.5 days, a 50-year temperature would be seen once in every 5.5 days, a 100-year temperature would be seen once in every week. Additional variables are given in Table 4.7.

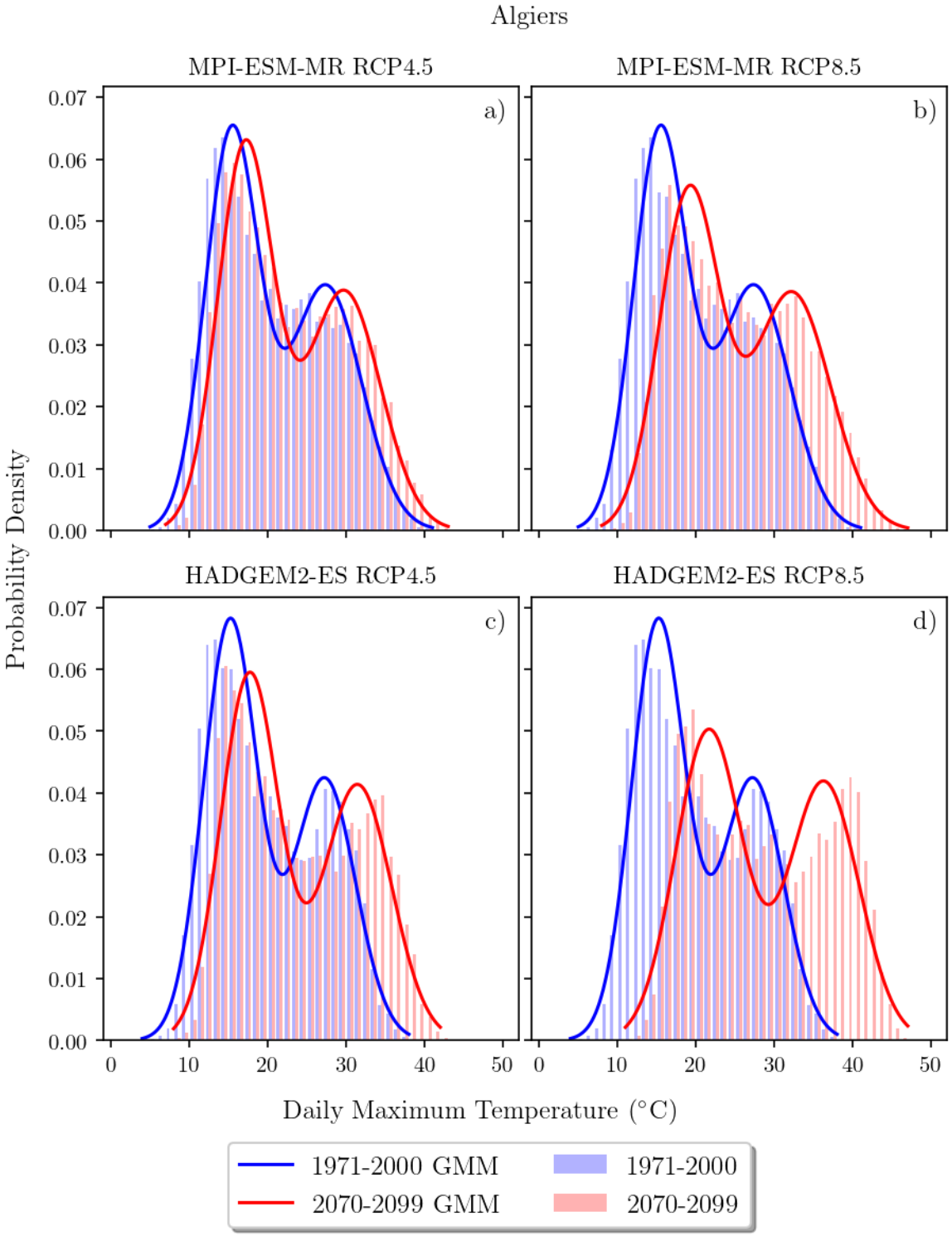

Figure 4.2. Algiers Daily Maximum Temperatures histogram at sea level for 1971-2000 and 2070-2099 and corresponding Gaussian Mixture Model fits: (a) MPI-ESM-MR RCP4.5, (b) MPI-ESM-MR RCP8.5, (c) HadGEM2-ES RCP4.5, (d) HadGEM2-ES RCP8.5

4.3. Amman

Amman is the capital of Jordan and has a population in urban agglomeration of 2,065,000 in 2018. Its mountainous terrain and high elevation affect its climate. Surrounding mountains prevents moderating effect of the Mediterranean Sea. Amman has an arid steppe hot climate *BSh* according to Köppen-Geiger classification as summers are hot and breezy and winters are moderate.

For MPI-ESM-MR RCP4.5 dataset, parameters of the Gaussians are $\mu_{cold}^{past} = 18.76°C$, $\sigma_{cold}^{past} = 5.02°C$ for the cold side, $\mu_{hot}^{past} = 34.79°C$, $\sigma_{hot}^{past} = 4.88°C$ for the hot side in 1971-2000 curve. Between 2070-2099, parameters are $\mu_{cold}^{future} = 20.81°C$, $\sigma_{cold}^{future} = 5.33°C$ for the cold side, $\mu_{hot}^{future} = 37.26°C$, $\sigma_{hot}^{future} = 4.95°C$ for the hot side. The mean temperatures will increase as shown in Figure 4.3 according to 1971-2000 base. Also, the peaks will diverge about 0.41°C from each other in the future with respect to 1971-2000, which will further increase the occurrence of extreme events. The hot period has 206.9 days in the past as shown in Table 4.1 and taken as the length of a year. Then, 1-year, 10-year, 30-year, 50-year and 100-year temperature events are calculated for the length of future hot period that they would be seen in every 0.215, 1.483, 3.784, 5.863 and 10.647 years, respectively. This means that a 1-year temperature would be seen 5 times in every year, a 10-year temperature would be seen twice in every 3 years, a 30-year temperature would be seen once in every 4 years, a 50-year temperature would be seen once in every 6 years, a 100-year temperature would be seen once in every 10 years. Additional variables are given in Table 4.1.

For HADGEM2-ES RCP4.5 dataset, parameters of the Gaussians are $\mu_{cold}^{past} = 18.57°C$, $\sigma_{cold}^{past} = 4.94°C$ for the cold side, $\mu_{hot}^{past} = 34.07°C$, $\sigma_{hot}^{past} = 4.51°C$ for the hot side in 1971-2000 curve. For 2070-2099, parameters are $\mu_{cold}^{future} = 21.53°C$, $\sigma_{cold}^{future} = 5.16°C$ for the cold side, $\mu_{hot}^{future} = 38.21°C$, $\sigma_{hot}^{future} = 4.58°C$ for the hot side. The peaks will diverge about 1.18°C from each other in the future with respect to 1971-2000 as shown in Figure 4.3, which will further increase the occurrence of extreme events. The hot period has 191.4 days in the past as shown in Table 4.5 and taken as the length of a year. Then, 1-year, 10-year, 30-year, 50-year and 100-year temperature

events are calculated for the length of future hot period that they would be seen in every 0.08, 0.434, 0.997, 1.474 and 2.515 years, respectively. This means that a 1-year temperature would be seen once in every 15.4 days, a 10-year temperature would be seen twice in every year, a 30-year temperature would be seen once in every year, a 50-year temperature would be seen twice in every 3 years, a 100-year temperature would be seen twice in every 5 years. Additional variables are given in Table 4.5.

For MPI-ESM-MR RCP8.5 dataset, parameters of the Gaussians are $\mu_{cold}^{past} = 18.79°C$, $\sigma_{cold}^{past} = 5.04°C$ for the cold side, $\mu_{hot}^{past} = 34.81°C$, $\sigma_{hot}^{past} = 4.86°C$ for the hot side in 1971-2000 curve. Between 2070-2099, parameters are $\mu_{cold}^{future} = 22.44°C$, $\sigma_{cold}^{future} = 5.73°C$ for the cold side, $\mu_{hot}^{future} = 39.63°C$, $\sigma_{hot}^{future} = 5.04°C$ for the hot side. The peaks will diverge about 1.16°C from each other in the future with respect to 1971-2000 as shown in Figure 4.3, which will further increase the occurrence of extreme events. The hot period has 206.5 days in the past as shown in Table 4.3 and taken as the length of a year. Then, 1-year, 10-year, 30-year, 50-year and 100-year temperature events are calculated for the length of future hot period that they would be seen in every 0.063, 0.31, 0.678, 0.98 and 1.624 years, respectively. This means that a 1-year temperature would be seen once in every 12.8 days, a 10-year temperature would be seen 3 times in every year, a 30-year temperature would be seen 3 times in every 2 years, a 50-year temperature would be seen once in every year, a 100-year temperature would be seen twice in every 3 years. Additional variables are given in Table 4.3.

For HADGEM2-ES RCP8.5 dataset, parameters of the Gaussians are $\mu_{cold}^{past} = 18.57°C$, $\sigma_{cold}^{past} = 4.94°C$ for the cold side, $\mu_{hot}^{past} = 34.07°C$, $\sigma_{hot}^{past} = 4.51°C$ for the hot side in 1971-2000 curve. For 2070-2099, parameters are $\mu_{cold}^{future} = 25.75°C$, $\sigma_{cold}^{future} = 5.71°C$ for the cold side, $\mu_{hot}^{future} = 42.63°C$, $\sigma_{hot}^{future} = 4.99°C$ for the hot side. The mean temperatures will increase as shown in Figure 4.3 according to 1971-2000 base. Also, the peaks will diverge about 1.37°C from each other in the future with respect to 1971-2000, which will further increase the occurrence of extreme events. The hot period has 191.4 days in the past as shown in Table 4.7 and taken as the length of a year. Then, 1-year, 10-year, 30-year, 50-year and 100-year temperature events are

calculated for the length of future hot period that they would be seen in every 0.012, 0.033, 0.056, 0.071 and 0.099 years, respectively. This means that a 1-year temperature would be seen once in every 2.4 days, a 10-year temperature would be seen once in every week, a 30-year temperature would be seen 3 times in every month, a 50-year temperature would be seen once in every two weeks, a 100-year temperature would be seen once in every 19 days. Additional variables are given in Table 4.7.

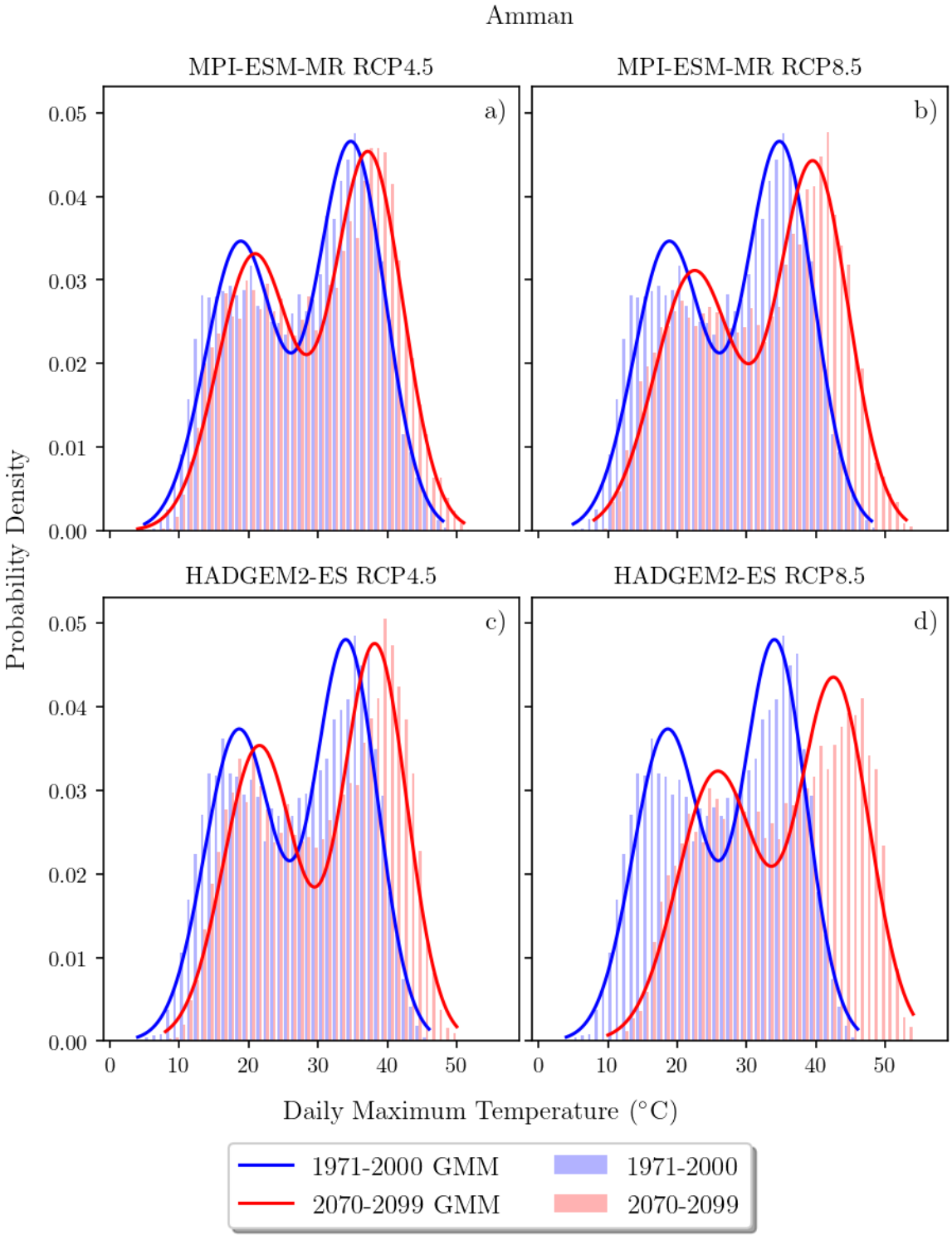

Figure 4.3. Amman Daily Maximum Temperatures histogram at sea level for 1971-2000 and 2070-2099 and corresponding Gaussian Mixture Model fits: (a) MPI-ESM-MR RCP4.5, (b) MPI-ESM-MR RCP8.5, (c) HadGEM2-ES RCP4.5, (d) HadGEM2-ES RCP8.5

4.4. Baghdad

The capital of Iraq is located on the Tigris riverbed which splits the city in half. Thus, city lies on almost flat and low-lying land. The climate of Baghdad is arid hot desert *Bwh* according to Köppen-Geiger classification as shown in Figure 3.11 with extremely hot, dry summers and mild winters. Urban agglomeration of the city is 6,812,00 in 2018 [5].

For MPI-ESM-MR RCP4.5 dataset, parameters of the Gaussians are $\mu_{cold}^{past} = 18.66°C$, $\sigma_{cold}^{past} = 5.81°C$ for the cold side, $\mu_{hot}^{past} = 39.11°C$, $\sigma_{hot}^{past} = 5.28°C$ for the hot side in 1971-2000 curve. Between 2070-2099, parameters are $\mu_{cold}^{future} = 20.81°C$, $\sigma_{cold}^{future} = 6.33°C$ for the cold side, $\mu_{hot}^{future} = 41.99°C$, $\sigma_{hot}^{future} = 5.31°C$ for the hot side. The peaks will diverge about 0.73°C from each other in the future with respect to 1971-2000 as shown in Figure 4.4, which will further increase the occurrence of extreme events. The hot period has 185.1 days in the past as shown in Table 4.1 and taken as the length of a year. Then, 1-year, 10-year, 30-year, 50-year and 100-year temperature events are calculated for the length of future hot period that they would be seen in every 0.205, 1.421, 3.64, 5.654 and 10.303 years, respectively. This means that a 1-year temperature would be seen 5 times in every year, a 10-year temperature would be seen twice in every 3 years, a 30-year temperature would be seen once in every 3.6 years, a 50-year temperature would be seen once in every 5.6 years, a 100-year temperature would be seen once in every 10 years. Additional variables are given in Table 4.1.

For HADGEM2-ES RCP4.5 dataset, parameters of the Gaussians are $\mu_{cold}^{past} = 18.14°C$, $\sigma_{cold}^{past} = 5.75°C$ for the cold side, $\mu_{hot}^{past} = 38.19°C$, $\sigma_{hot}^{past} = 5.34°C$ for the hot side in 1971-2000 curve. For 2070-2099, parameters are $\mu_{cold}^{future} = 21.11°C$, $\sigma_{cold}^{future} = 6.31°C$ for the cold side, $\mu_{hot}^{future} = 42.62°C$, $\sigma_{hot}^{future} = 4.97°C$ for the hot side. The peaks will diverge about 1.45°C from each other in the future with respect to 1971-2000 as shown in Figure 4.4, which will further increase the occurrence of extreme events. The hot period has 174.3 days in the past as shown in Table 4.5 and taken as the length of a year. Then, 1-year, 10-year, 30-year, 50-year and 100-year temperature events are

calculated for the length of future hot period that they would be seen in every 0.152, 1.154, 3.137, 5.021 and 9.556 years, respectively. This means that a 1-year temperature would be seen once in every month, a 10-year temperature would be seen once in every year, a 30-year temperature would be seen once in every 3 years, a 50-year temperature would be seen once in every 5 years, a 100-year temperature would be seen once in every 10 years. Additional variables are given in Table 4.5.

For MPI-ESM-MR RCP8.5 dataset, parameters of the Gaussians are $\mu_{cold}^{past} = 18.66°C$, $\sigma_{cold}^{past} = 5.81°C$ for the cold side, $\mu_{hot}^{past} = 39.11°C$, $\sigma_{hot}^{past} = 5.28°C$ for the hot side in 1971-2000 curve. Between 2070-2099, parameters are $\mu_{cold}^{future} = 22.29°C$, $\sigma_{cold}^{future} = 6.58°C$ for the cold side, $\mu_{hot}^{future} = 44.38°C$, $\sigma_{hot}^{future} = 5.59°C$ for the hot side. The peaks will diverge about 1.64°C from each other in the future with respect to 1971-2000 as shown in Figure 4.4, which will further increase the occurrence of extreme events. The hot period has 185.1 days in the past as shown in Table 4.3 and taken as the length of a year. Then, 1-year, 10-year, 30-year, 50-year and 100-year temperature events are calculated for the length of future hot period that they would be seen in every 0.059, 0.269, 0.569, 0.81 and 1.314 years, respectively. This means that a 1-year temperature would be seen once in every 11 days, a 10-year temperature would be seen 5 times in every year, a 30-year temperature would be seen twice in every year, a 50-year temperature would be seen once in every year, a 100-year temperature would be seen 4 times in every 3 years. Additional variables are given in Table 4.3.

For HADGEM2-ES RCP8.5 dataset, parameters of the Gaussians are $\mu_{cold}^{past} = 18.13°C$, $\sigma_{cold}^{past} = 5.75°C$ for the cold side, $\mu_{hot}^{past} = 38.19°C$, $\sigma_{hot}^{past} = 5.34°C$ for the hot side in 1971-2000 curve. For 2070-2099, parameters are $\mu_{cold}^{future} = 26.04°C$, $\sigma_{cold}^{future} = 6.19°C$ for the cold side, $\mu_{hot}^{future} = 46.69°C$, $\sigma_{hot}^{future} = 5.6°C$ for the hot side. The peaks will diverge about 0.58°C from each other in the future with respect to 1971-2000 as shown in Figure 4.4, which will further increase the occurrence of extreme events. The hot period has 174.4 days in the past as shown in Table 4.7 and taken as the length of a year. Then, 1-year, 10-year, 30-year, 50-year and 100-year temperature events are calculated for the length of future hot period that they would be seen in every 0.022, 0.075, 0.14, 0.189 and 0.284 years, respectively. This means that a 1-year temperature

would be seen once in every 4 days, a 10-year temperature would be seen once in every 2 weeks, a 30-year temperature would be seen once in every 24.4 days, a 50-year temperature would be seen once in every month, a 100-year temperature would be seen 5 times in every year. Additional variables are given in Table 4.7.

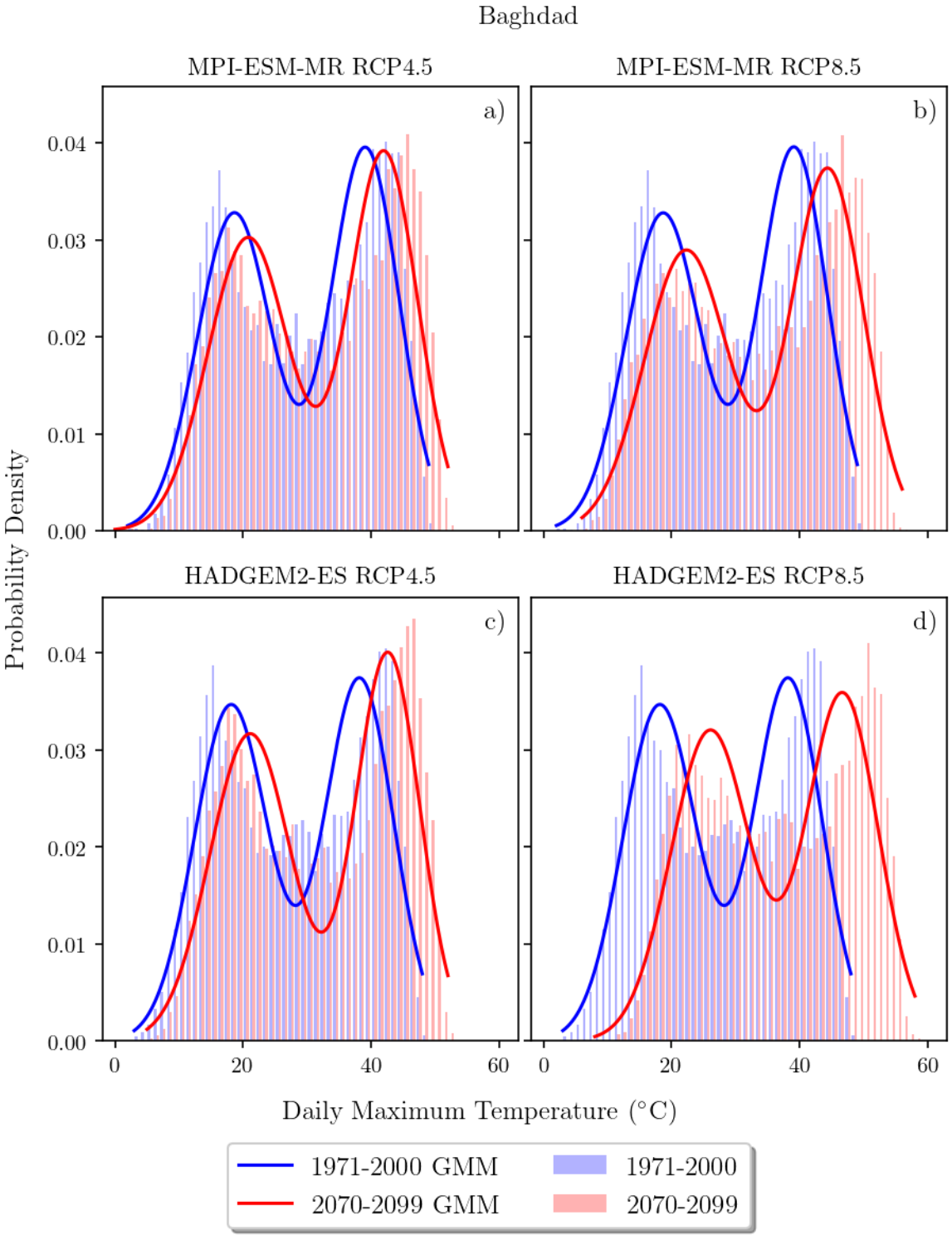

Figure 4.4. Baghdad Daily Maximum Temperatures histogram at sea level for 1971-2000 and 2070-2099 and corresponding Gaussian Mixture Model fits: (a) MPI-ESM-MR RCP4.5, (b) MPI-ESM-MR RCP8.5, (c) HadGEM2-ES RCP4.5, (d) HadGEM2-ES RCP8.5

4.5. Basrah

Basrah is the economic capital of Iraq located on the Shatt-Al-Arab waterway with an urban agglomeration of 1,299,000 in 2018. Complex network of canals and streams of the city are of value for agricultural use. The city has an arid hot desert *Bwh* climate according to Köppen-Gieger classification with slightly more precipitation due to its location near the coast.

For MPI-ESM-MR RCP4.5 dataset, parameters of the Gaussians are $\mu_{cold}^{past} = 20.98°C$, $\sigma_{cold}^{past} = 5.77°C$ for the cold side, $\mu_{hot}^{past} = 40.35°C$, $\sigma_{hot}^{past} = 4.87°C$ for the hot side in 1971-2000 curve. Between 2070-2099, parameters are $\mu_{cold}^{future} = 23.0°C$, $\sigma_{cold}^{future} = 6.17°C$ for the cold side, $\mu_{hot}^{future} = 43.15°C$, $\sigma_{hot}^{future} = 4.81°C$ for the hot side. The peaks will diverge about 0.78°C from each other in the future with respect to 1971-2000 as shown in Figure 4.5, which will further increase the occurrence of extreme events. The hot period has 183.3 days in the past as shown in Table 4.1 and taken as the length of a year. Then, 1-year, 10-year, 30-year, 50-year and 100-year temperature events are calculated for the length of future hot period that they would be seen in every 0.211, 1.538, 4.037, 6.344 and 11.751 years, respectively. This means that a 1-year temperature would be seen once in every 38.8 days, a 10-year temperature would be seen twice in every 3 years, a 30-year temperature would be seen once in every 4 years, a 50-year temperature would be seen once in every 6 years, a 100-year temperature would be seen once in every 12 years. Additional variables are given in Table 4.1.

For HADGEM2-ES RCP4.5 dataset, parameters of the Gaussians are $\mu_{cold}^{past} = 20.19°C$, $\sigma_{cold}^{past} = 5.77°C$ for the cold side, $\mu_{hot}^{past} = 39.92°C$, $\sigma_{hot}^{past} = 4.84°C$ for the hot side in 1971-2000 curve. For 2070-2099, parameters are $\mu_{cold}^{future} = 23.93°C$, $\sigma_{cold}^{future} = 6.83°C$ for the cold side, $\mu_{hot}^{future} = 44.88°C$, $\sigma_{hot}^{future} = 4.12°C$ for the hot side. The peaks will diverge about 1.22°C from each other in the future with respect to 1971-2000 as shown in Figure 4.5, which will further increase the occurrence of extreme events. The hot period has 173.0 days in the past as shown in Table 4.5 and taken as the length of a year. Then, 1-year, 10-year, 30-year, 50-year and 100-year temperature

events are calculated for the length of future hot period that they would be seen in every 0.149, 1.377, 4.181, 7.068 and 14.525 years, respectively. This means that a 1-year temperature would be seen once in every 24.2 days, a 10-year temperature would be seen twice in every 3 years, a 30-year temperature would be seen once in every 4 years, a 50-year temperature would be seen once in every 7 years, a 100-year temperature would be seen once in every 15 years. Additional variables are given in Table 4.5.

For MPI-ESM-MR RCP8.5 dataset, parameters of the Gaussians are $\mu_{cold}^{past} = 20.98°C$, $\sigma_{cold}^{past} = 5.77°C$ for the cold side, $\mu_{hot}^{past} = 40.35°C$, $\sigma_{hot}^{past} = 4.87°C$ for the hot side in 1971-2000 curve. Between 2070-2099, parameters are $\mu_{cold}^{future} = 24.71°C$, $\sigma_{cold}^{future} = 6.5°C$ for the cold side, $\mu_{hot}^{future} = 45.4°C$, $\sigma_{hot}^{future} = 5.13°C$ for the hot side. The peaks will diverge about 1.32°C from each other in the future with respect to 1971-2000 as shown in Figure 4.5, which will further increase the occurrence of extreme events. The hot period has 183.3 days in the past as shown in Table 4.3 and taken as the length of a year. Then, 1-year, 10-year, 30-year, 50-year and 100-year temperature events are calculated for the length of future hot period that they would be seen in every 0.054, 0.246, 0.518, 0.737 and 1.192 years, respectively. This means that a 1-year temperature would be seen once in every 10 days, a 10-year temperature would be seen 5 times in every year, a 30-year temperature would be seen twice in every year, a 50-year temperature would be seen 3 times in every 2 years, a 100-year temperature would be seen 5 times in every 6 years. Additional variables are given in Table 4.3.

For HADGEM2-ES RCP8.5 dataset, parameters of the Gaussians are $\mu_{cold}^{past} = 20.18°C$, $\sigma_{cold}^{past} = 5.77°C$ for the cold side, $\mu_{hot}^{past} = 39.92°C$, $\sigma_{hot}^{past} = 4.85°C$ for the hot side in 1971-2000 curve. For 2070-2099, parameters are $\mu_{cold}^{future} = 28.28°C$, $\sigma_{cold}^{future} = 6.13°C$ for the cold side, $\mu_{hot}^{future} = 47.79°C$, $\sigma_{hot}^{future} = 4.64°C$ for the hot side. The peaks will converge about -0.23°C to each other in the future with respect to 1971-2000 as shown in Figure 4.5. The hot period has 173.1 days in the past as shown in Table 4.7 and taken as the length of a year. Then, 1-year, 10-year, 30-year, 50-year and 100-year temperature events are calculated for the length of future hot period that they would be seen in every 0.025, 0.104, 0.214, 0.302 and 0.487 years, respectively. This means

that a 1-year temperature would be seen once in every 4 days, a 10-year temperature would be seen once in every 2 weeks, a 30-year temperature would be seen once in every month, a 50-year temperature would be seen 3 times in every year, a 100-year temperature would be seen twice in every year. Additional variables are given in Table 4.7.

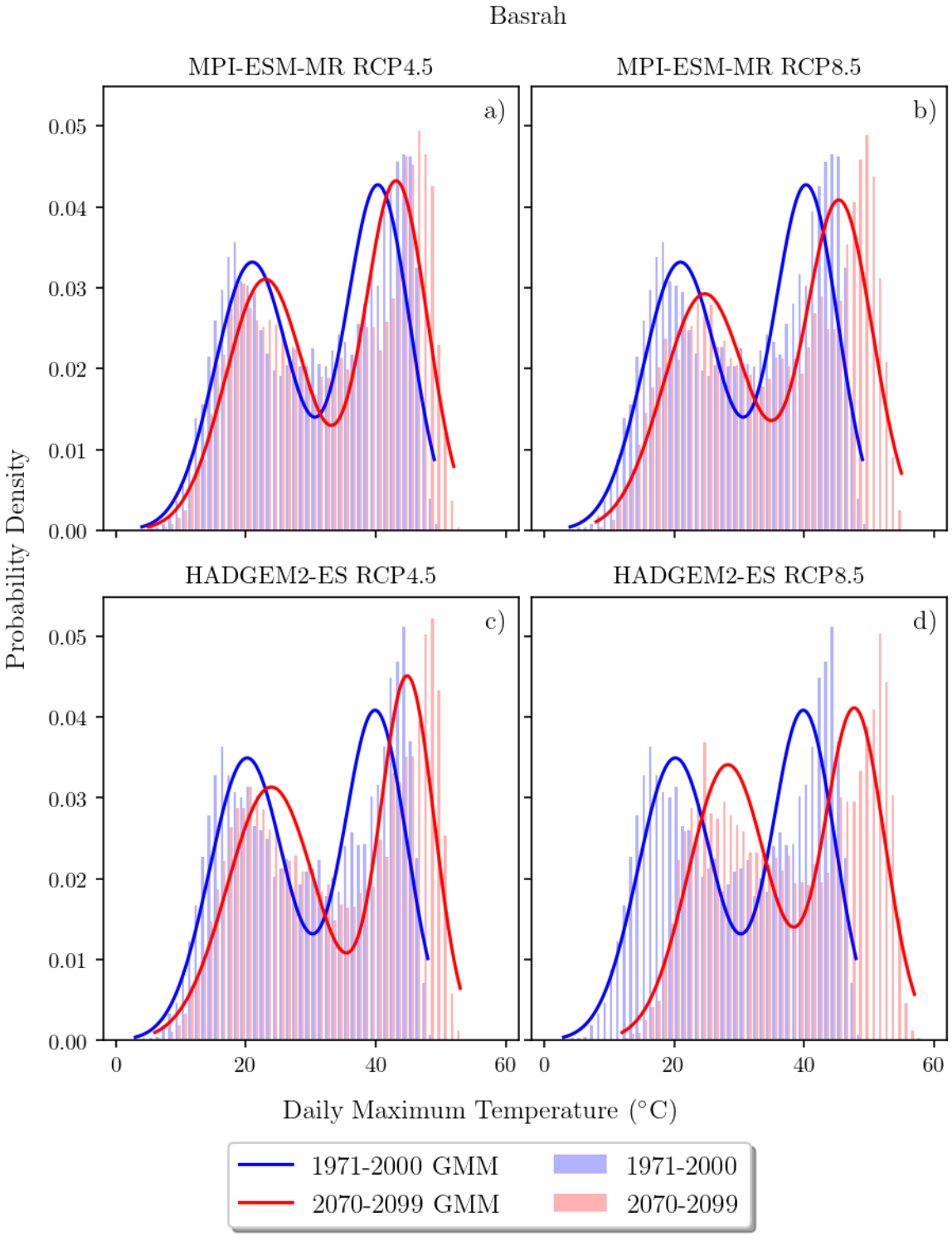

Figure 4.5. Basrah Daily Maximum Temperatures histogram at sea level for 1971-2000 and 2070-2099 and corresponding Gaussian Mixture Model fits: (a) MPI-ESM-MR RCP4.5, (b) MPI-ESM-MR RCP8.5, (c) HadGEM2-ES RCP4.5, (d) HadGEM2-ES RCP8.5

4.6. Cairo

Cairo is the capital of Egypt with an urban agglomeration of 20,076,000 in 2018. The city is located along the Nile River in Lower Egypt. The city has an arid hot desert climate BWh according to Köppen-Geiger classification as shown in Figure 3.11. Frequent windstorms brings Saharan dust into city which decreases the air quality and the air is often very dry.

For MPI-ESM-MR RCP4.5 dataset, parameters of the Gaussians are $\mu_{cold}^{past} = 19.83°C$, $\sigma_{cold}^{past} = 4.41°C$ for the cold side, $\mu_{hot}^{past} = 34.94°C$, $\sigma_{hot}^{past} = 4.22°C$ for the hot side in 1971-2000 curve. Between 2070-2099, parameters are $\mu_{cold}^{future} = 22.14°C$, $\sigma_{cold}^{future} = 4.75°C$ for the cold side, $\mu_{hot}^{future} = 37.45°C$, $\sigma_{hot}^{future} = 4.14°C$ for the hot side. The peaks will diverge about 0.19°C from each other in the future with respect to 1971-2000 as shown in Figure 4.6, which will further increase the occurrence of extreme events. The hot period has 202.7 days in the past as shown in Table 4.1 and taken as the length of a year. Then, 1-year, 10-year, 30-year, 50-year and 100-year temperature events are calculated for the length of future hot period that they would be seen in every 0.216, 1.603, 4.251, 6.714 and 12.521 years, respectively. This means that a 1-year temperature would be seen once in every 42 days, a 10-year temperature would be seen twice in every 3 years, a 30-year temperature would be seen once in every 4 years, a 50-year temperature would be seen once in every 7 years, a 100-year temperature would be seen once in every 13 years. Additional variables are given in Table 4.1.

For HADGEM2-ES RCP4.5 dataset, parameters of the Gaussians are $\mu_{cold}^{past} = 19.59°C$, $\sigma_{cold}^{past} = 4.54°C$ for the cold side, $\mu_{hot}^{past} = 35.25°C$, $\sigma_{hot}^{past} = 4.38°C$ for the hot side in 1971-2000 curve. For 2070-2099, parameters are $\mu_{cold}^{future} = 22.34°C$, $\sigma_{cold}^{future} = 4.74°C$ for the cold side, $\mu_{hot}^{future} = 39.08°C$, $\sigma_{hot}^{future} = 4.61°C$ for the hot side. The peaks will diverge about 1.08°C from each other in the future with respect to 1971-2000 as shown in Figure 4.6, which will further increase the occurrence of extreme events. The hot period has 193.6 days in the past as shown in Table 4.5 and taken as the length of a year. Then, 1-year, 10-year, 30-year, 50-year and 100-year temperature

events are calculated for the length of future hot period that they would be seen in every 0.076, 0.377, 0.829, 1.201 and 1.992 years, respectively. This means that a 1-year temperature would be seen once in every 2 weeks, a 10-year temperature would be seen 3 times in every year, a 30-year temperature would be seen once in every year, a 50-year temperature would be seen 5 times in every 6 years days, a 100-year temperature would be seen once in every 2 years. Additional variables are given in Table 4.5.

For MPI-ESM-MR RCP8.5 dataset, parameters of the Gaussians are $\mu_{cold}^{past} = 19.83°C$, $\sigma_{cold}^{past} = 4.41°C$ for the cold side, $\mu_{hot}^{past} = 34.94°C$, $\sigma_{hot}^{past} = 4.22°C$ for the hot side in 1971-2000 curve. Between 2070-2099, parameters are $\mu_{cold}^{future} = 23.63°C$, $\sigma_{cold}^{future} = 5.04°C$ for the cold side, $\mu_{hot}^{future} = 39.69°C$, $\sigma_{hot}^{future} = 4.47°C$ for the hot side. The peaks will diverge about 0.94°C from each other in the future with respect to 1971-2000 as shown in Figure 4.6, which will further increase the occurrence of extreme events. The hot period has 202.7 days in the past as shown in Table 4.3 and taken as the length of a year. Then, 1-year, 10-year, 30-year, 50-year and 100-year temperature events are calculated for the length of future hot period that they would be seen in every 0.046, 0.196, 0.404, 0.568 and 0.905 years, respectively. This means that a 1-year temperature would be seen once in every 9 days, a 10-year temperature would be seen 5 times in every year, a 30-year temperature would be seen 5 times in every 2 years, a 50-year temperature would be seen 3 times in every 2 years, a 100-year temperature would be seen once in every year. Additional variables are given in Table 4.3.

For HADGEM2-ES RCP8.5 dataset, parameters of the Gaussians are $\mu_{cold}^{past} = 19.59°C$, $\sigma_{cold}^{past} = 4.54°C$ for the cold side, $\mu_{hot}^{past} = 35.25°C$, $\sigma_{hot}^{past} = 4.38°C$ for the hot side in 1971-2000 curve. For 2070-2099, parameters are $\mu_{cold}^{future} = 27.63°C$, $\sigma_{cold}^{future} = 5.11°C$ for the cold side, $\mu_{hot}^{future} = 42.37°C$, $\sigma_{hot}^{future} = 4.4°C$ for the hot side. The peaks will converge about -0.92°C to each other in the future with respect to 1971-2000 as shown in Figure 4.6, which means number of cold days will decrease. The hot period has 193.6 days in the past as shown in Table 4.7 and taken as the length of a year. Then, 1-year, 10-year, 30-year, 50-year and 100-year temperature events are calculated for the length of future hot period that they would be seen in every 0.021, 0.078, 0.152,

0.209 and 0.325 years, respectively. This means that a 1-year temperature would be seen once in every 4 days, a 10-year temperature would be seen once in every 2 weeks, a 30-year temperature would be seen once in every month, a 50-year temperature would be seen 5 times in every year, a 100-year temperature would be seen 3 times in every year. Additional variables are given in Table 4.7.

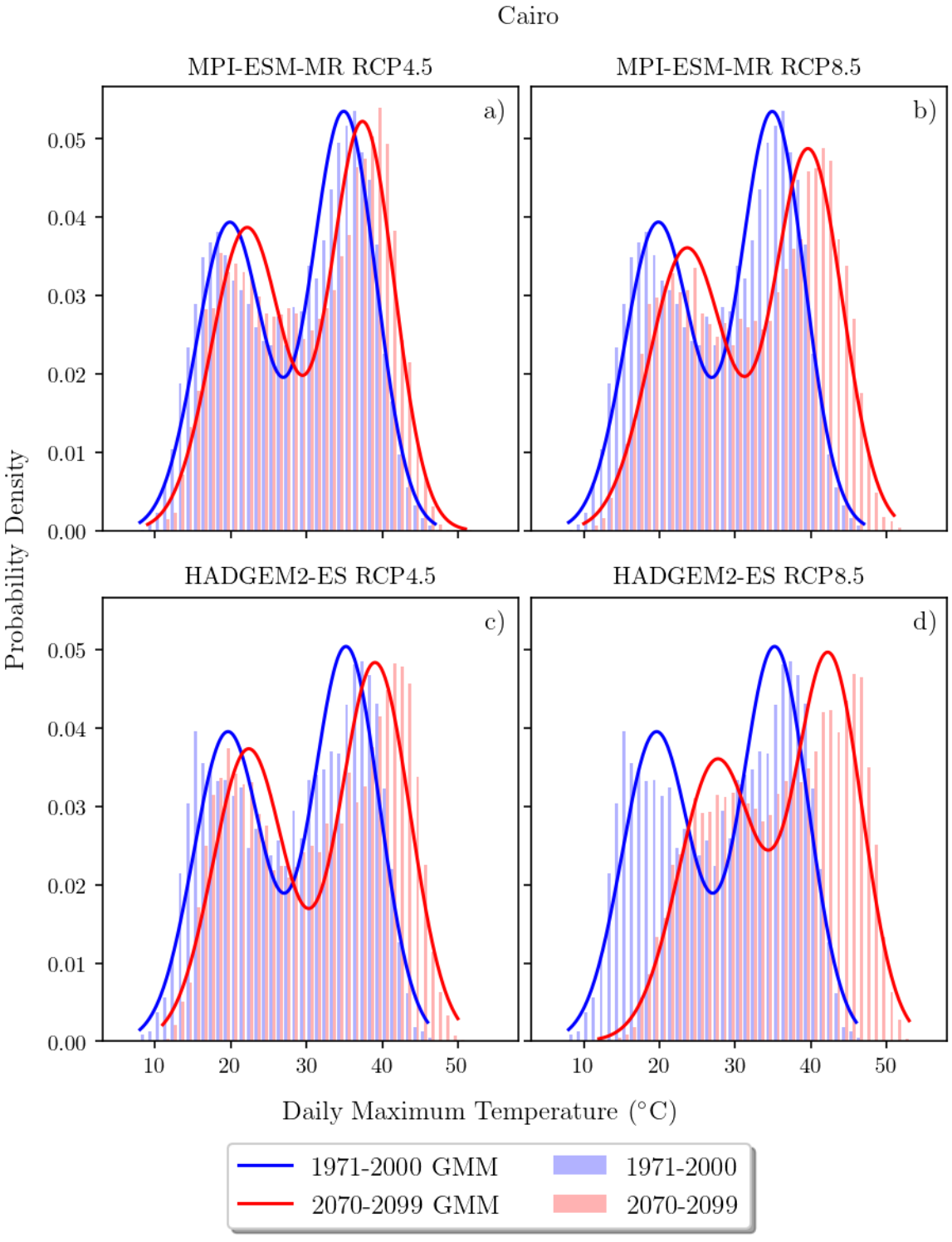

Figure 4.6. Cairo Daily Maximum Temperatures histogram at sea level for 1971-2000 and 2070-2099 and corresponding Gaussian Mixture Model fits: (a) MPI-ESM-MR RCP4.5, (b) MPI-ESM-MR RCP8.5, (c) HadGEM2-ES RCP4.5, (d) HadGEM2-ES RCP8.5

4.7. Casablanca

Casablanca is the largest city in Morocco with an urban agglomeration of 3,684,000 in 2018. The city is located on the coast of Atlantic Ocean. The climate of the city falls into temperate dry hot summer *Csa* climate category according to Köppen-Geiger classification. City's moderate temperatures are due to the cool Canary Current of Atlantic Ocean.

For MPI-ESM-MR RCP4.5 dataset, parameters of the Gaussians are $\mu_{cold}^{past} = 17.34°C$, $\sigma_{cold}^{past} = 3.1°C$ for the cold side, $\mu_{hot}^{past} = 26.35°C$, $\sigma_{hot}^{past} = 4.3°C$ for the hot side in 1971-2000 curve. Between 2070-2099, parameters are $\mu_{cold}^{future} = 18.98°C$, $\sigma_{cold}^{future} = 3.33°C$ for the cold side, $\mu_{hot}^{future} = 28.64°C$, $\sigma_{hot}^{future} = 4.46°C$ for the hot side. The peaks will diverge about 0.64°C from each other in the future with respect to 1971-2000 as shown in Figure 4.7, which will further increase the occurrence of extreme events. The hot period has 164.7 days in the past as shown in Table 4.1 and taken as the length of a year. Then, 1-year, 10-year, 30-year, 50-year and 100-year temperature events are calculated for the length of future hot period that they would be seen in every 0.184, 1.166, 2.856, 4.342 and 7.684 years, respectively. This means that a 1-year temperature would be seen once in every month, a 10-year temperature would be seen once in every year, a 30-year temperature would be seen once in every 3 years, a 50-year temperature would be seen once in every 4 years, a 100-year temperature would be seen once in every 8 years. Additional variables are given in Table 4.1.

For HADGEM2-ES RCP4.5 dataset, parameters of the Gaussians are $\mu_{cold}^{past} = 16.5°C$, $\sigma_{cold}^{past} = 3.12°C$ for the cold side, $\mu_{hot}^{past} = 25.48°C$, $\sigma_{hot}^{past} = 4.23°C$ for the hot side in 1971-2000 curve. For 2070-2099, parameters are $\mu_{cold}^{future} = 18.98°C$, $\sigma_{cold}^{future} = 3.16°C$ for the cold side, $\mu_{hot}^{future} = 27.67°C$, $\sigma_{hot}^{future} = 4.36°C$ for the hot side. The peaks will converge about -0.29°C to each other in the future with respect to 1971-2000 as shown in Figure 4.7. The hot period has 157.0 days in the past as shown in Table 4.5 and taken as the length of a year. Then, 1-year, 10-year, 30-year, 50-year and 100-year temperature events are calculated for the length of future hot period that they would be seen in every 0.169, 1.101, 2.732, 4.18 and 7.46 years, respectively. This means that

a 1-year temperature would be seen once in every month, a 10-year temperature would be seen once in every year, a 30-year temperature would be seen once in every 3 years, a 50-year temperature would be seen once in every 4 years, a 100-year temperature would be seen once in every 8 years. Additional variables are given in Table 4.5.

For MPI-ESM-MR RCP8.5 dataset, parameters of the Gaussians are $\mu_{cold}^{past} = 17.34°C$, $\sigma_{cold}^{past} = 3.1°C$ for the cold side, $\mu_{hot}^{past} = 26.35°C$, $\sigma_{hot}^{past} = 4.3°C$ for the hot side in 1971-2000 curve. Between 2070-2099, parameters are $\mu_{cold}^{future} = 20.51°C$, $\sigma_{cold}^{future} = 3.3°C$ for the cold side, $\mu_{hot}^{future} = 29.85°C$, $\sigma_{hot}^{future} = 4.65°C$ for the hot side. The peaks will diverge about 0.33°C from each other in the future with respect to 1971-2000 as shown in Figure 4.7, which will further increase the occurrence of extreme events. The hot period has 164.7 days in the past as shown in Table 4.3 and taken as the length of a year. Then, 1-year, 10-year, 30-year, 50-year and 100-year temperature events are calculated for the length of future hot period that they would be seen in every 0.069, 0.331, 0.711, 1.017 and 1.661 years, respectively. This means that a 1-year temperature would be seen once in every 2 weeks, a 10-year temperature would be seen 3 times in every year, a 30-year temperature would be seen 3 times in every 2 years, a 50-year temperature would be seen once in every year, a 100-year temperature would be seen twice in every 3 years. Additional variables are given in Table 4.3.

For HADGEM2-ES RCP8.5 dataset, parameters of the Gaussians are $\mu_{cold}^{past} = 16.5°C$, $\sigma_{cold}^{past} = 3.11°C$ for the cold side, $\mu_{hot}^{past} = 25.48°C$, $\sigma_{hot}^{past} = 4.23°C$ for the hot side in 1971-2000 curve. For 2070-2099, parameters are $\mu_{cold}^{future} = 22.92°C$, $\sigma_{cold}^{future} = 3.61°C$ for the cold side, $\mu_{hot}^{future} = 33.26°C$, $\sigma_{hot}^{future} = 4.08°C$ for the hot side. The mean temperatures will increase as shown in Figure 4.7 according to 1971-2000 base. Also, the peaks will diverge about 1.36°C from each other in the future with respect to 1971-2000, which will further increase the occurrence of extreme events. The hot period has 157.1 days in the past as shown in Table 4.7 and taken as the length of a year. Then, 1-year, 10-year, 30-year, 50-year and 100-year temperature events are calculated for the length of future hot period that they would be seen in every 0.015, 0.053, 0.102, 0.14 and 0.217 years, respectively. This means that a 1-year temperature would be

seen once in every 3 days, a 10-year temperature would be seen once in every 10 days, a 30-year temperature would be seen once in every 20 days, a 50-year temperature would be seen once in every 26 days, a 100-year temperature would be seen 5 times in every year. Additional variables are given in Table 4.7.

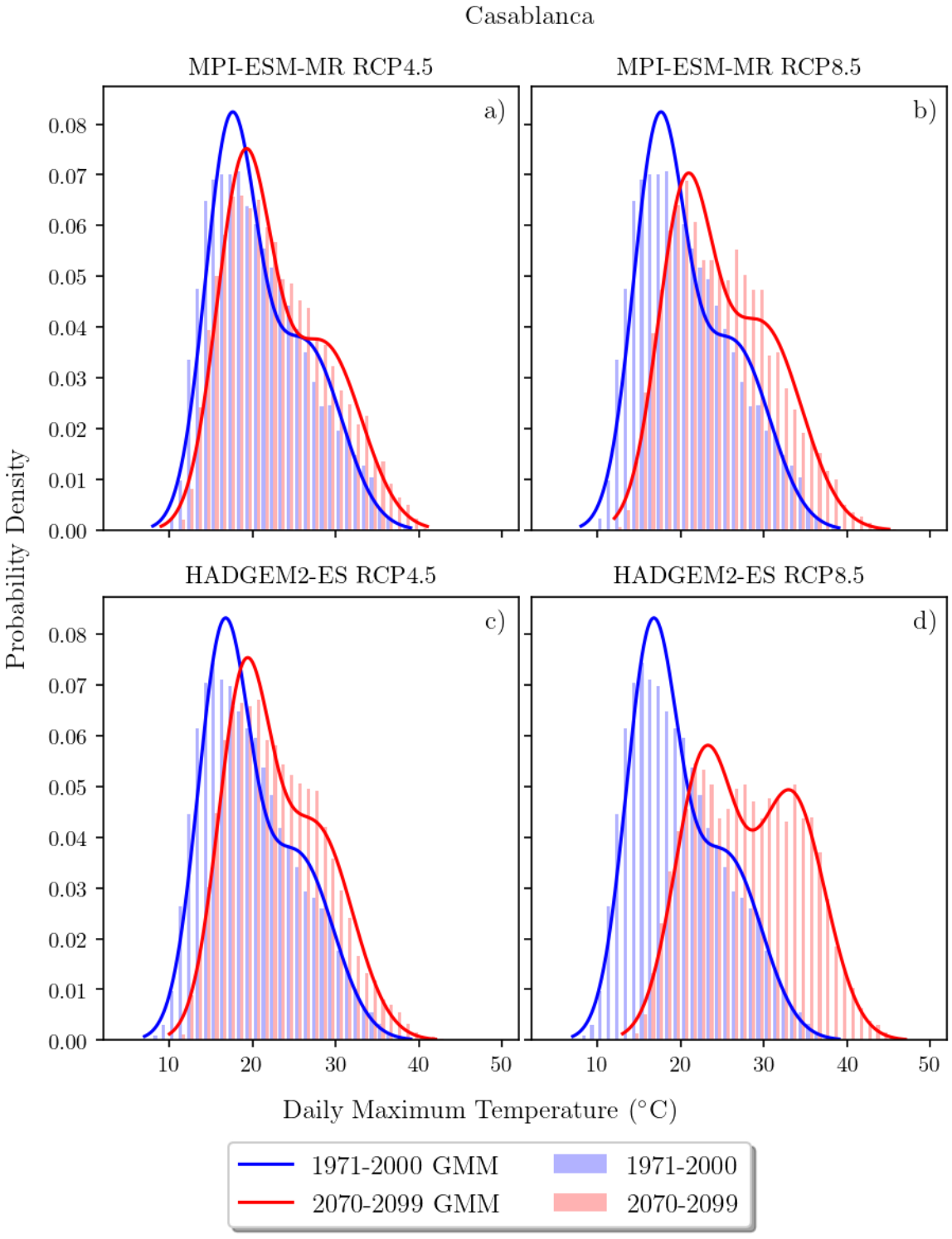

Figure 4.7. Casablanca Daily Maximum Temperatures histogram at sea level for 1971-2000 and 2070-2099 and corresponding Gaussian Mixture Model fits: (a) MPI-ESM-MR RCP4.5, (b) MPI-ESM-MR RCP8.5, (c) HadGEM2-ES RCP4.5, (d) HadGEM2-ES RCP8.5

4.8. Dubai

Dubai is located on the coast of Persian Gulf at sea level and lies within the Arabian Desert. Thus, the city has an arid hot desert climate BWh according to Köppen-Geiger classification. In summers, humidity levels are very high which makes the weather more uncomfortable. Population of urban agglomeration is 2,785,000 in 2018.

For MPI-ESM-MR RCP4.5 dataset, parameters of the Gaussians are $\mu_{cold}^{past} = 23.75°C$, $\sigma_{cold}^{past} = 3.51°C$ for the cold side, $\mu_{hot}^{past} = 34.83°C$, $\sigma_{hot}^{past} = 2.96°C$ for the hot side in 1971-2000 curve. Between 2070-2099, parameters are $\mu_{cold}^{future} = 25.38°C$, $\sigma_{cold}^{future} = 3.52°C$ for the cold side, $\mu_{hot}^{future} = 37.06°C$, $\sigma_{hot}^{future} = 3.03°C$ for the hot side. The peaks will diverge about 0.61°C from each other in the future with respect to 1971-2000 as shown in Figure 4.8, which will further increase the occurrence of extreme events. The hot period has 175.4 days in the past as shown in Table 4.1 and taken as the length of a year. Then, 1-year, 10-year, 30-year, 50-year and 100-year temperature events are calculated for the length of future hot period that they would be seen in every 0.112, 0.644, 1.517, 2.269 and 3.93 years, respectively. This means that a 1-year temperature would be seen once in every 20 days, a 10-year temperature would be seen once in every 116.2 days, a 30-year temperature would be seen twice in every 3 years, a 50-year temperature would be seen once in every 2 years, a 100-year temperature would be seen once in every 4 years. Additional variables are given in Table 4.1.

For HADGEM2-ES RCP4.5 dataset, parameters of the Gaussians are $\mu_{cold}^{past} = 22.63°C$, $\sigma_{cold}^{past} = 3.38°C$ for the cold side, $\mu_{hot}^{past} = 34.05°C$, $\sigma_{hot}^{past} = 2.79°C$ for the hot side in 1971-2000 curve. For 2070-2099, parameters are $\mu_{cold}^{future} = 25.74°C$, $\sigma_{cold}^{future} = 3.5°C$ for the cold side, $\mu_{hot}^{future} = 37.45°C$, $\sigma_{hot}^{future} = 2.8°C$ for the hot side. The peaks will diverge about 0.28°C from each other in the future with respect to 1971-2000 as shown in Figure 4.8, which will further increase the occurrence of extreme events. The hot period has 188.8 days in the past as shown in Table 4.5 and taken as the length of a year. Then, 1-year, 10-year, 30-year, 50-year and 100-year temperature events are

calculated for the length of future hot period that they would be seen in every 0.045, 0.214, 0.465, 0.672 and 1.111 years, respectively. This means that a 1-year temperature would be seen once in every week, a 10-year temperature would be seen 5 times in every year, a 30-year temperature would be seen twice in every year, a 50-year temperature would be seen 3 times in every 2 years, a 100-year temperature would be seen once in almost every year. Additional variables are given in Table 4.5.

For MPI-ESM-MR RCP8.5 dataset, parameters of the Gaussians are $\mu_{cold}^{past} = 23.75°C$, $\sigma_{cold}^{past} = 3.51°C$ for the cold side, $\mu_{hot}^{past} = 34.83°C$, $\sigma_{hot}^{past} = 2.96°C$ for the hot side in 1971-2000 curve. Between 2070-2099, parameters are $\mu_{cold}^{future} = 27.08°C$, $\sigma_{cold}^{future} = 3.64°C$ for the cold side, $\mu_{hot}^{future} = 39.0°C$, $\sigma_{hot}^{future} = 3.12°C$ for the hot side. The peaks will diverge about 0.84°C from each other in the future with respect to 1971-2000 as shown in Figure 4.8, which will further increase the occurrence of extreme events. The hot period has 175.4 days in the past as shown in Table 4.3 and taken as the length of a year. Then, 1-year, 10-year, 30-year, 50-year and 100-year temperature events are calculated for the length of future hot period that they would be seen in every 0.028, 0.104, 0.201, 0.275 and 0.424 years, respectively. This means that a 1-year temperature would be seen once in every 5 days, a 10-year temperature would be seen once in every 3 weeks, a 30-year temperature would be seen 5 times in every year, a 50-year temperature would be seen 3 times in every year, a 100-year temperature would be seen twice in every year. Additional variables are given in Table 4.3.

For HADGEM2-ES RCP8.5 dataset, parameters of the Gaussians are $\mu_{cold}^{past} = 22.63°C$, $\sigma_{cold}^{past} = 3.38°C$ for the cold side, $\mu_{hot}^{past} = 34.05°C$, $\sigma_{hot}^{past} = 2.79°C$ for the hot side in 1971-2000 curve. For 2070-2099, parameters are $\mu_{cold}^{future} = 29.34°C$, $\sigma_{cold}^{future} = 3.24°C$ for the cold side, $\mu_{hot}^{future} = 40.54°C$, $\sigma_{hot}^{future} = 2.89°C$ for the hot side. The peaks will diverge about -0.22°C from each other in the future with respect to 1971-2000 as shown in Figure 4.8, which will further increase the occurrence of extreme events. The hot period has 188.8 days in the past as shown in Table 4.7 and taken as the length of a year. Then, 1-year, 10-year, 30-year, 50-year and 100-year temperature events are calculated for the length of future hot period that they would be seen in

every 0.009, 0.021, 0.033, 0.042 and 0.058 years, respectively. This means that a 1-year temperature would be seen twice in every 3 days, a 10-year temperature would be seen twice in every week, a 30-year temperature would be seen once in every 6 days, a 50-year temperature would be seen once in every 7.6 days, a 100-year temperature would be seen once in every 10.5 days. Additional variables are given in Table 4.7.

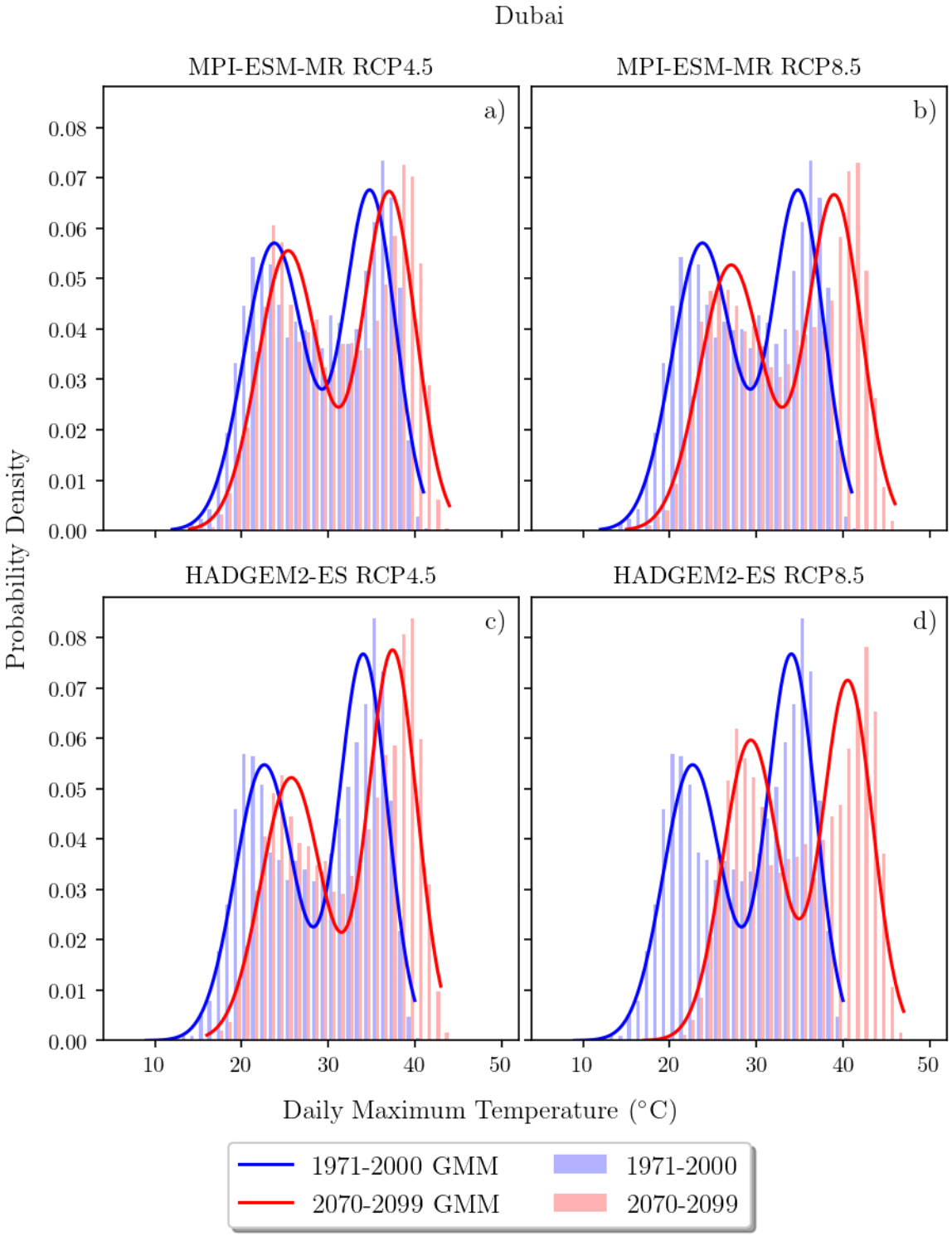

Figure 4.8. Dubai Daily Maximum Temperatures histogram at sea level for 1971-2000 and 2070-2099 and corresponding Gaussian Mixture Model fits: (a) MPI-ESM-MR RCP4.5, (b) MPI-ESM-MR RCP8.5, (c) HadGEM2-ES RCP4.5, (d) HadGEM2-ES RCP8.5

4.9. Istanbul

Istanbul is the most populous city of Turkey with an urban agglomeration of 14,751,000 in 2018. The city is surrounded by the Sea of Marmara at south and the Black Sea at north connected by the Bosporus which divides Istanbul in half by separating Asia from Europe. Furthermore, the Golden Horn divides the city, shaping a natural peninsula. The city shows the characteristics of multiple Köppen-Geiger classifications, temperate dry summer hot summer *Csa*, temperate no dry season hot summer *Cfa* and temperate no dry season warm summer *Cfb* due to its transitional climatic zone.

For MPI-ESM-MR RCP4.5 dataset, parameters of the Gaussians are $\mu_{cold}^{past} = 11.83°C$, $\sigma_{cold}^{past} = 3.89°C$ for the cold side, $\mu_{hot}^{past} = 23.54°C$, $\sigma_{hot}^{past} = 3.81°C$ for the hot side in 1971-2000 curve. Between 2070-2099, parameters are $\mu_{cold}^{future} = 13.41°C$, $\sigma_{cold}^{future} = 3.77°C$ for the cold side, $\mu_{hot}^{future} = 25.32°C$, $\sigma_{hot}^{future} = 3.92°C$ for the hot side. The mean temperatures will increase as shown in Figure 4.9 according to 1971-2000 base. Also, the peaks will diverge about 0.19°C from each other in the future with respect to 1971-2000, which will further increase the occurrence of extreme events. The hot period has 176.3 days in the past as shown in Table 4.2 and taken as the length of a year. Then, 1-year, 10-year, 30-year, 50-year and 100-year temperature events are calculated for the length of future hot period that they would be seen in every 0.23, 1.556, 3.924, 6.046 and 10.894 years, respectively. This means that a 1-year temperature would be seen 5 times in every year, a 10-year temperature would be seen twice in every 3 years, a 30-year temperature would be seen once in every 4 years, a 50-year temperature would be seen once in every 6 years, a 100-year temperature would be seen once in every 11 years. Additional variables are given in Table 4.2.

For HADGEM2-ES RCP4.5 dataset, parameters of the Gaussians are $\mu_{cold}^{past} = 12.05°C$, $\sigma_{cold}^{past} = 3.88°C$ for the cold side, $\mu_{hot}^{past} = 23.62°C$, $\sigma_{hot}^{past} = 3.65°C$ for the hot side in 1971-2000 curve. For 2070-2099, parameters are $\mu_{cold}^{future} = 14.52°C$, $\sigma_{cold}^{future} = 4.03°C$ for the cold side, $\mu_{hot}^{future} = 27.47°C$, $\sigma_{hot}^{future} = 4.13°C$ for the hot side. The mean temperatures will increase as shown in Figure 4.9 according to 1971-2000 base.

Also, the peaks will diverge about 1.37°C from each other in the future with respect to 1971-2000, which will further increase the occurrence of extreme events. The hot period has 162.4 days in the past as shown in Table 4.6 and taken as the length of a year. Then, 1-year, 10-year, 30-year, 50-year and 100-year temperature events are calculated for the length of future hot period that they would be seen in every 0.044, 0.166, 0.318, 0.432 and 0.658 years, respectively. This means that a 1-year temperature would be seen once in every week, a 10-year temperature would be seen once in every month, a 30-year temperature would be seen 3 times in every year, a 50-year temperature would be seen twice in every year, a 100-year temperature would be seen 3 times in every 2 years. Additional variables are given in Table 4.6.

For MPI-ESM-MR RCP8.5 dataset, parameters of the Gaussians are $\mu_{cold}^{past} = 11.83°C$, $\sigma_{cold}^{past} = 3.89°C$ for the cold side, $\mu_{hot}^{past} = 23.54°C$, $\sigma_{hot}^{past} = 3.81°C$ for the hot side in 1971-2000 curve. Between 2070-2099, parameters are $\mu_{cold}^{future} = 14.62°C$, $\sigma_{cold}^{future} = 4.02°C$ for the cold side, $\mu_{hot}^{future} = 27.37°C$, $\sigma_{hot}^{future} = 4.06°C$ for the hot side. The mean temperatures will increase as shown in Figure 4.9 according to 1971-2000 base. Also, the peaks will diverge about 1.03°C from each other in the future with respect to 1971-2000, which will further increase the occurrence of extreme events. The hot period has 176.3 days in the past as shown in Table 4.4 and taken as the length of a year. Then, 1-year, 10-year, 30-year, 50-year and 100-year temperature events are calculated for the length of future hot period that they would be seen in every 0.058, 0.26, 0.545, 0.773 and 1.246 years, respectively. This means that a 1-year temperature would be seen once in every 10.2 days, a 10-year temperature would be seen 4 times in every year, a 30-year temperature would be seen twice in every year, a 50-year temperature would be seen 4 times in every 3 years, a 100-year temperature would be seen 4 times in every 5 year. Additional variables are given in Table 4.4.

For HADGEM2-ES RCP8.5 dataset, parameters of the Gaussians are $\mu_{cold}^{past} = 12.05°C$, $\sigma_{cold}^{past} = 3.88°C$ for the cold side, $\mu_{hot}^{past} = 23.62°C$, $\sigma_{hot}^{past} = 3.65°C$ for the hot side in 1971-2000 curve. For 2070-2099, parameters are $\mu_{cold}^{future} = 17.42°C$, $\sigma_{cold}^{future} = 3.25°C$ for the cold side, $\mu_{hot}^{future} = 28.5°C$, $\sigma_{hot}^{future} = 3.67°C$ for the hot side. The peaks will converge about -0.49°C to each other in the future with respect to 1971-2000 as

shown in Figure 4.9. The hot period has 162.5 days in the past as shown in Table 4.8 and taken as the length of a year. Then, 1-year, 10-year, 30-year, 50-year and 100-year temperature events are calculated for the length of future hot period that they would be seen in every 0.038, 0.162, 0.339, 0.48 and 0.776 years, respectively. This means that a 1-year temperature would be seen once in every week, a 10-year temperature would be seen once in every month, a 30-year temperature would be seen 3 times in every year, a 50-year temperature would be seen twice in every year, a 100-year temperature would be seen 3 times in every 2 years. Additional variables are given in Table 4.8.

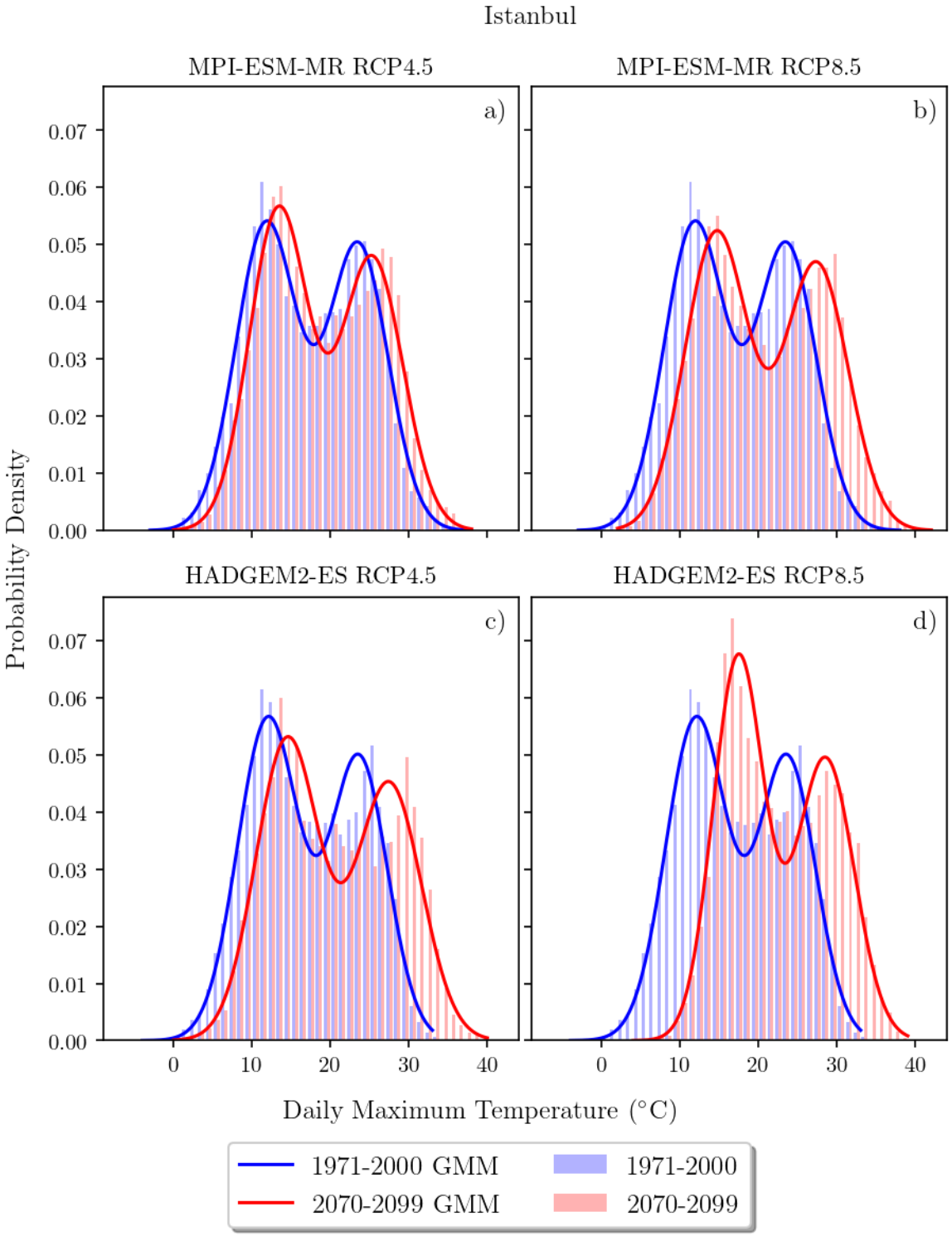

Figure 4.9. Istanbul Daily Maximum Temperatures histogram at sea level for 1971-2000 and 2070-2099 and corresponding Gaussian Mixture Model fits: (a) MPI-ESM-MR RCP4.5, (b) MPI-ESM-MR RCP8.5, (c) HadGEM2-ES RCP4.5, (d) HadGEM2-ES RCP8.5

4.10. Jeddah

Jeddah is located on the coast of Red Sea, which it is the largest seaport. Population of urban agglomeration is 4,433,000 in 2018. City has an arid desert hot climate according to Köppen-Geiger classification and is affected from dust storms coming from the deserts in Arabian Peninsula.

For MPI-ESM-MR RCP4.5 dataset, parameters of the Gaussians are $\mu_{cold}^{past} = 26.43°C$, $\sigma_{cold}^{past} = 2.85°C$ for the cold side, $\mu_{hot}^{past} = 34.95°C$, $\sigma_{hot}^{past} = 2.29°C$ for the hot side in 1971-2000 curve. Between 2070-2099, parameters are $\mu_{cold}^{future} = 27.79°C$, $\sigma_{cold}^{future} = 3.01°C$ for the cold side, $\mu_{hot}^{future} = 37.0°C$, $\sigma_{hot}^{future} = 2.44°C$ for the hot side. The peaks will diverge about 0.69°C from each other in the future with respect to 1971-2000 as shown in Figure 4.10, which will further increase the occurrence of extreme events. The hot period has 199.6 days in the past as shown in Table 4.2 and taken as the length of a year. Then, 1-year, 10-year, 30-year, 50-year and 100-year temperature events are calculated for the length of future hot period that they would be seen in every 0.066, 0.314, 0.675, 0.967 and 1.579 years, respectively. This means that a 1-year temperature would be seen once in every 2 weeks, a 10-year temperature would be seen 3 times in every year, a 30-year temperature would be seen 3 times in every 2 years, a 50-year temperature would be seen once in every year, a 100-year temperature would be seen twice in every 3 years. Additional variables are given in Table 4.2.

For HADGEM2-ES RCP4.5 dataset, parameters of the Gaussians are $\mu_{cold}^{past} = 26.14°C$, $\sigma_{cold}^{past} = 2.85°C$ for the cold side, $\mu_{hot}^{past} = 35.46°C$, $\sigma_{hot}^{past} = 2.34°C$ for the hot side in 1971-2000 curve. For 2070-2099, parameters are $\mu_{cold}^{future} = 28.97°C$, $\sigma_{cold}^{future} = 3.14°C$ for the cold side, $\mu_{hot}^{future} = 39.16°C$, $\sigma_{hot}^{future} = 2.27°C$ for the hot side. The peaks will diverge about 0.87°C from each other in the future with respect to 1971-2000, which will further increase the occurrence of extreme events. The hot period has 196.4 days in the past as shown in Table 4.6 and taken as the length of a year. Then, 1-year, 10-year, 30-year, 50-year and 100-year temperature events are calculated for the length of future hot period that they would be seen in every 0.025, 0.105, 0.217, 0.307 and 0.496 years, respectively. This means that a 1-year temperature would be seen

once in every 5 days, a 10-year temperature would be seen 10 times in every year, a 30-year temperature would be seen 5 times in every year, a 50-year temperature would be seen 3 times in every year, a 100-year temperature would be seen twice in every year. Additional variables are given in Table 4.6.

For MPI-ESM-MR RCP8.5 dataset, parameters of the Gaussians are $\mu_{cold}^{past} = 26.43°C$, $\sigma_{cold}^{past} = 2.85°C$ for the cold side, $\mu_{hot}^{past} = 34.95°C$, $\sigma_{hot}^{past} = 2.29°C$ for the hot side in 1971-2000 curve. Between 2070-2099, parameters are $\mu_{cold}^{future} = 29.85°C$, $\sigma_{cold}^{future} = 3.28°C$ for the cold side, $\mu_{hot}^{future} = 39.46°C$, $\sigma_{hot}^{future} = 2.55°C$ for the hot side. The peaks will diverge about 1.09°C from each other in the future with respect to 1971-2000 as shown in Figure 4.10, which will further increase the occurrence of extreme events. The hot period has 199.6 days in the past as shown in Table 4.4 and taken as the length of a year. Then, 1-year, 10-year, 30-year, 50-year and 100-year temperature events are calculated for the length of future hot period that they would be seen in every 0.011, 0.029, 0.047, 0.06 and 0.083 years, respectively. This means that a 1-year temperature would be seen once in every 3 days, a 10-year temperature would be seen once in every 6 days, a 30-year temperature would be seen once in every 10 days, a 50-year temperature would be seen once in every 12 days, a 100-year temperature would be seen once in every 16 days. Additional variables are given in Table 4.4.

For HADGEM2-ES RCP8.5 dataset, parameters of the Gaussians are $\mu_{cold}^{past} = 26.14°C$, $\sigma_{cold}^{past} = 2.85°C$ for the cold side, $\mu_{hot}^{past} = 35.46°C$, $\sigma_{hot}^{past} = 2.34°C$ for the hot side in 1971-2000 curve. For 2070-2099, parameters are $\mu_{cold}^{future} = 33.16°C$, $\sigma_{cold}^{future} = 2.77°C$ for the cold side, $\mu_{hot}^{future} = 42.01°C$, $\sigma_{hot}^{future} = 2.25°C$ for the hot side. The peaks will converge about -0.47°C to each other in the future with respect to 1971-2000. The hot period has 196.4 days in the past as shown in Table 4.8 and taken as the length of a year. Then, 1-year, 10-year, 30-year, 50-year and 100-year temperature events are calculated for the length of future hot period that they would be seen in every 0.005, 0.011, 0.017, 0.021 and 0.028 years, respectively. This means that a 1-year temperature would be seen every day, a 10-year temperature would be seen once in every 2.1 days, a 30-year temperature would be seen once in every 3.2 days, a 50-year

temperature would be seen once in every 3.9 days, a 100-year temperature would be seen once in every 5.3 days. Additional variables are given in Table 4.8.

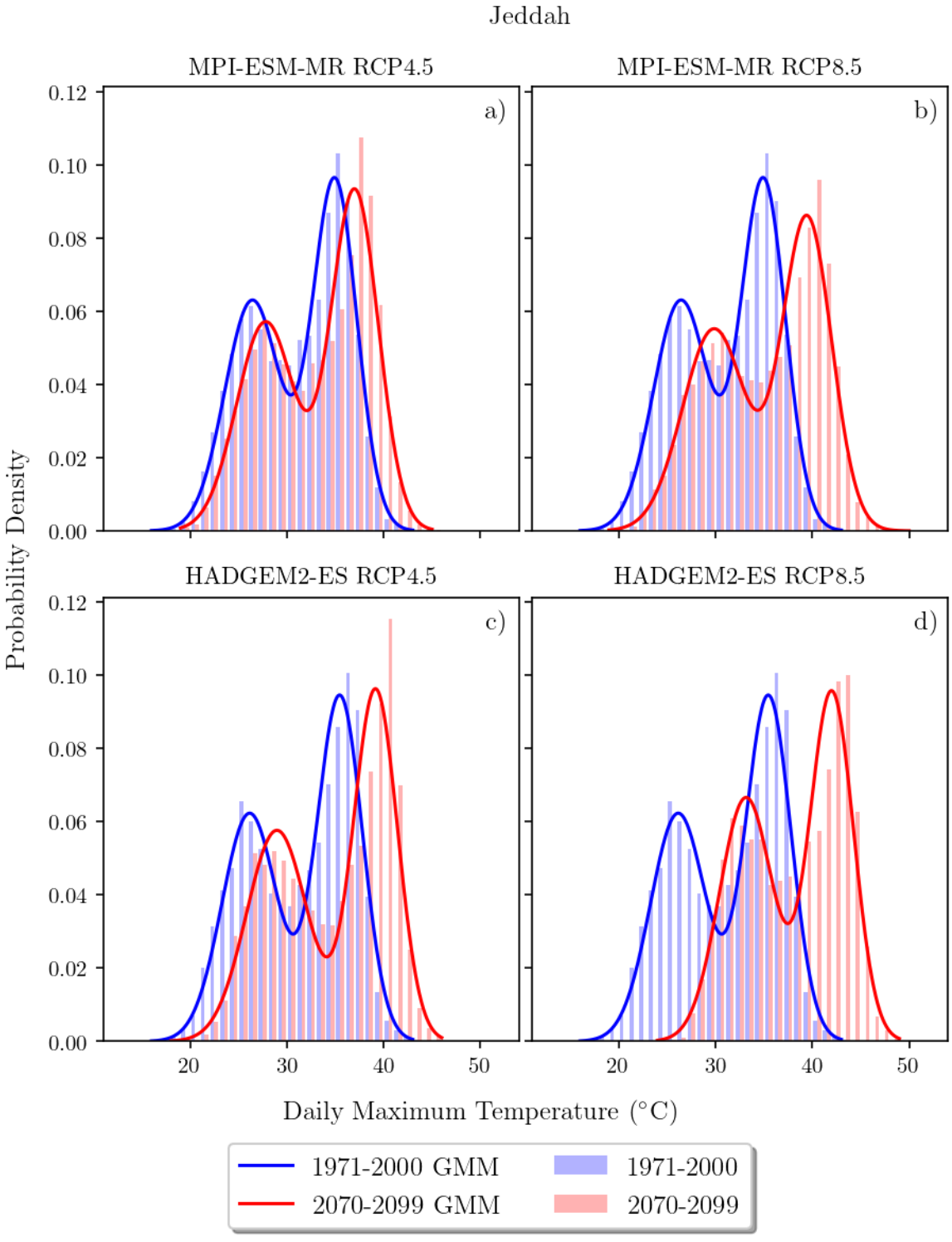

Figure 4.10. Jeddah Daily Maximum Temperatures histogram at sea level for 1971-2000 and 2070-2099 and corresponding Gaussian Mixture Model fits: (a) MPI-ESM-MR RCP4.5, (b) MPI-ESM-MR RCP8.5, (c) HadGEM2-ES RCP4.5, (d) HadGEM2-ES RCP8.5

4.11. Khartoum

Khartoum is the capital of Sudan. The city is the largest city of the country with an urban agglomeration of 5,534,000 in 2018. Khartoum is located where the White Nile and the Blue Nile meet and forms the Nile. City features an arid desert hot climate *BWh* according to Köppen-Geiger classification and one of the hottest major cities on Earth.

For MPI-ESM-MR RCP4.5 dataset, parameters of the Gaussians are $\mu_{cold}^{past} = 30.81°C$, $\sigma_{cold}^{past} = 3.73°C$ for the cold side, $\mu_{hot}^{past} = 39.92°C$, $\sigma_{hot}^{past} = 2.42°C$ for the hot side in 1971-2000 curve. Between 2070-2099, parameters are $\mu_{cold}^{future} = 32.48°C$, $\sigma_{cold}^{future} = 4.07°C$ for the cold side, $\mu_{hot}^{future} = 42.69°C$, $\sigma_{hot}^{future} = 2.64°C$ for the hot side. The peaks will diverge about 1.1°C from each other in the future with respect to 1971-2000 as shown in Figure 4.11, which will further increase the occurrence of extreme events. The hot period has 228.7 days in the past as shown in Table 4.2 and taken as the length of a year. Then, 1-year, 10-year, 30-year, 50-year and 100-year temperature events are calculated for the length of future hot period that they would be seen in every 0.037, 0.145, 0.288, 0.397 and 0.617 years, respectively. This means that a 1-year temperature would be seen once in every 8.5 days, a 10-year temperature would be seen once in every month, a 30-year temperature would be seen once in every 2 months, a 50-year temperature would be seen 5 times in every 2 years, a 100-year temperature would be seen 3 times in every 2 years. Additional variables are given in Table 4.2.

For HADGEM2-ES RCP4.5 dataset, parameters of the Gaussians are $\mu_{cold}^{past} = 30.51°C$, $\sigma_{cold}^{past} = 4.01°C$ for the cold side, $\mu_{hot}^{past} = 40.36°C$, $\sigma_{hot}^{past} = 2.9°C$ for the hot side in 1971-2000 curve. For 2070-2099, parameters are $\mu_{cold}^{future} = 33.51°C$, $\sigma_{cold}^{future} = 4.29°C$ for the cold side, $\mu_{hot}^{future} = 44.2°C$, $\sigma_{hot}^{future} = 2.94°C$ for the hot side. The peaks will diverge about 0.85°C from each other in the future with respect to 1971-2000, which will further increase the occurrence of extreme events. The hot period has 208.0 days in the past as shown in Table 4.6 and taken as the length of a year. Then, 1-year, 10-year, 30-year, 50-year and 100-year temperature events are calculated for the length

of future hot period that they would be seen in every 0.033, 0.14, 0.289, 0.409 and 0.657 years, respectively. This means that a 1-year temperature would be seen once in every week, a 10-year temperature would be seen once in every month, a 30-year temperature would be seen once in every 2 months, a 50-year temperature would be seen 5 times in every 2 years, a 100-year temperature would be seen 3 times in every 2 years. Additional variables are given in Table 4.6.

For MPI-ESM-MR RCP8.5 dataset, parameters of the Gaussians are $\mu_{cold}^{past} = 30.82°C$, $\sigma_{cold}^{past} = 3.74°C$ for the cold side, $\mu_{hot}^{past} = 39.92°C$, $\sigma_{hot}^{past} = 2.42°C$ for the hot side in 1971-2000 curve. Between 2070-2099, parameters are $\mu_{cold}^{future} = 34.56°C$, $\sigma_{cold}^{future} = 4.46°C$ for the cold side, $\mu_{hot}^{future} = 45.19°C$, $\sigma_{hot}^{future} = 2.96°C$ for the hot side. The peaks will diverge about 1.54°C from each other in the future with respect to 1971-2000 as shown in Figure 4.11, which will further increase the occurrence of extreme events. The hot period has 228.5 days in the past as shown in Table 4.4 and taken as the length of a year. Then, 1-year, 10-year, 30-year, 50-year and 100-year temperature events are calculated for the length of future hot period that they would be seen in every 0.007, 0.016, 0.023, 0.028 and 0.036 years, respectively. This means that a 1-year temperature would be seen once in every 1.7 days, a 10-year temperature would be seen once in every 3.6 days, a 30-year temperature would be seen once in every 5.4 days, a 50-year temperature would be seen once in every 6.5 days, a 100-year temperature would be seen once in every 8.4 days. Additional variables are given in Table 4.4.

For HADGEM2-ES RCP8.5 dataset, parameters of the Gaussians are $\mu_{cold}^{past} = 30.51°C$, $\sigma_{cold}^{past} = 4.01°C$ for the cold side, $\mu_{hot}^{past} = 40.36°C$, $\sigma_{hot}^{past} = 2.9°C$ for the hot side in 1971-2000 curve. For 2070-2099, parameters are $\mu_{cold}^{future} = 40.37°C$, $\sigma_{cold}^{future} = 3.13°C$ for the cold side, $\mu_{hot}^{future} = 48.27°C$, $\sigma_{hot}^{future} = 2.18°C$ for the hot side. The peaks will diverge about -1.94°C from each other in the future with respect to 1971-2000 as shown in Figure 4.11. The hot period has 208.0 days in the past as shown in Table 4.8 and taken as the length of a year. Then, 1-year, 10-year, 30-year, 50-year and 100-year temperature events are calculated for the length of future hot period that they would be seen in every 0.005, 0.014, 0.027, 0.037 and 0.059 years, respectively. This means

that a 1-year temperature would be seen once in every 1.1 days, a 10-year temperature would be seen once in every 3.2 days, a 30-year temperature would be seen once in every 6.1 days, a 50-year temperature would be seen once in every 8.4 days, a 100-year temperature would be seen once in every 13.2 days. Additional variables are given in Table 4.8.

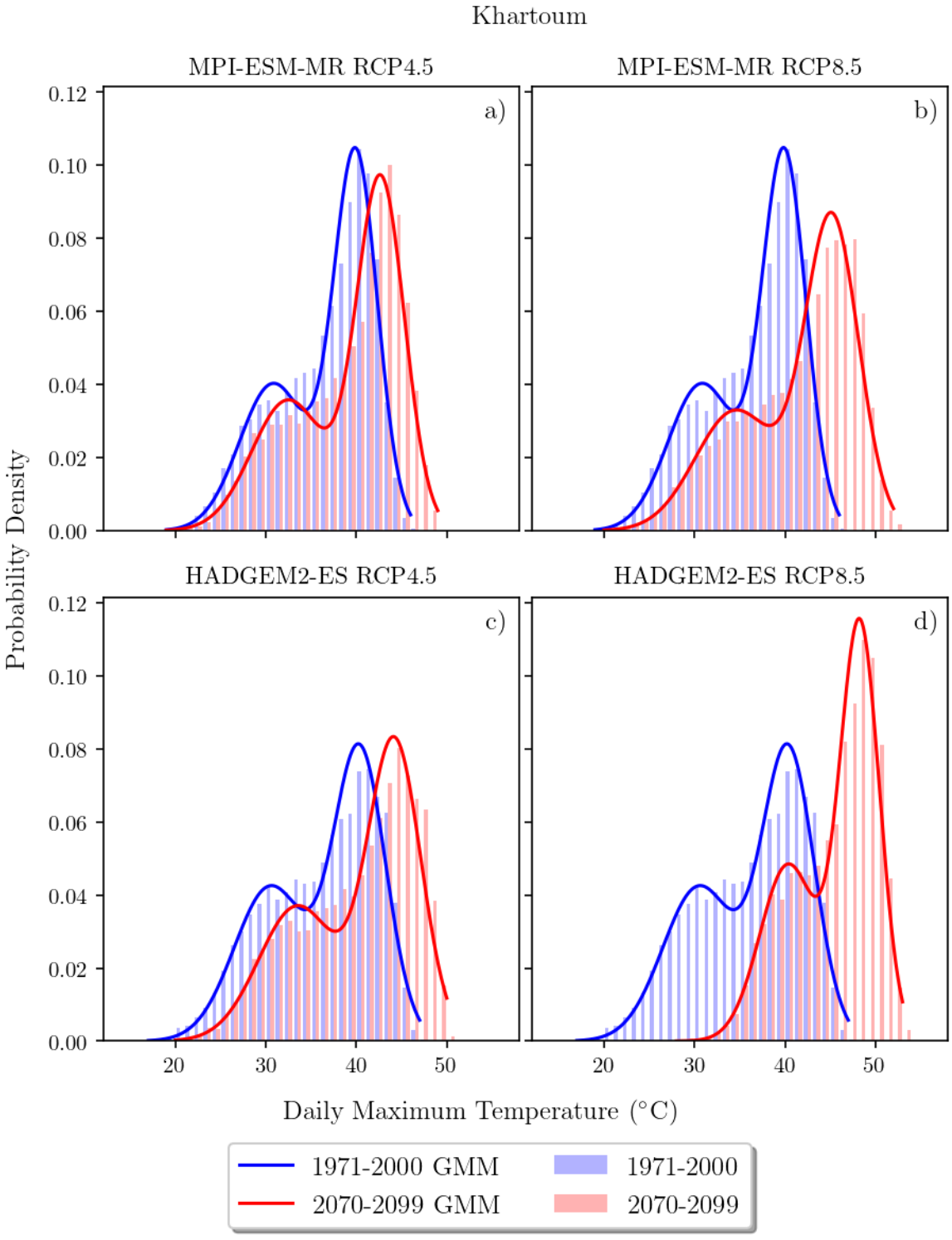

Figure 4.11. Khartoum Daily Maximum Temperatures histogram at sea level for 1971-2000 and 2070-2099 and corresponding Gaussian Mixture Model fits: (a) MPI-ESM-MR RCP4.5, (b) MPI-ESM-MR RCP8.5, (c) HadGEM2-ES RCP4.5, (d) HadGEM2-ES RCP8.5

4.12. Madrid

Madrid is the capital of Spain with an urban agglomeration of 6,497,000 in 2018. The city is located at the center of Spain. Madrid has borderline temperate dry hot summer *Csa* and arid steppe cold *BSk* climate according to Köppen-Geiger classification system.

For MPI-ESM-MR RCP4.5 dataset, parameters of the Gaussians are $\mu_{cold}^{past} = 14.77°C$, $\sigma_{cold}^{past} = 4.35°C$ for the cold side, $\mu_{hot}^{past} = 30.68°C$, $\sigma_{hot}^{past} = 5.21°C$ for the hot side in 1971-2000 curve. Between 2070-2099, parameters are $\mu_{cold}^{future} = 15.99°C$, $\sigma_{cold}^{future} = 4.4°C$ for the cold side, $\mu_{hot}^{future} = 33.22°C$, $\sigma_{hot}^{future} = 5.43°C$ for the hot side. The mean temperatures will increase as shown in Figure 4.12 according to 1971-2000 base. Also, the peaks will diverge about 1.32°C from each other in the future with respect to 1971-2000, which will further increase the occurrence of extreme events. The hot period has 136.5 days in the past as shown in Table 4.2 and taken as the length of a year. Then, 1-year, 10-year, 30-year, 50-year and 100-year temperature events are calculated for the length of future hot period that they would be seen in every 0.188, 1.186, 2.898, 4.401 and 7.772 years, respectively. This means that a 1-year temperature would be seen once in every month, a 10-year temperature would be seen once in every year, a 30-year temperature would be seen once in every 3 years, a 50-year temperature would be seen once in every 4 years, a 100-year temperature would be seen once in every 8 years. Additional variables are given in Table 4.2.

For HADGEM2-ES RCP4.5 dataset, parameters of the Gaussians are $\mu_{cold}^{past} = 14.58°C$, $\sigma_{cold}^{past} = 4.55°C$ for the cold side, $\mu_{hot}^{past} = 31.57°C$, $\sigma_{hot}^{past} = 5.2°C$ for the hot side in 1971-2000 curve. For 2070-2099, parameters are $\mu_{cold}^{future} = 16.96°C$, $\sigma_{cold}^{future} = 4.83°C$ for the cold side, $\mu_{hot}^{future} = 36.14°C$, $\sigma_{hot}^{future} = 5.66°C$ for the hot side. The mean temperatures will increase as shown in Figure 4.12 according to 1971-2000 base. Also, the peaks will diverge about 2.19°C from each other in the future with respect to 1971-2000, which will further increase the occurrence of extreme events. The hot period has 145.6 days in the past as shown in Table 4.6 and taken as the length of a year. Then, 1-year, 10-year, 30-year, 50-year and 100-year temperature events are calculated for

the length of future hot period that they would be seen in every 0.069, 0.31, 0.648, 0.916 and 1.47 years, respectively. This means that a 1-year temperature would be seen once in every 10 days, a 10-year temperature would be seen 3 times in every year, a 30-year temperature would be seen 3 times in every 2 years, a 50-year temperature would be seen once in every year, a 100-year temperature would be seen twice in every 3 years. Additional variables are given in Table 4.6.

For MPI-ESM-MR RCP8.5 dataset, parameters of the Gaussians are $\mu_{cold}^{past} = 14.77°C$, $\sigma_{cold}^{past} = 4.35°C$ for the cold side, $\mu_{hot}^{past} = 30.68°C$, $\sigma_{hot}^{past} = 5.21°C$ for the hot side in 1971-2000 curve. Between 2070-2099, parameters are $\mu_{cold}^{future} = 17.58°C$, $\sigma_{cold}^{future} = 4.46°C$ for the cold side, $\mu_{hot}^{future} = 36.08°C$, $\sigma_{hot}^{future} = 5.67°C$ for the hot side. The mean temperatures will increase as shown in Figure 4.12 according to 1971-2000 base. Also, the peaks will diverge about 2.59°C from each other in the future with respect to 1971-2000, which will further increase the occurrence of extreme events. The hot period has 136.5 days in the past as shown in Table 4.4 and taken as the length of a year. Then, 1-year, 10-year, 30-year, 50-year and 100-year temperature events are calculated for the length of future hot period that they would be seen in every 0.048, 0.198, 0.399, 0.555 and 0.873 years, respectively. This means that a 1-year temperature would be seen once in every week, a 10-year temperature would be seen once in every month, a 30-year temperature would be seen 5 times in every 2 years, a 50-year temperature would be seen twice in every year, a 100-year temperature would be seen 8 times in every 7 years. Additional variables are given in Table 4.4.

For HADGEM2-ES RCP8.5 dataset, parameters of the Gaussians are $\mu_{cold}^{past} = 14.57°C$, $\sigma_{cold}^{past} = 4.54°C$ for the cold side, $\mu_{hot}^{past} = 31.55°C$, $\sigma_{hot}^{past} = 5.21°C$ for the hot side in 1971-2000 curve. For 2070-2099, parameters are $\mu_{cold}^{future} = 19.08°C$, $\sigma_{cold}^{future} = 4.34°C$ for the cold side, $\mu_{hot}^{future} = 39.57°C$, $\sigma_{hot}^{future} = 6.67°C$ for the hot side. The peaks will diverge about 3.51°C from each other in the future with respect to 1971-2000, which will further increase the occurrence of extreme events. The hot period has 145.7 days in the past as shown in Table 4.8 and taken as the length of a year. Then, 1-year, 10-year, 30-year, 50-year and 100-year temperature events are calculated for the length of future hot period that they would be seen in every 0.014, 0.036, 0.056,

0.069 and 0.093 years, respectively. This means that a 1-year temperature would be seen 3 times in every week, a 10-year temperature would be seen once in every week, a 30-year temperature would be seen once in every 10.7 days, a 50-year temperature would be seen once in every 13.2 days, a 100-year temperature would be seen once in every 17.7 days. Additional variables are given in Table 4.8.

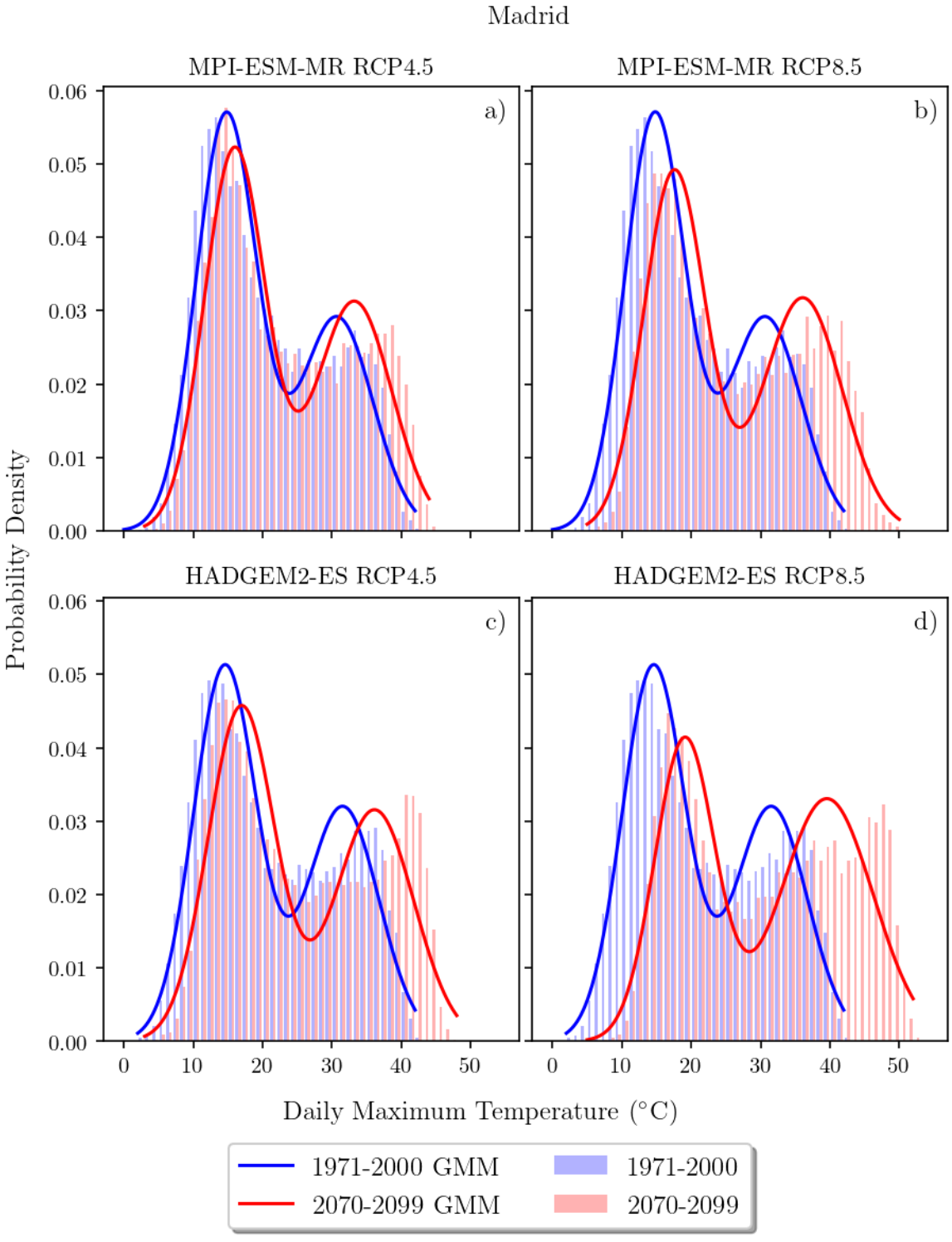

Figure 4.12. Madrid Daily Maximum Temperatures histogram at sea level for 1971-2000 and 2070-2099 and corresponding Gaussian Mixture Model fits: (a) MPI-ESM-MR RCP4.5, (b) MPI-ESM-MR RCP8.5, (c) HadGEM2-ES RCP4.5, (d) HadGEM2-ES RCP8.5

4.13. N'Djamena

N'Djamena is the capital of Chad with an urban agglomeration of 1,323,000 in 2018. The city lies along the Chari River at the confluence with the Logone River. The city features arid steppe hot *BSh* climate according to Köppen-Geiger classification.

For MPI-ESM-MR RCP4.5 dataset, parameters of the Gaussians are $\mu_{cold}^{past} = 33.6°C$, $\sigma_{cold}^{past} = 3.66°C$ for the cold side, $\mu_{hot}^{past} = 39.1°C$, $\sigma_{hot}^{past} = 2.66°C$ for the hot side in 1971-2000 curve. Between 2070-2099, parameters are $\mu_{cold}^{future} = 36.25°C$, $\sigma_{cold}^{future} = 3.76°C$ for the cold side, $\mu_{hot}^{future} = 42.07°C$, $\sigma_{hot}^{future} = 2.78°C$ for the hot side. The peaks will diverge about 0.33°C from each other in the future with respect to 1971-2000 as shown in Figure 4.13, which will further increase the occurrence of extreme events. The hot period has 250.9 days in the past as shown in Table 4.2 and taken as the length of a year. Then, 1-year, 10-year, 30-year, 50-year and 100-year temperature events are calculated for the length of future hot period that they would be seen in every 0.044, 0.2, 0.421, 0.597 and 0.966 years, respectively. This means that a 1-year temperature would be seen once in every 11 days, a 10-year temperature would be seen 5 times in every year, a 30-year temperature would be seen 5 times in every 2 years, a 50-year temperature would be seen 3 times in every 2 years, a 100-year temperature would be seen once in every year. Additional variables are given in Table 4.2.

For HADGEM2-ES RCP4.5 dataset, parameters of the Gaussians are $\mu_{cold}^{past} = 33.43°C$, $\sigma_{cold}^{past} = 3.78°C$ for the cold side, $\mu_{hot}^{past} = 39.7°C$, $\sigma_{hot}^{past} = 3.08°C$ for the hot side in 1971-2000 curve. For 2070-2099, parameters are $\mu_{cold}^{future} = 36.69°C$, $\sigma_{cold}^{future} = 3.76°C$ for the cold side, $\mu_{hot}^{future} = 43.67°C$, $\sigma_{hot}^{future} = 2.82°C$ for the hot side. The mean temperatures will increase as shown in Figure 4.13 according to 1971-2000 base. Also, the peaks will diverge about 0.72°C from each other in the future with respect to 1971-2000, which will further increase the occurrence of extreme events. The hot period has 236.6 days in the past as shown in Table 4.6 and taken as the length of a year. Then, 1-year, 10-year, 30-year, 50-year and 100-year temperature events are calculated for the length of future hot period that they would be seen in every 0.049, 0.289, 0.702,

1.07 and 1.909 years, respectively. This means that a 1-year temperature would be seen once in every 11.4 days, a 10-year temperature would be seen 4 times in every year, a 30-year temperature would be seen 3 times in every 2 years, a 50-year temperature would be seen once in every year, a 100-year temperature would be seen once in every 2 years. Additional variables are given in Table 4.6.

For MPI-ESM-MR RCP8.5 dataset, parameters of the Gaussians are $\mu_{cold}^{past} = 33.6°C$, $\sigma_{cold}^{past} = 3.66°C$ for the cold side, $\mu_{hot}^{past} = 39.1°C$, $\sigma_{hot}^{past} = 2.66°C$ for the hot side in 1971-2000 curve. Between 2070-2099, parameters are $\mu_{cold}^{future} = 38.53°C$, $\sigma_{cold}^{future} = 4.04°C$ for the cold side, $\mu_{hot}^{future} = 44.56°C$, $\sigma_{hot}^{future} = 3.03°C$ for the hot side. The peaks will diverge about 0.54°C from each other in the future with respect to 1971-2000 as shown in Figure 4.13, which will further increase the occurrence of extreme events. The hot period has 250.9 days in the past as shown in Table 4.4 and taken as the length of a year. Then, 1-year, 10-year, 30-year, 50-year and 100-year temperature events are calculated for the length of future hot period that they would be seen in every 0.009, 0.021, 0.033, 0.041 and 0.056 years, respectively. This means that a 1-year temperature would be seen once in every 2.1 days, a 10-year temperature would be seen once in every 5.2 days, a 30-year temperature would be seen once in every 8.3 days, a 50-year temperature would be seen once in every 10.4 days, a 100-year temperature would be seen once in every week. Additional variables are given in Table 4.4.

For HADGEM2-ES RCP8.5 dataset, parameters of the Gaussians are $\mu_{cold}^{past} = 33.43°C$, $\sigma_{cold}^{past} = 3.78°C$ for the cold side, $\mu_{hot}^{past} = 39.7°C$, $\sigma_{hot}^{past} = 3.08°C$ for the hot side in 1971-2000 curve. For 2070-2099, parameters are $\mu_{cold}^{future} = 44.75°C$, $\sigma_{cold}^{future} = 2.58°C$ for the cold side, $\mu_{hot}^{future} = 50.1°C$, $\sigma_{hot}^{future} = 2.09°C$ for the hot side. The peaks will converge about -0.92°C to each other in the future with respect to 1971-2000. The hot period has 236.8 days in the past as shown in Table 4.8 and taken as the length of a year. Then, 1-year, 10-year, 30-year, 50-year and 100-year temperature events are calculated for the length of future hot period that they would be seen in every 0.003, 0.006, 0.01, 0.012 and 0.018 years, respectively. This means that a 1-year temperature would be seen once in every 0.6 days, a 10-year temperature would be seen once in

every 1.2 days, a 30-year temperature would be seen once in every 1.9 days, a 50-year temperature would be seen once in every 2.4 days, a 100-year temperature would be seen once in every 3.4 days. Additional variables are given in Table 4.8.

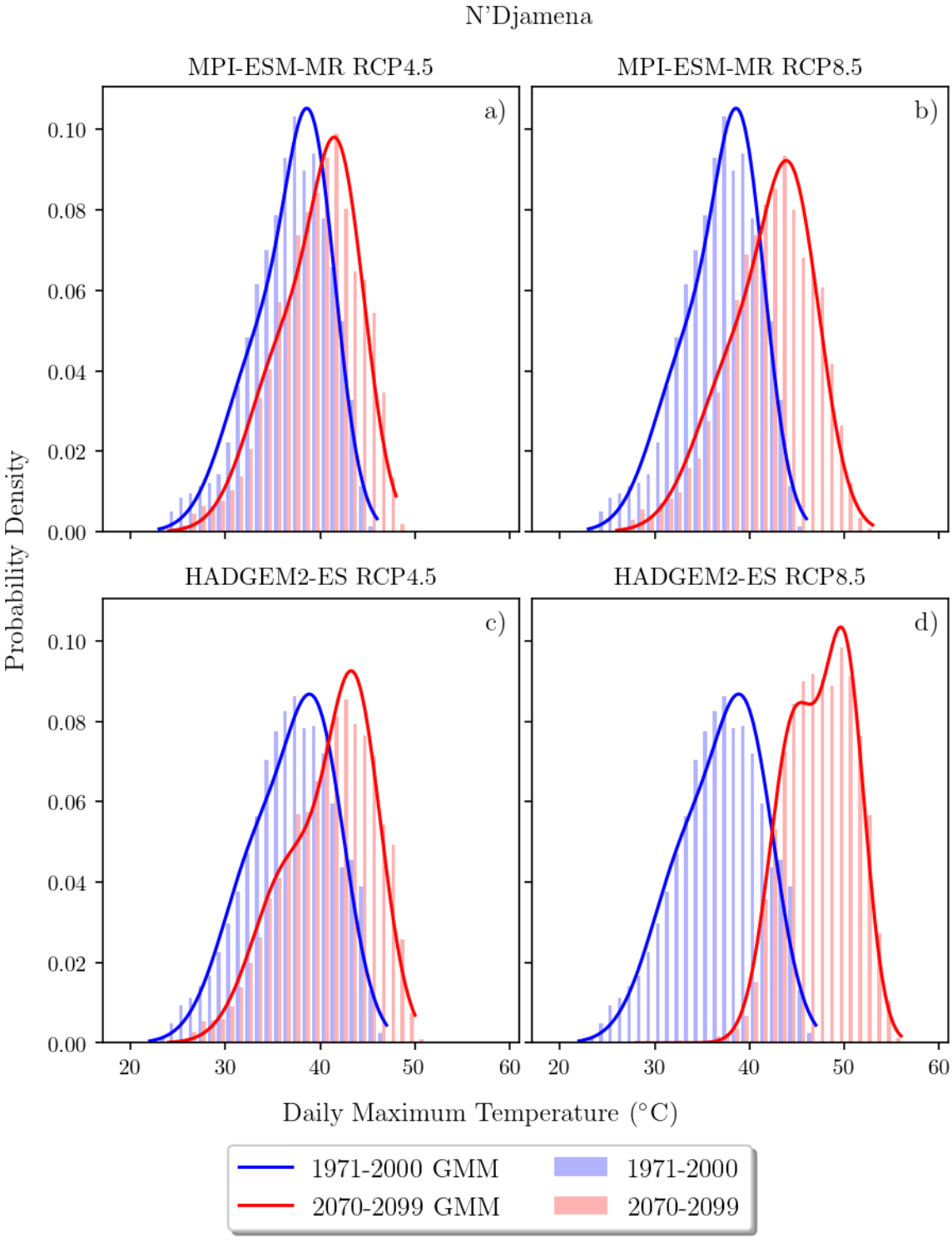

Figure 4.13. NDjamena Daily Maximum Temperatures histogram at sea level for 1971-2000 and 2070-2099 and corresponding Gaussian Mixture Model fits: (a) MPI-ESM-MR RCP4.5, (b) MPI-ESM-MR RCP8.5, (c) HadGEM2-ES RCP4.5, (d) HadGEM2-ES RCP8.5

4.14. Riyadh

The capital of Saudi Arabia is located on the east of the Najd plateau with urban agglomeration of 6,907,000 in 2018. Riyadh features arid desert hot BWh climate according to Köppen-Geiger.

For MPI-ESM-MR RCP4.5 dataset, parameters of the Gaussians are $\mu_{cold}^{past} = 26.4°C$, $\sigma_{cold}^{past} = 5.34°C$ for the cold side, $\mu_{hot}^{past} = 41.91°C$, $\sigma_{hot}^{past} = 3.82°C$ for the hot side in 1971-2000 curve. Between 2070-2099, parameters are $\mu_{cold}^{future} = 30.46°C$, $\sigma_{cold}^{future} = 7.1°C$ for the cold side, $\mu_{hot}^{future} = 46.08°C$, $\sigma_{hot}^{future} = 2.65°C$ for the hot side. The mean temperatures will increase as shown in Figure 4.14 according to 1971-2000 base. The hot period has 187.1 days in the past as shown in Table 4.2 and taken as the length of a year. Then, 1-year, 10-year, 30-year, 50-year and 100-year temperature events are calculated for the length of future hot period that they would be seen in every 0.436, 9.941, 48.37, 102.518 and 288.044 years, respectively. This means that a 1-year temperature would be seen once in every 2 months, a 10-year temperature would be seen once in every 10 year, a 30-year temperature would be seen once in every 50 years, a 50-year temperature would be seen once in every 100 years, a 100-year temperature would be seen once in every 290 years. To clarify, the frequencies seems to be not changing or even decreasing for this dataset. This is because the standard deviations would be decreasing thus causing more days to be at mean temperatures in the future, which would be $4.17°C$ hotter than the past. Additional variables are given in Table 4.2.

For HADGEM2-ES RCP4.5 dataset, parameters of the Gaussians are $\mu_{cold}^{past} = 27.17°C$, $\sigma_{cold}^{past} = 6.54°C$ for the cold side, $\mu_{hot}^{past} = 42.71°C$, $\sigma_{hot}^{past} = 2.68°C$ for the hot side in 1971-2000 curve. For 2070-2099, parameters are $\mu_{cold}^{future} = 30.45°C$, $\sigma_{cold}^{future} = 7.06°C$ for the cold side, $\mu_{hot}^{future} = 46.52°C$, $\sigma_{hot}^{future} = 2.72°C$ for the hot side. The mean temperatures will increase as shown in Figure 4.14 according to 1971-2000 base. Also, the peaks will diverge about 0.53°C from each other in the future with respect to 1971-2000, which will further increase the occurrence of extreme events. The hot period has 158.4 days in the past as shown in Table 4.6 and taken as the length of a year.

Then, 1-year, 10-year, 30-year, 50-year and 100-year temperature events are calculated for the length of future hot period that they would be seen in every 0.032, 0.125, 0.252, 0.352 and 0.556 years, respectively. This means that a 1-year temperature would be seen once in every 5 days, a 10-year temperature would be seen once in every 20 days, a 30-year temperature would be seen 4 times in every year, a 50-year temperature would be seen 3 times in every year, a 100-year temperature would be seen twice in every year. Additional variables are given in Table 4.6.

For MPI-ESM-MR RCP8.5 dataset, parameters of the Gaussians are $\mu_{cold}^{past} = 26.4°C$, $\sigma_{cold}^{past} = 5.34°C$ for the cold side, $\mu_{hot}^{past} = 41.91°C$, $\sigma_{hot}^{past} = 3.82°C$ for the hot side in 1971-2000 curve. Between 2070-2099, parameters are $\mu_{cold}^{future} = 32.53°C$, $\sigma_{cold}^{future} = 7.42°C$ for the cold side, $\mu_{hot}^{future} = 48.6°C$, $\sigma_{hot}^{future} = 2.93°C$ for the hot side. The mean temperatures will increase as shown in Figure 4.14 according to 1971-2000 base. Also, the peaks will diverge about 0.55°C from each other in the future with respect to 1971-2000, which will further increase the occurrence of extreme events. The hot period has 187.2 days in the past as shown in Table 4.4 and taken as the length of a year. Then, 1-year, 10-year, 30-year, 50-year and 100-year temperature events are calculated for the length of future hot period that they would be seen in every 0.037, 0.256, 0.712, 1.164 and 2.307 years, respectively. This means that a 1-year temperature would be seen once in every 5.6 days, a 10-year temperature would be seen 4 times in every year, a 30-year temperature would be seen 3 times in every year, a 50-year temperature would be seen once in every year, a 100-year temperature would be seen 3 times in every 7 years. Additional variables are given in Table 4.4.

For HADGEM2-ES RCP8.5 dataset, parameters of the Gaussians are $\mu_{cold}^{past} = 27.17°C$, $\sigma_{cold}^{past} = 6.54°C$ for the cold side, $\mu_{hot}^{past} = 42.71°C$, $\sigma_{hot}^{past} = 2.68°C$ for the hot side in 1971-2000 curve. For 2070-2099, parameters are $\mu_{cold}^{future} = 34.76°C$, $\sigma_{cold}^{future} = 6.38°C$ for the cold side, $\mu_{hot}^{future} = 49.79°C$, $\sigma_{hot}^{future} = 2.68°C$ for the hot side. The hot period has 158.4 days in the past as shown in Table 4.8 and taken as the length of a year. Then, 1-year, 10-year, 30-year, 50-year and 100-year temperature events are calculated for the length of future hot period that they would be seen in every 0.007, 0.015, 0.023, 0.029 and 0.038 years, respectively. This means that a 1-year temperature

would be seen once in every 1.1 days, a 10-year temperature would be seen once in every 2.3 days, a 30-year temperature would be seen once in every 3.4 days, a 50-year temperature would be seen once in every 4.2 days, a 100-year temperature would be seen once in every 5.6 days. Additional variables are given in Table 4.8.

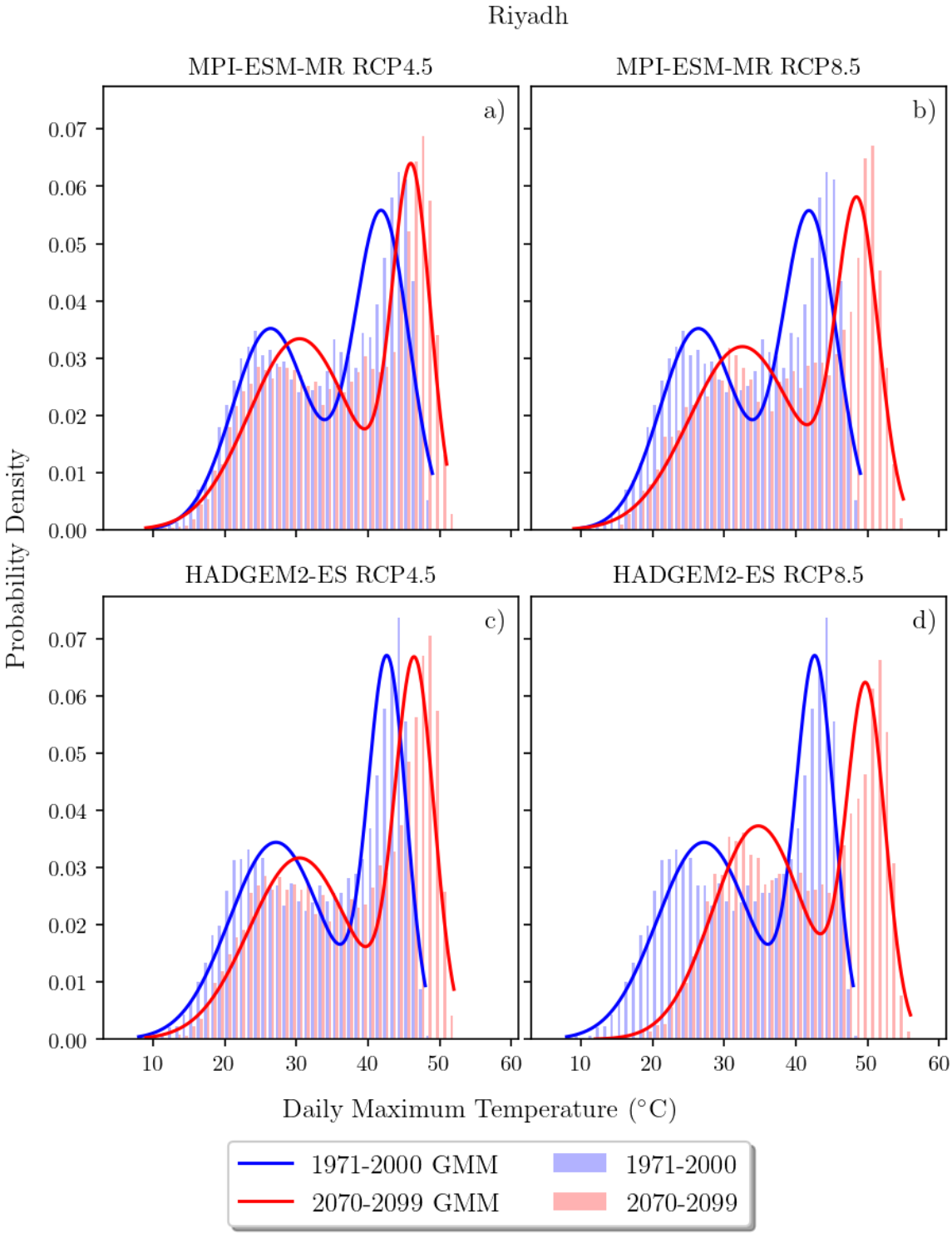

Figure 4.14. Riyadh Daily Maximum Temperatures histogram at sea level for 1971-2000 and 2070-2099 and corresponding Gaussian Mixture Model fits: (a) MPI-ESM-MR RCP4.5, (b) MPI-ESM-MR RCP8.5, (c) HadGEM2-ES RCP4.5, (d) HadGEM2-ES RCP8.5

4.15. Sana'a

Sana'a is the capital of Yemen with urban agglomeration of 2,779,000 in 2018. Sana'a is located at an elevation of 2,300 metres which makes it one of the highest capitals and this situtation affects the climate of the city. Sana'a features arid steppe cold *BSk* climate and has moderate temperatures due to its elevation.

For MPI-ESM-MR RCP4.5 dataset, parameters of the Gaussians are $\mu_{cold}^{past} = 33.87°C$, $\sigma_{cold}^{past} = 2.4°C$ for the cold side, $\mu_{hot}^{past} = 39.49°C$, $\sigma_{hot}^{past} = 2.17°C$ for the hot side in 1971-2000 curve. Between 2070-2099, parameters are $\mu_{cold}^{future} = 35.9°C$, $\sigma_{cold}^{future} = 2.44°C$ for the cold side, $\mu_{hot}^{future} = 42.05°C$, $\sigma_{hot}^{future} = 2.27°C$ for the hot side. The mean temperatures will increase as shown in Figure 4.15 according to 1971-2000 base. Also, the peaks will diverge about 0.53°C from each other in the future with respect to 1971-2000, which will further increase the occurrence of extreme events. The hot period has 199.0 days in the past as shown in Table 4.2 and taken as the length of a year. Then, 1-year, 10-year, 30-year, 50-year and 100-year temperature events are calculated for the length of future hot period that they would be seen in every 0.041, 0.178, 0.369, 0.52 and 0.833 years, respectively. This means that a 1-year temperature would be seen once in every 8.3 days, a 10-year temperature would be seen once in every month, a 30-year temperature would be seen 3 times in every year, a 50-year temperature would be seen twice in every year, a 100-year temperature would be seen once in every year. Additional variables are given in Table 4.2.

For HADGEM2-ES RCP4.5 dataset, parameters of the Gaussians are $\mu_{cold}^{past} = 34.01°C$, $\sigma_{cold}^{past} = 2.2°C$ for the cold side, $\mu_{hot}^{past} = 39.46°C$, $\sigma_{hot}^{past} = 1.96°C$ for the hot side in 1971-2000 curve. For 2070-2099, parameters are $\mu_{cold}^{future} = 37.31°C$, $\sigma_{cold}^{future} = 2.19°C$ for the cold side, $\mu_{hot}^{future} = 42.67°C$, $\sigma_{hot}^{future} = 2.05°C$ for the hot side. The peaks will converge about -0.09°C to each other in the future with respect to 1971-2000. The hot period has 173.9 days in the past as shown in Table 4.6 and taken as the length of a year. Then, 1-year, 10-year, 30-year, 50-year and 100-year temperature events are calculated for the length of future hot period that they would be seen in every 0.018, 0.06, 0.111, 0.149 and 0.223 years, respectively. This means that a 1-year temperature

would be seen once in every 3.5 days, a 10-year temperature would be seen once in every 11.8 days, a 30-year temperature would be seen once in every 21.8 days, a 50-year temperature would be seen once in every month, a 100-year temperature would be seen 4 times in every year. Additional variables are given in Table 4.6.

For MPI-ESM-MR RCP8.5 dataset, parameters of the Gaussians are $\mu_{cold}^{past} = 33.87°C$, $\sigma_{cold}^{past} = 2.4°C$ for the cold side, $\mu_{hot}^{past} = 39.49°C$, $\sigma_{hot}^{past} = 2.17°C$ for the hot side in 1971-2000 curve. Between 2070-2099, parameters are $\mu_{cold}^{future} = 38.2°C$, $\sigma_{cold}^{future} = 2.44°C$ for the cold side, $\mu_{hot}^{future} = 44.55°C$, $\sigma_{hot}^{future} = 2.5°C$ for the hot side. The mean temperatures will increase as shown in Figure 4.15 according to 1971-2000 base. Also, the peaks will diverge about 0.72°C from each other in the future with respect to 1971-2000, which will further increase the occurrence of extreme events. The hot period has 199.0 days in the past as shown in Table 4.4 and taken as the length of a year. Then, 1-year, 10-year, 30-year, 50-year and 100-year temperature events are calculated for the length of future hot period that they would be seen in every 0.007, 0.015, 0.023, 0.028 and 0.036 years, respectively. This means that a 1-year temperature would be seen once in every 1.5 days, a 10-year temperature would be seen once in every 3.1 days, a 30-year temperature would be seen once in every 4.7 days, a 50-year temperature would be seen once in every 5.7 days, a 100-year temperature would be seen once in every 7.4 days. Additional variables are given in Table 4.4.

For HADGEM2-ES RCP8.5 dataset, parameters of the Gaussians are $\mu_{cold}^{past} = 34.01°C$, $\sigma_{cold}^{past} = 2.2°C$ for the cold side, $\mu_{hot}^{past} = 39.46°C$, $\sigma_{hot}^{past} = 1.96°C$ for the hot side in 1971-2000 curve. For 2070-2099, parameters are $\mu_{cold}^{future} = 41.71°C$, $\sigma_{cold}^{future} = 2.62°C$ for the cold side, $\mu_{hot}^{future} = 46.76°C$, $\sigma_{hot}^{future} = 2.15°C$ for the hot side. The peaks will converge about -0.39°C to each other in the future with respect to 1971-2000. The hot period has 174.0 days in the past as shown in Table 4.8 and taken as the length of a year. Then, 1-year, 10-year, 30-year, 50-year and 100-year temperature events are calculated for the length of future hot period that they would be seen in every 0.003, 0.004, 0.005, 0.005 and 0.006 years, respectively. This means that a 1-year temperature would be seen once in every 0.6 days, a 10-year temperature would be seen once in every 0.8 days, a 30-year temperature would be seen once in every 1.0 days, a 50-year

temperature would be seen once in every 1.1 days, a 100-year temperature would be seen once in every 1.3 days. Additional variables are given in Table 4.8.

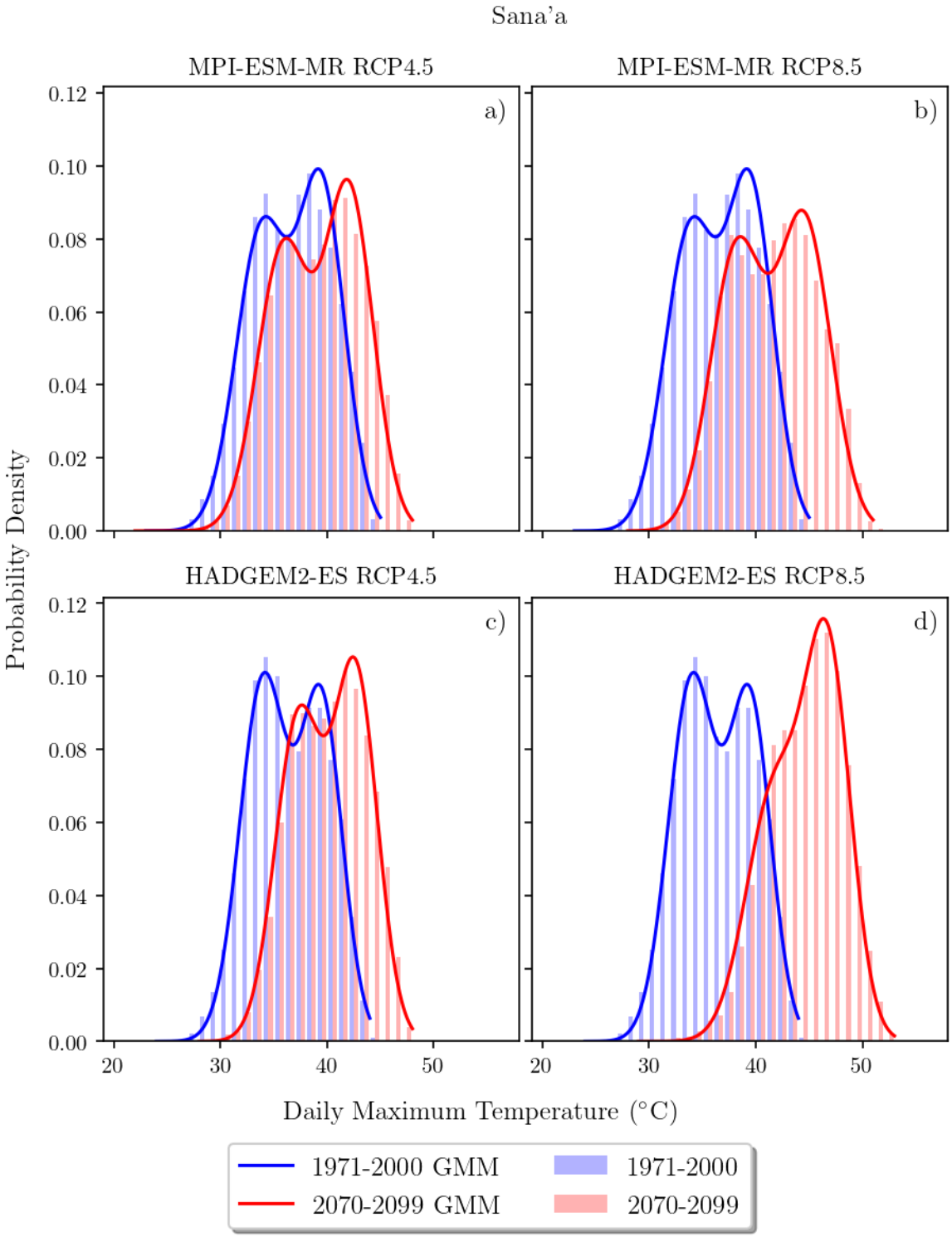

Figure 4.15. Sanaa Daily Maximum Temperatures histogram at sea level for 1971-2000 and 2070-2099 and corresponding Gaussian Mixture Model fits: (a) MPI-ESM-MR RCP4.5, (b) MPI-ESM-MR RCP8.5, (c) HadGEM2-ES RCP4.5, (d) HadGEM2-ES RCP8.5

4.16. Tehran

Tehran is the capital of Iran with an urban agglomeration of 8,896,000 in 2018. Tehran features temperate dry hot summer climate *Csa* according to Köppen-Geiger classification influenced by the Alborz mountains to its north and desert to its south.

For MPI-ESM-MR RCP4.5 dataset, parameters of the Gaussians are $\mu_{cold}^{past} = 16.97°C$, $\sigma_{cold}^{past} = 6.09°C$ for the cold side, $\mu_{hot}^{past} = 35.58°C$, $\sigma_{hot}^{past} = 5.6°C$ for the hot side in 1971-2000 curve. Between 2070-2099, parameters are $\mu_{cold}^{future} = 18.62°C$, $\sigma_{cold}^{future} = 6.43°C$ for the cold side, $\mu_{hot}^{future} = 38.19°C$, $\sigma_{hot}^{future} = 5.76°C$ for the hot side. The mean temperatures will increase as shown in Figure 4.16 according to 1971-2000 base. Also, the peaks will diverge about 0.96°C from each other in the future with respect to 1971-2000, which will further increase the occurrence of extreme events. The hot period has 184.6 days in the past as shown in Table 4.2 and taken as the length of a year. Then, 1-year, 10-year, 30-year, 50-year and 100-year temperature events are calculated for the length of future hot period that they would be seen in every 0.218, 1.479, 3.733, 5.755 and 10.375 years, respectively. This means that a 1-year temperature would be seen once in every 41.3 days, a 10-year temperature would be seen 2 times in every 3 years, a 30-year temperature would be seen once in every 4 years, a 50-year temperature would be seen once in every 6 years, a 100-year temperature would be seen once in every 10 years. Additional variables are given in Table 4.2.

For HADGEM2-ES RCP4.5 dataset, parameters of the Gaussians are $\mu_{cold}^{past} = 15.35°C$, $\sigma_{cold}^{past} = 5.65°C$ for the cold side, $\mu_{hot}^{past} = 34.67°C$, $\sigma_{hot}^{past} = 5.34°C$ for the hot side in 1971-2000 curve. For 2070-2099, parameters are $\mu_{cold}^{future} = 18.94°C$, $\sigma_{cold}^{future} = 6.4°C$ for the cold side, $\mu_{hot}^{future} = 39.25°C$, $\sigma_{hot}^{future} = 5.48°C$ for the hot side. The mean temperatures will increase as shown in Figure 4.16 according to 1971-2000 base. Also, the peaks will diverge about 0.99°C from each other in the future with respect to 1971-2000, which will further increase the occurrence of extreme events. The hot period has 171.2 days in the past as shown in Table 4.6 and taken as the length of a year. Then, 1-year, 10-year, 30-year, 50-year and 100-year temperature events are calculated for the length of future hot period that they would be seen in every 0.091, 0.492, 1.127,

1.663 and 2.831 years, respectively. This means that a 1-year temperature would be seen once in every 2 weeks, a 10-year temperature would be seen 2 times in every year, a 30-year temperature would be seen once in every year, a 50-year temperature would be seen 3 times in every 5 years, a 100-year temperature would be seen once in every 3 years. Additional variables are given in Table 4.6.

For MPI-ESM-MR RCP8.5 dataset, parameters of the Gaussians are $\mu_{cold}^{past} = 16.97°C$, $\sigma_{cold}^{past} = 6.09°C$ for the cold side, $\mu_{hot}^{past} = 35.58°C$, $\sigma_{hot}^{past} = 5.6°C$ for the hot side in 1971-2000 curve. Between 2070-2099, parameters are $\mu_{cold}^{future} = 20.21°C$, $\sigma_{cold}^{future} = 6.84°C$ for the cold side, $\mu_{hot}^{future} = 40.29°C$, $\sigma_{hot}^{future} = 6.02°C$ for the hot side.The mean temperatures will increase as shown in Figure 4.16 according to 1971-2000 base. Also, the peaks will diverge about 1.48°C from each other in the future with respect to 1971-2000, which will further increase the occurrence of extreme events. The hot period has 184.6 days in the past as shown in Table 4.4 and taken as the length of a year. Then, 1-year, 10-year, 30-year, 50-year and 100-year temperature events are calculated for the length of future hot period that they would be seen in every 0.075, 0.358, 0.771, 1.104 and 1.805 years, respectively. This means that a 1-year temperature would be seen once in every 2 weeks, a 10-year temperature would be seen 3 times in every 3 years, a 30-year temperature would be seen 3 times in every 2 years, a 50-year temperature would be seen once in every year, a 100-year temperature would be seen once in every 2 years. Additional variables are given in Table 4.4.

For HADGEM2-ES RCP8.5 dataset, parameters of the Gaussians are $\mu_{cold}^{past} = 15.35°C$, $\sigma_{cold}^{past} = 5.65°C$ for the cold side, $\mu_{hot}^{past} = 34.67°C$, $\sigma_{hot}^{past} = 5.34°C$ for the hot side in 1971-2000 curve. For 2070-2099, parameters are $\mu_{cold}^{future} = 22.13°C$, $\sigma_{cold}^{future} = 6.49°C$ for the cold side, $\mu_{hot}^{future} = 43.05°C$, $\sigma_{hot}^{future} = 5.79°C$ for the hot side. The mean temperatures will increase as shown in Figure 4.16 according to 1971-2000 base. Also, the peaks will diverge about 1.6°C from each other in the future with respect to 1971-2000, which will further increase the occurrence of extreme events. The hot period has 171.2 days in the past as shown in Table 4.8 and taken as the length of a year. Then, 1-year, 10-year, 30-year, 50-year and 100-year temperature events are calculated for the length of future hot period that they would be seen in every 0.021,

0.067, 0.122, 0.162 and 0.239 years, respectively. This means that a 1-year temperature would be seen once in every 3.7 days, a 10-year temperature would be seen once in every 11.8 days, a 30-year temperature would be seen once in every 3 weeks, a 50-year temperature would be seen once in every month, a 100-year temperature would be seen 4 times in every year. Additional variables are given in Table 4.8.

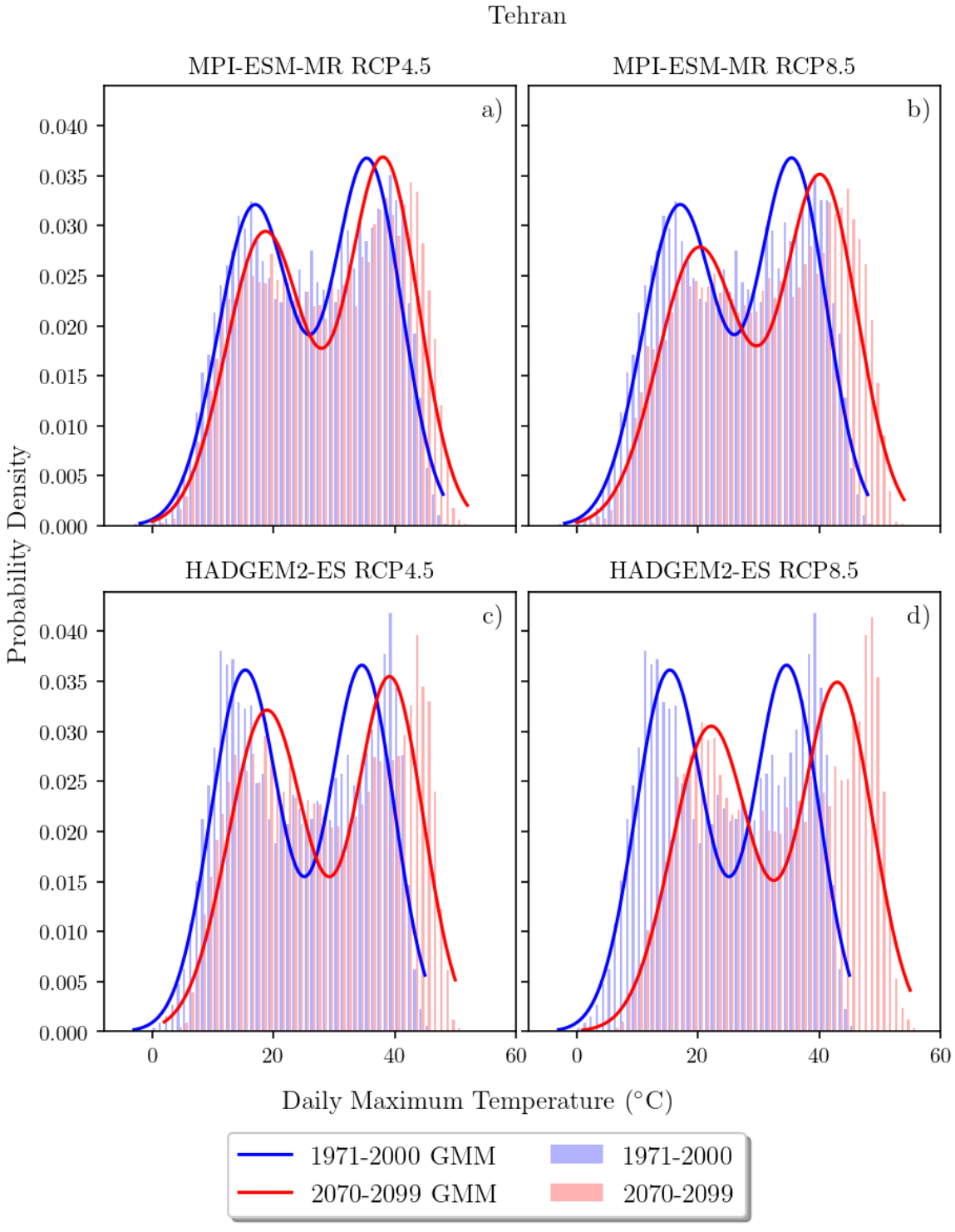

Figure 4.16. Tehran Daily Maximum Temperatures histogram at sea level for 1971-2000 and 2070-2099 and corresponding Gaussian Mixture Model fits: (a) MPI-ESM-MR RCP4.5, (b) MPI-ESM-MR RCP8.5, (c) HadGEM2-ES RCP4.5, (d) HadGEM2-ES RCP8.5

Table 4.1. Gaussian Parameter for city histograms (MPI-ESM-MR RCP4.5)

	Alexandria	Algiers	Amman	Baghdad	Basrah	Cairo	Casablanca	Dubai
μ_{hot}^{past}	29.6	27.4	34.8	39.1	40.3	34.9	26.4	34.8
σ_{hot}^{past}	3.4	4.6	4.9	5.3	4.9	4.2	4.3	3.0
μ_{cold}^{past}	18.1	15.4	18.8	18.7	21.0	19.8	17.3	23.8
σ_{cold}^{past}	3.4	3.4	5.0	5.8	5.8	4.4	3.1	3.5
$\lvert\mathcal{N}(\mu_{hot}^{past}, \sigma_{hot}^{past})\rvert$	199.2	168.6	206.9	185.1	183.3	202.7	164.7	175.4
$\Delta\mu^{past}$	11.5	12.0	16.0	20.4	19.4	15.1	9.0	11.1
μ_{hot}^{future}	31.6	29.7	37.3	42.0	43.1	37.5	28.6	37.1
σ_{hot}^{future}	3.5	4.6	5.0	5.3	4.8	4.1	4.5	3.0
μ_{cold}^{future}	20.0	17.1	20.8	20.8	23.0	22.1	19.0	25.4
σ_{cold}^{future}	3.5	3.5	5.3	6.3	6.2	4.7	3.3	3.5
$\lvert\mathcal{N}(\mu_{hot}^{future}, \sigma_{hot}^{future})\rvert$	193.6	166.6	204.2	186.0	183.4	195.0	166.8	180.4
$\Delta\mu^{future}$	11.6	12.6	16.4	21.2	20.1	15.3	9.7	11.7
$\Delta\mu^{future} - \Delta\mu^{past}$	0.1	0.6	0.4	0.7	0.8	0.2	0.6	0.6
1-year event	0.1786	0.2180	0.2147	0.2046	0.2114	0.2160	0.1840	0.1116
10-year event	1.1805	1.4855	1.4831	1.4206	1.5376	1.6026	1.1664	0.6438
30-year event	2.9569	3.7668	3.7837	3.6400	4.0370	4.2514	2.8562	1.5174
50-year event	4.5451	5.8209	5.8633	5.6538	6.3444	6.7144	4.3423	2.2690
100-year event	8.1671	10.5311	10.6473	10.3026	11.7506	12.5210	7.6839	3.9299

Table 4.2. Gaussian Parameter for city histograms (MPI-ESM-MR RCP4.5) (continued)

	Istanbul	Jeddah	Khartoum	Madrid	NDjamena	Riyadh	Sanaa	Tehran
μ_{hot}^{past}	23.5	34.9	39.9	30.7	39.1	41.9	39.5	35.6
σ_{hot}^{past}	3.8	2.3	2.4	5.2	2.7	3.8	2.2	5.6
μ_{cold}^{past}	11.8	26.4	30.8	14.8	33.6	26.4	33.9	17.0
σ_{cold}^{past}	3.9	2.8	3.7	4.4	3.7	5.3	2.4	6.1
$\lvert\mathcal{N}(\mu_{hot}^{past}, \sigma_{hot}^{past})\rvert$	176.3	199.6	228.7	136.5	250.9	187.1	199.0	184.6
$\Delta\mu^{past}$	11.7	8.5	9.1	15.9	5.5	15.5	5.6	18.6
μ_{hot}^{future}	25.3	37.0	42.7	33.2	42.1	46.1	42.1	38.2
σ_{hot}^{future}	3.9	2.4	2.6	5.4	2.8	2.7	2.3	5.8
μ_{cold}^{future}	13.4	27.8	32.5	16.0	36.2	30.5	35.9	18.6
σ_{cold}^{future}	3.8	3.0	4.1	4.4	3.8	7.1	2.4	6.4
$\lvert\mathcal{N}(\mu_{hot}^{future}, \sigma_{hot}^{future})\rvert$	172.1	204.7	232.1	150.5	245.4	153.2	202.2	189.2
$\Delta\mu^{future}$	11.9	9.2	10.2	17.2	5.8	15.6	6.2	19.6
$\Delta\mu^{future} - \Delta\mu^{past}$	0.2	0.7	1.1	1.3	0.3	0.1	0.5	1.0
1-year event	0.2300	0.0662	0.0366	0.1875	0.0443	0.4361	0.0413	0.2181
10-year event	1.5557	0.3143	0.1455	1.1862	0.1996	9.9415	0.1782	1.4789
30-year event	3.9236	0.6750	0.2880	2.8982	0.4205	48.3704	0.3688	3.7333
50-year event	6.0461	0.9667	0.3973	4.4006	0.5975	102.5177	0.5200	5.7552
100-year event	10.8937	1.5790	0.6174	7.7724	0.9665	288.0444	0.8328	10.3750

Table 4.3. Gaussian Parameter for city histograms (MPI-ESM-MR RCP8.5)

	Alexandria	Algiers	Amman	Baghdad	Basrah	Cairo	Casablanca	Dubai
μ_{hot}^{past}	29.6	27.4	34.8	39.1	40.3	34.9	26.3	34.8
σ_{hot}^{past}	3.4	4.6	4.9	5.3	4.9	4.2	4.3	3.0
μ_{cold}^{past}	18.1	15.4	18.8	18.7	21.0	19.8	17.3	23.8
σ_{cold}^{past}	3.4	3.4	5.0	5.8	5.8	4.4	3.1	3.5
$\lvert\mathcal{N}(\mu_{hot}^{past}, \sigma_{hot}^{past})\rvert$	199.3	168.6	206.5	185.1	183.3	202.7	164.7	175.4
$\Delta\mu^{past}$	11.5	12.0	16.0	20.4	19.4	15.1	9.0	11.1
μ_{hot}^{future}	33.6	32.2	39.6	44.4	45.4	39.7	29.9	39.0
σ_{hot}^{future}	3.7	4.9	5.0	5.6	5.1	4.5	4.6	3.1
μ_{cold}^{future}	21.4	19.1	22.4	22.3	24.7	23.6	20.5	27.1
σ_{cold}^{future}	3.8	3.8	5.7	6.6	6.5	5.0	3.3	3.6
$\lvert\mathcal{N}(\mu_{hot}^{future}, \sigma_{hot}^{future})\rvert$	193.9	176.2	202.9	184.7	186.4	196.4	195.0	182.8
$\Delta\mu^{future}$	12.2	13.1	17.2	22.1	20.7	16.1	9.3	11.9
$\Delta\mu^{future} - \Delta\mu^{past}$	0.673	1.106	1.164	1.643	1.317	0.941	0.334	0.840
1-year event	0.0386	0.0490	0.0632	0.0587	0.0542	0.0457	0.0693	0.0277
10-year event	0.1513	0.2066	0.3095	0.2686	0.2456	0.1962	0.3308	0.1036
30-year event	0.2982	0.4208	0.6779	0.5690	0.5182	0.4039	0.7106	0.2010
50-year event	0.4106	0.5882	0.9804	0.8102	0.7367	0.5678	1.0174	0.2754
100-year event	0.6364	0.9303	1.6243	1.3136	1.1922	0.9053	1.6606	0.4243

Table 4.4. Gaussian Parameter for city histograms (MPI-ESM-MR RCP8.5) (continued)

	Istanbul	Jeddah	Khartoum	Madrid	NDjamena	Riyadh	Sanaa	Tehran
μ_{hot}^{past}	23.5	34.9	39.9	30.7	39.1	41.9	39.5	35.6
σ_{hot}^{past}	3.8	2.3	2.4	5.2	2.7	3.8	2.2	5.6
μ_{cold}^{past}	11.8	26.4	30.8	14.8	33.6	26.4	33.9	17.0
σ_{cold}^{past}	3.9	2.8	3.7	4.4	3.7	5.3	2.4	6.1
$\lvert\mathcal{N}(\mu_{hot}^{past}, \sigma_{hot}^{past})\rvert$	176.3	199.6	228.5	136.5	250.9	187.2	199.0	184.6
$\Delta\mu^{past}$	11.7	8.5	9.1	15.9	5.5	15.5	5.6	18.6
μ_{hot}^{future}	27.4	39.5	45.2	36.1	44.6	48.6	44.5	40.3
σ_{hot}^{future}	4.1	2.5	3.0	5.7	3.0	2.9	2.5	6.0
μ_{cold}^{future}	14.6	29.8	34.6	17.6	38.5	32.5	38.2	20.2
σ_{cold}^{future}	4.0	3.3	4.5	4.5	4.0	7.4	2.4	6.8
$\lvert\mathcal{N}(\mu_{hot}^{future}, \sigma_{hot}^{future})\rvert$	176.0	197.7	233.0	159.9	250.9	152.0	204.8	188.0
$\Delta\mu^{future}$	12.7	9.6	10.6	18.5	6.0	16.1	6.3	20.1
$\Delta\mu^{future} - \Delta\mu^{past}$	1.0	1.1	1.5	2.6	0.5	0.6	0.7	1.5
1-year event	0.0579	0.0112	0.0073	0.0478	0.0085	0.0371	0.0072	0.0748
10-year event	0.2600	0.0289	0.0156	0.1977	0.0208	0.2562	0.0153	0.3580
30-year event	0.5455	0.0473	0.0230	0.3990	0.0331	0.7116	0.0229	0.7706
50-year event	0.7732	0.0598	0.0277	0.5554	0.0413	1.1643	0.0278	1.1044
100-year event	1.2461	0.0829	0.0359	0.8734	0.0561	2.3068	0.0364	1.8054

Table 4.5. Gaussian Parameter for city histograms (HadGEM2-ES RCP4.5)

	Alexandria	Algiers	Amman	Baghdad	Basrah	Cairo	Casablanca	Dubai
μ_{hot}^{past}	29.8	27.3	34.1	38.2	39.9	35.2	25.5	34.1
σ_{hot}^{past}	3.7	3.9	4.5	5.3	4.8	4.4	4.2	2.8
μ_{cold}^{past}	17.8	15.2	18.6	18.1	20.2	19.6	16.5	22.6
σ_{cold}^{past}	3.4	3.4	4.9	5.7	5.8	4.5	3.1	3.4
$\lvert\mathcal{N}(\mu_{hot}^{past}, \sigma_{hot}^{past})\rvert$	192.9	147.1	191.4	174.3	173.0	193.6	157.0	188.8
$\Delta\mu^{past}$	12.0	12.0	15.5	20.1	19.7	15.7	9.0	11.4
μ_{hot}^{future}	33.4	31.4	38.2	42.6	44.9	39.1	27.7	37.5
σ_{hot}^{future}	3.9	4.3	4.6	5.0	4.1	4.6	4.4	2.8
μ_{cold}^{future}	20.5	17.7	21.5	21.1	23.9	22.3	19.0	25.7
σ_{cold}^{future}	3.5	3.7	5.2	6.3	6.8	4.7	3.2	3.5
$\lvert\mathcal{N}(\mu_{hot}^{future}, \sigma_{hot}^{future})\rvert$	191.2	157.1	191.5	174.4	162.4	193.9	186.7	189.5
$\Delta\mu^{future}$	12.9	13.7	16.7	21.5	21.0	16.7	8.7	11.7
$\Delta\mu^{future} - \Delta\mu^{past}$	0.9	1.7	1.2	1.4	1.2	1.1	-0.3	0.3
1-year event	0.0615	0.0464	0.0804	0.1518	0.1493	0.0757	0.1689	0.0454
10-year event	0.2848	0.1836	0.4344	1.1541	1.3771	0.3771	1.1010	0.2144
30-year event	0.6058	0.3622	0.9969	3.1368	4.1807	0.8294	2.7324	0.4654
50-year event	0.8640	0.4988	1.4736	5.0214	7.0677	1.2011	4.1803	0.6716
100-year event	1.4039	0.7731	2.5147	9.5558	14.5248	1.9922	7.4604	1.1110

Table 4.6. Gaussian Parameter for city histograms (HadGEM2-ES RCP4.5) (continued)

	Istanbul	Jeddah	Khartoum	Madrid	NDjamena	Riyadh	Sanaa	Tehran
μ_{hot}^{past}	23.6	35.5	40.4	31.6	39.7	42.7	39.5	34.7
σ_{hot}^{past}	3.6	2.3	2.9	5.2	3.1	2.7	2.0	5.3
μ_{cold}^{past}	12.0	26.1	30.5	14.6	33.4	27.2	34.0	15.3
σ_{cold}^{past}	3.9	2.9	4.0	4.5	3.8	6.5	2.2	5.7
$\lvert\mathcal{N}(\mu_{hot}^{past}, \sigma_{hot}^{past})\rvert$	162.4	196.4	208.0	145.6	236.6	158.4	173.9	171.2
$\Delta\mu^{past}$	11.6	9.3	9.8	17.0	6.3	15.5	5.4	19.3
μ_{hot}^{future}	27.5	39.2	44.2	36.1	43.7	46.5	42.7	39.2
σ_{hot}^{future}	4.1	2.3	2.9	5.7	2.8	2.7	2.1	5.5
μ_{cold}^{future}	14.5	29.0	33.5	17.0	36.7	30.5	37.3	18.9
σ_{cold}^{future}	4.0	3.1	4.3	4.8	3.8	7.1	2.2	6.4
$\lvert\mathcal{N}(\mu_{hot}^{future}, \sigma_{hot}^{future})\rvert$	165.2	192.0	216.5	153.4	231.7	159.6	196.6	170.6
$\Delta\mu^{future}$	12.9	10.2	10.7	19.2	7.0	16.1	5.4	20.3
$\Delta\mu^{future} - \Delta\mu^{past}$	1.4	0.9	0.9	2.2	0.7	0.5	-0.1	1.0
1-year event	0.0441	0.0253	0.0326	0.0691	0.0494	0.0315	0.0179	0.0912
10-year event	0.1656	0.1050	0.1395	0.3101	0.2886	0.1255	0.0600	0.4921
30-year event	0.3179	0.2173	0.2893	0.6480	0.7019	0.2525	0.1110	1.1267
50-year event	0.4321	0.3074	0.4086	0.9160	1.0697	0.3520	0.1489	1.6630
100-year event	0.6577	0.4958	0.6565	1.4700	1.9089	0.5559	0.2232	2.8314

Table 4.7. Gaussian Parameter for city histograms (HadGEM2-ES RCP8.5)

	Alexandria	Algiers	Amman	Baghdad	Basrah	Cairo	Casablanca	Dubai
μ_{hot}^{past}	29.9	27.3	34.1	38.2	39.9	35.2	25.5	34.1
σ_{hot}^{past}	3.7	3.9	4.5	5.3	4.8	4.4	4.2	2.8
μ_{cold}^{past}	17.8	15.2	18.6	18.1	20.2	19.6	16.5	22.6
σ_{cold}^{past}	3.4	3.4	4.9	5.7	5.8	4.5	3.1	3.4
$\lvert\mathcal{N}(\mu_{hot}^{past}, \sigma_{hot}^{past})\rvert$	192.7	147.1	191.4	174.4	173.1	193.6	157.1	188.8
$\Delta\mu^{past}$	12.0	12.0	15.5	20.1	19.7	15.7	9.0	11.4
μ_{hot}^{future}	36.8	36.3	42.6	46.7	47.8	42.4	33.3	40.5
σ_{hot}^{future}	3.8	4.5	5.0	5.6	4.6	4.4	4.1	2.9
μ_{cold}^{future}	24.7	21.6	25.7	26.0	28.3	27.6	22.9	29.3
σ_{cold}^{future}	3.9	4.2	5.7	6.2	6.1	5.1	3.6	3.2
$\lvert\mathcal{N}(\mu_{hot}^{future}, \sigma_{hot}^{future})\rvert$	190.4	162.8	191.6	174.4	167.2	191.7	186.1	179.6
$\Delta\mu^{future}$	12.1	14.7	16.9	20.6	19.5	14.7	10.3	11.2
$\Delta\mu^{future} - \Delta\mu^{past}$	0.1	2.6	1.4	0.6	-0.2	-0.9	1.4	-0.2
1-year event	0.0139	0.0085	0.0124	0.0218	0.0254	0.0213	0.0151	0.0086
10-year event	0.0430	0.0185	0.0334	0.0748	0.1038	0.0783	0.0531	0.0208
30-year event	0.0773	0.0278	0.0556	0.1399	0.2139	0.1524	0.1023	0.0335
50-year event	0.1023	0.0339	0.0709	0.1886	0.3022	0.2094	0.1402	0.0422
100-year event	0.1510	0.0447	0.0993	0.2845	0.4870	0.3246	0.2170	0.0582

Table 4.8. Gaussian Parameter for city histograms (HadGEM2-ES RCP8.5) (continued)

	Istanbul	Jeddah	Khartoum	Madrid	NDjamena	Riyadh	Sanaa	Tehran
μ_{hot}^{past}	23.6	35.5	40.4	31.6	39.7	42.7	39.5	34.7
σ_{hot}^{past}	3.6	2.3	2.9	5.2	3.1	2.7	2.0	5.3
μ_{cold}^{past}	12.0	26.1	30.5	14.6	33.4	27.2	34.0	15.3
σ_{cold}^{past}	3.9	2.9	4.0	4.5	3.8	6.5	2.2	5.7
$\lvert\mathcal{N}(\mu_{hot}^{past}, \sigma_{hot}^{past})\rvert$	162.5	196.4	208.0	145.7	236.8	158.4	174.0	171.2
$\Delta\mu^{past}$	11.6	9.3	9.8	17.0	6.3	15.5	5.4	19.3
μ_{hot}^{future}	28.5	42.0	48.3	39.6	50.1	49.8	46.8	43.1
σ_{hot}^{future}	3.7	2.2	2.2	6.7	2.1	2.7	2.1	5.8
μ_{cold}^{future}	17.4	33.2	40.4	19.1	44.7	34.8	41.7	22.1
σ_{cold}^{future}	3.2	2.8	3.1	4.3	2.6	6.4	2.6	6.5
$\lvert\mathcal{N}(\mu_{hot}^{future}, \sigma_{hot}^{future})\rvert$	162.1	189.3	224.6	190.7	191.9	147.2	223.2	175.8
$\Delta\mu^{future}$	11.1	8.9	7.9	20.5	5.4	15.0	5.1	20.9
$\Delta\mu^{future} - \Delta\mu^{past}$	-0.5	-0.5	-1.9	3.5	-0.9	-0.5	-0.4	1.6
1-year event	0.0377	0.0053	0.0049	0.0144	0.0033	0.0073	0.0028	0.0208
10-year event	0.1625	0.0111	0.0143	0.0356	0.0063	0.0154	0.0037	0.0673
30-year event	0.3390	0.0169	0.0271	0.0559	0.0098	0.0233	0.0045	0.1220
50-year event	0.4805	0.0208	0.0373	0.0692	0.0124	0.0287	0.0050	0.1618
100-year event	0.7760	0.0279	0.0588	0.0928	0.0177	0.0383	0.0057	0.2389

5. CONCLUSION

Gaussian mixture model and empirical rule are used to calculate the return periods of extreme weather events in 16 most populous cities in MENA region. The extreme events consistently become more frequent for RCP8.5 scenarios for both GCM, except Riyadh where the largest decrease in standard deviations occurs unlike other cities as the city's climate would change in the future. Even though it seems like frequencies of extreme events are increasing in Riyadh, this would mean that there would be constant heatwaves over Riyadh with mean temperatures much higher than current temperatures.

The change in frequencies follow similar patterns in all cities. Also, mean temperature increases are seen in all cities. The hot side means for daily maximum temperatures will increase 2.56°C, 4.83°C, 3.88°C and 7.68°C on average for all cities in the future for MPI-ESM-MR RCP4.5, MPI-ESM-MR RCP8.5, HadGEM2-ES RCP4.5 and HadGEM2-ES RCP8.5, respectively.

In general, the peak differences will further increase in the future. This divergence would cause cities to have shorter transition seasons and transform into only 2 seasons. In some cities, change in peak difference seems to be negative for HadGEM2-ES dataset on the contrary to MPI-ESM-MR dataset, which might be resulted from the differences in model components. These increases in peak differences would cause more severe extreme events.

Temperatures of cities on south of the Sahara Desert show a single Gaussian as they have tropical climates. These cities would have bimodal temperature distribution in the future as the climate classification pattern move northward with climate change. Decrease observed in peak differences in some cities would also occur due to this climate shift. 2 most populous cities in MENA region, Cairo and Istanbul, would have hundredfold more frequent extreme hot weather events between 2070 and 2099. These two cities would be exposed to temperatures never seen before throughout hu-

man history. Considering their high population, extreme weather events would cause devastating results.

The health effects of climate change become more apparent with extreme events such as long heat waves. Sherwood and Huber proposed that humans cannot tolerate wet-bulb temperatures exceeding 35°C for long periods, as dissipation of metabolic heat becomes impossible [26]. With the change in frequency of extreme events and increase in means, probability of heat waves occurring would be expected to increase. As the MENA region and the 16 cities in question have population of 556,246,000 and 95,621,000, respectively, the aftermath of an extreme event might be devastating. Also, increased mean temperatures and frequent extreme events would affect agriculture and vegetation, cause wildfires, black outs due to increased demand, and landslides due to permafrost changes. IPCC's Special Report on Climate Change and Land states that climate change creates additional stresses on land, exacerbating existing risks to livelihoods, biodiversity, human and ecosystem health, infrastructure, and food systems. Increasing impacts on land are projected under all future Greenhouse Gas emission scenarios [47].

In this study, coarse-resolution GCM outputs are dynamically downscaled to 50 km, elevation correction for sea level is applied and temperatures at city centers are calculated from the nearest 4 grid points using inverse distance squared weighted interpolation method from aforementioned 50-km resolution RCM dataset. For further studies, higher resolution RCM outputs can be used to obtain better results on city scale. Thus, the city topographies and their effects on city's climate might be modelled better and more robust statistics could be obtained.

REFERENCES

1. Masson-Delmotte, V., P. Zhai, H. O. Pörtner, D. Roberts, J. Skea, P. Shukla, A. Pirani, W. Moufouma-Okia, C. Péan, R. Pidcock, S. Connors, J. B. R. Matthews, Y. Chen, X. Zhou, M. I. Gomis, E. Lonnoy, T. Maycock, M. Tignor and T. Waterfield (Editors), *Global warming of 1.5°C. An IPCC Special Report on the impacts of global warming of 1.5°C above pre-industrial levels and related global greenhouse gas emission pathways, in the context of strengthening the global response to the threat of climate change, sustainable development, and efforts to eradicate poverty*, IPCC, In Press, 2018.

2. IPCC, *Climate Change 2013: The Physical Science Basis. Contribution of Working Group I to the Fifth Assessment Report of the Intergovernmental Panel on Climate Change*, Cambridge University Press, Cambridge, United Kingdom and New York, NY, USA, 2013, `www.climatechange2013.org`.

3. Crimmins, A., J. Balbus, J. Gamble, C. Beard, J. Bell, D. Dodgen, R. Eisen, N. Fann, M. Hawkins, S. Herring, L. Jantarasami, D. Mills, S. Saha, M. Sarofim, J. Trtanj and L. Ziska, *The Impacts of Climate Change on Human Health in the United States: A Scientific Assessment*, Tech. rep., 2016, `https://doi.org/10.7930/j0r49nqx`.

4. Robine, J.-M., S. L. K. Cheung, S. L. Roy, H. V. Oyen, C. Griffiths, J.-P. Michel and F. R. Herrmann, "Death toll exceeded 70,000 in Europe during the summer of 2003", *Comptes Rendus Biologies*, Vol. 331, No. 2, pp. 171 – 178, 2008, `http://www.sciencedirect.com/science/article/pii/S1631069107003770`.

5. United Nations, Department of Economic and Social Affairs, Population Division, *World Urbanization Prospects: The 2018 Revision*, online edn., 2018.

6. Van Bavel, J., "The world population explosion: causes, backgrounds and - projections for the future.", *Facts, views Vis. ObGyn*, Vol. 5, No. 4, pp.

281–91, 2013, http://www.ncbi.nlm.nih.gov/pubmed/24753956http://www.pubmedcentral.nih.gov/articlerender.fcgi?artid=PMC3987379.

7. Burgess, E., "General remarks on the temperature of the terrestrial globe and planetary spaces", *American Journal of Science*, Vol. 32, pp. 1–20, 2019.

8. Tyndall, J., *On the Absorption And Radiation Of Heat By Gases And Vapours, And On The Physical Connexion Of Radiation, Absorption, And Conduction*, p. 1–1, Cambridge Library Collection - Physical Sciences, Cambridge University Press, 2014.

9. Arrhenius, S. and E. S. Holden, "On The Influence Of Carbonic Acid In The Air Upon The Temperature Of The Earth", *Publications of the Astronomical Society of the Pacific*, Vol. 9, No. 54, pp. 14–24, 1897, http://www.jstor.org/stable/40670917.

10. F. Richardson, L., *Weather Prediction by Numerical Process*, Vol. 20, Jan 1922.

11. Milanković, M. and J. akademija znanosti i umjetnosti, *Théorie mathématique des phénomènes thermiques produits par la radiation solaire*, Gauthier-Villars et Cie, 1920, https://books.google.com.tr/books?id=1oJZAAAAYAAJ.

12. Lüthi, D., M. Le Floch, B. Bereiter, T. Blunier, J.-M. Barnola, U. Siegenthaler, R. Dominique, J. Jouzel, H. Fischer, K. Kawamura and T. Stocker, "High-resolution carbon dioxide concentration record 650,000-800,000 years before present", *Nature*, Vol. 453, pp. 379–82, Jun 2008.

13. Callendar, G. S., "The artificial production of carbon dioxide and its influence on temperature", *Quarterly Journal of the Royal Meteorological Society*, Vol. 64, No. 275, pp. 223–240, 1938, https://rmets.onlinelibrary.wiley.com/doi/abs/10.1002/qj.49706427503.

14. Phillips, N. A., "The general circulation of the atmosphere: A numerical ex-

periment", *Quarterly Journal of the Royal Meteorological Society*, Vol. 82, No. 352, pp. 123–164, 1956, https://rmets.onlinelibrary.wiley.com/doi/abs/10.1002/qj.49708235202.

15. Möller, F., "On the influence of changes in the CO2 concentration in air on the radiation balance of the Earth's surface and on the climate", *Journal of Geophysical Research (1896-1977)*, Vol. 68, No. 13, pp. 3877–3886, 1963, https://agupubs.onlinelibrary.wiley.com/doi/abs/10.1029/JZ068i013p03877.

16. Manabe, S. and R. T. Wetherald, "Thermal Equilibrium of the Atmosphere with a Given Distribution of Relative Humidity", *Journal of the Atmospheric Sciences*, Vol. 24, No. 3, pp. 241–259, 1967, https://doi.org/10.1175/1520-0485(1975)005%3C0003:AGOACM%3E2.0.CO;2.

17. Manabe, S., K. Bryan and M. J. Spelman, "A Global Ocean-Atmosphere Climate Model. Part I. The Atmospheric Circulation", *Journal of Physical Oceanography*, Vol. 5, No. 1, pp. 3–29, 1975, https://doi.org/10.1175/1520-0485(1975)005<0003:AGOACM>2.0.CO;2.

18. NJ, N., J. Alcamo, G. Davis, B. de Vries, J. Fenhann, S. Gaffin, K. Gregory, A. Grubler, T. Jung, T. Kram, E. La Rovere, L. Michaelis, S. Mori, T. Morita, W. Pepper, P. HM, L. Price, K. Riahi, A. Roehrl and D. Z, *IPCC Special Report on Emissions Scenarios*, Jan 2000.

19. De Bono, A., P. Peduzzi, S. Kluser and G. Giuliani, "Impacts of summer 2003 heat wave in Europe", *United Nations Environment Programme*, 2004.

20. Kuglitsch, F. G., A. Toreti, E. Xoplaki, P. M. Della-Marta, C. S. Zerefos, M. Türkeş and J. Luterbacher, "Heat wave changes in the eastern Mediterranean since 1960", *Geophysical Research Letters*, Vol. 37, No. 4, 2010, https://agupubs.onlinelibrary.wiley.com/doi/abs/10.1029/2009GL041841.

21. Lelieveld, J., P. Hadjinicolaou, E. Kostopoulou, J. Chenoweth, M. El Maayar,

C. Giannakopoulos, C. Hannides, M. A. Lange, M. Tanarhte, E. Tyrlis and E. Xoplaki, "Climate change and impacts in the Eastern Mediterranean and the Middle East", *Climatic Change*, Vol. 114, No. 3, pp. 667–687, Oct 2012, https://doi.org/10.1007/s10584-012-0418-4.

22. Lelieveld, J., Y. Proestos, P. Hadjinicolaou, M. Tanarhte, E. Tyrlis and G. Zittis, "Strongly increasing heat extremes in the Middle East and North Africa (MENA) in the 21st century", *Climatic Change*, Vol. 137, No. 1, pp. 245–260, Jul 2016, https://doi.org/10.1007/s10584-016-1665-6.

23. Öztürk, T., Z. P. Ceber, M. Türkeş and M. L. Kurnaz, "Projections of climate change in the Mediterranean Basin by using downscaled global climate model outputs", *International Journal of Climatology*, Vol. 35, No. 14, pp. 4276–4292, 2015, https://rmets.onlinelibrary.wiley.com/doi/abs/10.1002/joc.4285.

24. Sillmann, J., V. V. Kharin, F. W. Zwiers, X. Zhang and D. Bronaugh, "Climate extremes indices in the CMIP5 multimodel ensemble: Part 2. Future climate projections", *Journal of Geophysical Research: Atmospheres*, Vol. 118, No. 6, pp. 2473–2493, 2013, https://agupubs.onlinelibrary.wiley.com/doi/abs/10.1002/jgrd.50188.

25. Efthymiadis, D., C. M. Goodess and P. D. Jones, "Trends in Mediterranean gridded temperature extremes and large-scale circulation influences", *Natural Hazards and Earth System Sciences*, Vol. 11, No. 8, pp. 2199–2214, 2011, https://www.nat-hazards-earth-syst-sci.net/11/2199/2011/.

26. Sherwood, S. C. and M. Huber, "An adaptability limit to climate change due to heat stress", *Proceedings of the National Academy of Sciences*, Vol. 107, No. 21, pp. 9552–9555, 2010, https://www.pnas.org/content/107/21/9552.

27. Houghton, J., Y. Ding, D. Griggs, M. Noguer, P. van der Linden, X. Dai, K. Maskell and C. Johnson (Editors), *Climate Change 2001: The Scientific Basis. Contribution of Working Group I to the Third Assessment Report of the Intergovernmental*

Panel on Climate Change, IPCC, Cambridge University Press, United Kingdom and New York, NY, USA, 881pp, 2001.

28. Wilby, R. L., J. Troni, Y. Biot, L. Tedd, B. C. Hewitson, D. M. Smith and R. T. Sutton, "A review of climate risk information for adaptation and development planning", *International Journal of Climatology*, Vol. 29, No. 9, pp. 1193–1215, 2009, https://rmets.onlinelibrary.wiley.com/doi/abs/10.1002/joc.1839.

29. National Oceanic and Atmospheric Administration, *Top Tens: Breakthroughs The First Climate Model*, 2007, https://celebrating200years.noaa.gov/breakthroughs/climate_model/welcome.html.

30. Giorgetta, M. A., J. Jungclaus, C. H. Reick, S. Legutke, J. Bader, M. Böttinger, V. Brovkin, T. Crueger, M. Esch, K. Fieg, K. Glushak, V. Gayler, H. Haak, H.-D. Hollweg, T. Ilyina, S. Kinne, L. Kornblueh, D. Matei, T. Mauritsen, U. Mikolajewicz, W. Mueller, D. Notz, F. Pithan, T. Raddatz, S. Rast, R. Redler, E. Roeckner, H. Schmidt, R. Schnur, J. Segschneider, K. D. Six, M. Stockhause, C. Timmreck, J. Wegner, H. Widmann, K.-H. Wieners, M. Claussen, J. Marotzke and B. Stevens, "Climate and carbon cycle changes from 1850 to 2100 in MPI-ESM simulations for the Coupled Model Intercomparison Project phase 5", *Journal of Advances in Modeling Earth Systems*, Vol. 5, No. 3, pp. 572–597, 2013, https://agupubs.onlinelibrary.wiley.com/doi/abs/10.1002/jame.20038.

31. Martin, T. H. D. T. G. M., N. Bellouin, W. J. Collins, I. D. Culverwell, P. R. Halloran, S. C. Hardiman, T. J. Hinton, C. D. Jones, R. E. McDonald, A. J. McLaren, F. M. O'Connor, M. J. Roberts, J. M. Rodriguez, S. Woodward, M. J. Best, M. E. Brooks, A. R. Brown, N. Butchart, C. Dearden, S. H. Derbyshire, I. Dharssi, M. Doutriaux-Boucher, J. M. Edwards, P. D. Falloon, N. Gedney, L. J. Gray, H. T. Hewitt, M. Hobson, M. R. Huddleston, J. Hughes, S. Ineson, W. J. Ingram, P. M. James, T. C. Johns, C. E. Johnson, A. Jones, C. P. Jones, M. M. Joshi, A. B. Keen, S. Liddicoat, A. P. Lock, A. V. Maidens, J. C. Manners, S. F. Milton, J. G. L. Rae, J. K. Ridley, A. Sellar, C. A. Senior, I. J. Totterdell, A. Ver-

hoef, P. L. Vidale and A. Wiltshire, "The HadGEM2 family of Met Office Unified Model climate configurations", *Geoscientific Model Development*, Vol. 4, No. 3, pp. 723–757, 2011, https://www.geosci-model-dev.net/4/723/2011/.

32. Elguindi, N., X. Bi, F. Giorgi, B. Nagarajan, J. Pal, F. Solmon, S. Rauscher, A. Zakey, T. O'Brien, R. Nogherotto and G. Giuliani, *Regional Climate Model RegCM Reference Manual Version 4.7*, The Abdus Salam International Centre for Theoretical Physics, Trieste, Italy, Jan 2017.

33. van Vuuren, D. P., J. Edmonds, M. Kainuma, K. Riahi, A. Thomson, K. Hibbard, G. C. Hurtt, T. Kram, V. Krey, J.-F. Lamarque, T. Masui, M. Meinshausen, N. Nakicenovic, S. J. Smith and S. K. Rose, "The representative concentration pathways: an overview", *Climatic Change*, Vol. 109, No. 1, p. 5, Aug 2011, https://doi.org/10.1007/s10584-011-0148-z.

34. Riahi, K., A. Grübler and N. Nakicenovic, "Scenarios of long-term socio-economic and environmental development under climate stabilization", *Technological Forecasting and Social Change*, Vol. 74, No. 7, pp. 887 – 935, 2007, http://www.sciencedirect.com/science/article/pii/S0040162506001387, greenhouse Gases - Integrated Assessment.

35. Fujino, J., R. Nair, M. Kainuma, T. Masui and Y. Matsuoka, "Multi-gas Mitigation Analysis on Stabilization Scenarios Using Aim Global Model", *The Energy Journal*, Vol. 27, pp. 343–353, 2006, http://www.jstor.org/stable/23297089.

36. Hijioka, Y., Y. Matsuoka, H. Nishimoto, T. Masui and M. Kainuma, "Global GHG emission scenarios under GHG concentration stabilization targets", *Journal of Global Environment Engineering*, Vol. 13, pp. 97–108, Mar 2008.

37. Clarke, L., J. Edmonds, H. Jacoby, H. Pitcher, J. Reilly and R. Richels, "Scenarios of greenhouse gas emissions and atmospheric concentrations", , 2007.

38. Smith, S. J. and T. Wigley, "Multi-gas forcing stabilization with Minicam", *The*

Energy Journal, pp. 373–391, 2006.

39. Wise, M., K. Calvin, A. Thomson, L. Clarke, B. Bond-Lamberty, R. Sands, S. J. Smith, A. Janetos and J. Edmonds, "Implications of limiting CO2 concentrations for land use and energy", *Science*, Vol. 324, No. 5931, pp. 1183–1186, 2009.

40. Van Vuuren, D., B. Eickhout, P. Lucas and M. Den Elzen, "Long-term multi-gas scenarios to stabilise radiative forcing—exploring costs and benefits within an integrated assessment framework", *The energy journal*, pp. 201–233, 2006.

41. Van Vuuren, D. P., M. G. Den Elzen, P. L. Lucas, B. Eickhout, B. J. Strengers, B. Van Ruijven, S. Wonink and R. Van Houdt, "Stabilizing greenhouse gas concentrations at low levels: an assessment of reduction strategies and costs", *Climatic change*, Vol. 81, No. 2, pp. 119–159, 2007.

42. *The Coordinated Regional Climate Downscaling Experiment (CORDEX)*, Tech. rep., WCRP, 2018, `https://www.wcrp-climate.org/news/wcrp-newsletter/wcrp-news-articles/1347-wcrp-spotlight-the-coordinated-regional-climate-downscaling-experiment-c`

43. Beck, H., N. Zimmermann, T. Mcvicar, N. Vergopolan, A. Berg and E. Wood, "Present and future Köppen-Geiger climate classification maps at 1-km resolution", *Scientific Data*, Vol. 5, p. 180214, Oct 2018.

44. Organization, I. C. A., *Manual de la Átmosfera Tipo de la OACI: Ampliada Hasta 80 Kilómetros (262 500 Pies)*, ICAO, 2002, `https://books.google.com.tr/books?id=vZO6AQAACAAJ`.

45. Pedregosa, F., G. Varoquaux, A. Gramfort, V. Michel, B. Thirion, O. Grisel, M. Blondel, P. Prettenhofer, R. Weiss, V. Dubourg, J. Vanderplas, A. Passos, D. Cournapeau, M. Brucher, M. Perrot and E. Duchesnay, "Scikit-learn: Machine Learning in Python", *Journal of Machine Learning Research*, Vol. 12, pp. 2825–2830, 2011.

46. Brilliant.org, *Gaussian Mixture Model*, Jul 2019, https://brilliant.org/wiki/gaussian-mixture-model/.

47. *Climate Change and Land, an IPCC special report on climate change, desertification, land degradation, sustainable land management, food security, and greenhouse gas fluxes in terrestrial ecosystems (SRCCL)*, Aug 2019, https://www.ipcc.ch/report/srccl/.

APPENDIX A: Gaussian Mixture Model Python code

```
import numpy as np
import matplotlib.pyplot as plt
import pandas as pd
from sklearn.mixture import GaussianMixture
import math
from os import getcwd, chdir, mkdir, listdir
from os.path import isfile, join, exists
import re
from scipy import special as sps
from scipy import signal as spsig
##########################################
pastStart = 1971
pastEnd = 2000
futureStart = 2070
futureEnd = 2099
areaName = 'THESIS'
model = 'MPI'
scenario = '85'
##########################################
titlefont = {'fontsize': 12,'fontweight': 'normal'}
labelfont = {'fontsize': 12}

# CREATE DIRECTORY
chdir('D:\\DATA\\graphs\\')

if not exists(areaName + '_' + model + '_' + scenario + '_' +
              str(pastStart) + '-' + str(pastEnd) + '_vs_' +
              str(futureStart) + '-' + str(futureEnd)):
    mkdir(areaName + '_' + model + '_' + scenario + '_' +
```

```
30            str(pastStart) + '-' + str(pastEnd) + '_vs_' +
31            str(futureStart) + '-' + str(futureEnd))
32
33  chdir('.\\' + areaName + '_' + model + '_' + scenario + '_' +
34        str(pastStart) + '-' + str(pastEnd) + '_vs_' + str(futureStart) +
35        '-' + str(futureEnd))
36  outputGraphFolder = getcwd()
37
38  if not exists('tas'):
39      mkdir('tas')
40  if not exists('tasmin'):
41      mkdir('tasmin')
42  if not exists('tasmax'):
43      mkdir('tasmax')
44
45  def round_down(num, divisor):
46      if num<0:
47          return num - (10-(-1*num % divisor))
48      else:
49          return num - (num % divisor)
50
51  def round_up(num, divisor):
52      if num % divisor <= 5:
53          return num + (5 - num % divisor)
54      else:
55          return num + (10 - num % divisor)
56
57  variable = {'tasmax': 'Maximum Daily Temperature',
58              'tasmin': 'Minimum Daily Temperature',
59              'tas': 'Mean Daily Temperature'}
60
61  path = 'D:\\DATA\\' + model + '_RCP' + scenario +
62         '_shifttime_elecor_' + areaName + '\\'
```

```
files = [f for f in listdir(path) if isfile(join(path, f))]
files = [f for f in files if f.endswith('.csv')]

excelColumns = ['city', 'variable', 'mu_hot_past', 'sigma_hot_past',
                'mu_cold_past', 'sigma_cold_past', 'hotPeriodDays_past',
                'peakDiffPast', 'mu_hot_future', 'sigma_hot_future',
                'mu_cold_future', 'sigma_cold_future',
                'hotPeriodDays_future', 'peakDiffFuture', 'changePeakDiff',
                '1-year event', '10-year event', '30-year event',
                '50-year event', '100-year event']
excelHolder = pd.DataFrame(columns=excelColumns)

# READ FILE FOR EACH CITY AND DRAW HIST AND FIT
for file in files:
    filename = path + '\\' + file
    datafile = pd.read_csv(filename, sep='\s+', header=0)
    datafile.columns = ['name', 'lon', 'lat', 'year', 'month', 'day',
                        'value', 'drop']
    datafile.drop('drop', axis=1, inplace=True)
    regex = r'(.*)_' + model + r'_RCP' + scenario + r'_1970-2100.csv'
    cityname = re.findall(regex, file)[0]
    array = ['tas', 'tasmin', 'tasmax']
    HistMinMaxSelector = datafile.loc[datafile['name'].isin(array)]['value']
    histMin = round_down(min(HistMinMaxSelector), 10)
    histMax = round_up(max(HistMinMaxSelector), 10)

    for key, value in variable.items():
        dataFuture = datafile.loc[(datafile['name'] == key) &
                                  (datafile['year'] >= futureStart) &
                                  (datafile['year'] <= futureEnd)]
        histFuture = dataFuture['value']
        dataPast = datafile.loc[(datafile['name'] == key) &
                                (datafile['year'] >= pastStart) &
```

```
96                              (datafile['year'] <= pastEnd)]
97          histPast = dataPast['value']
98
99          # gmmFuture FIT
100         gmmFuture = GaussianMixture(n_components=2,
101                                     covariance_type='full',
102                                     n_init=5)
103         gmmFuture = gmmFuture.fit(X=np.expand_dims(histFuture, 1))
104
105         # gmmPast FIT
106         gmmPast = GaussianMixture(n_components=2,
107                                   covariance_type='full',
108                                   n_init=5)
109         gmmPast = gmmPast.fit(X=np.expand_dims(histPast, 1))
110
111         # CREATE GAUSSIAN FROM PARAMETERS
112         gmmFuture_x = np.linspace(int(min(histFuture)),
113                                   int(max(histFuture)),
114                                   1000)
115         gmmFuture_y = np.exp(gmmFuture.score_samples(
116                           gmmFuture_x.reshape(-1, 1)))
117
118         # CREATE GAUSSIAN FOR FUTURE
119         gmmPast_x = np.linspace(int(min(histPast)),
120                                 int(max(histPast)),
121                                 1000)
122         gmmPast_y = np.exp(gmmPast.score_samples(
123                           gmmPast_x.reshape(-1, 1)))
124
125         # PLOT HISTOGAM AND GAUSSIAN FIT
126         fig = plt.figure(figsize=(6.1,5), dpi=150)
127         ax = fig.add_subplot(111)
128         fig.subplots_adjust(left=0.125,right=0.98,bottom=0.1,top=0.95)
```

```
129         # PLOT HISTOGRAM
130         n, bins, patches = ax.hist([histPast, histFuture],
131                                    bins=np.arange(histMin, histMax),
132                                    alpha=0.2,
133                                    color=['teal', 'firebrick'],
134                                    density=1,
135                                    label=[str(pastStart) + '-' + (pastEnd),
136                                           str(futureStart) + '-' +
137                                           str(futureEnd)])
138
139         # PLOT FUTURE AND PAST FIT
140         ax.plot(gmmPast_x, gmmPast_y,
141                 color="blue", lw=2,
142                 label=str(pastStart) + '-' + str(pastEnd) + ' GMM')
143
144         ax.plot(gmmFuture_x, gmmFuture_y,
145                 color="red", lw=2,
146                 label=str(futureStart) + '-' + str(futureEnd) + ' GMM')
147
148         # Annotate diagram
149         ax.set_ylabel("Probability density", fontdict=labelfont)
150         ax.set_xlabel(value + " ($^\circ$C)", fontdict=labelfont)
151
152         # DEFINE MU AND SIGMA
153         mu_past_cold = min(gmmPast.means_)
154         mu_past_hot = max(gmmPast.means_)
155         mu_past_cold_index = np.argmin(gmmPast.means_)
156         mu_past_hot_index = np.argmax(gmmPast.means_)
157         sigma_past_cold =
                    math.sqrt(gmmPast.covariances_[mu_past_cold_index])
158         sigma_past_hot = math.sqrt(gmmPast.covariances_[mu_past_hot_index])
159
160         mu_future_cold = min(gmmFuture.means_)
```

```
161         mu_future_hot = max(gmmFuture.means_)
162         mu_future_cold_index = np.argmin(gmmFuture.means_)
163         mu_future_hot_index = np.argmax(gmmFuture.means_)
164         sigma_future_cold =
                    math.sqrt(gmmFuture.covariances_[mu_future_cold_index])
165         sigma_future_hot =
                    math.sqrt(gmmFuture.covariances_[mu_future_hot_index])
166
167         # CHOOSE HOTTER DAYS THAN MEAN-STD
168         # FIND THE TOTAL POPULATION FROM 84.13%
169         back1sigma = 50+100*sps.erf(1/math.sqrt(2))/2
170
171         hotterData = datafile.loc[(datafile['name'] == key) &
172                                   (datafile['year'] >= pastStart) &
173                                   (datafile['year'] <= pastEnd)]
174
175         hotterDaysPAST = datafile.loc[(datafile['value'] >= mu_past_hot[0]
176                                        - sigma_past_hot) &
177                                        (datafile['name'] == key) &
178                                        (datafile['year'] >= pastStart) &
179                                        (datafile['year'] <= pastEnd)]
180
181         hotterDaysFUTURE = datafile.loc[(datafile['value'] >=
182                                          mu_future_hot[0]
183                                          - sigma_future_hot) &
184                                          (datafile['name'] == key) &
185                                          (datafile['year'] >= futureStart) &
186                                          (datafile['year'] <= futureEnd)]
187
188         hotPeriodNumberOfDays_Past = (hotterDaysPAST.shape[0] *
189                                       (100 / back1sigma))/ 30
190         hotPeriodNumberOfDays_Future = (hotterDaysFUTURE.shape[0] *
191                                         (100 / back1sigma)) / 30
```

```
192
193         peakDiffPast = mu_past_hot[0] - mu_past_cold[0]
194         peakDiffFuture = mu_future_hot[0] - mu_future_cold[0]
195         changePeakDiff = peakDiffFuture - peakDiffPast
196         returnPeriodHolder = [cityname, key, mu_past_hot[0], sigma_past_hot,
197                               mu_past_cold[0], sigma_past_cold,
198                               hotPeriodNumberOfDays_Past, peakDiffPast,
199                               mu_future_hot[0], sigma_future_hot,
200                               mu_future_cold[0], sigma_future_cold,
201                               hotPeriodNumberOfDays_Future, peakDiffFuture,
202                               changePeakDiff]
203
204         for multiplier in [1, 10, 30, 50, 100]:
205             # expected frequency of n-year events in the past Equation 3.20
206             pastReturnPeriod = multiplier*hotPeriodNumberOfDays_Past
207
208             # the expected frequency outside range Equation 3.21
209             sigmaRange = math.sqrt(2) *
210                          sps.erfinv(1 - (1 / pastReturnPeriod))
211
212             # temperature limit of range Equation 3.22
213             tau = mu_past_hot[0] + sigmaRange * sigma_past_hot
214
215             # calculation of x in mu-x*sigma for future Equation 3.23
216             futureSigmaRange = (tau - mu_future_hot[0]) / sigma_future_hot
217
218             # changed value of n-year event Equation 3.24
219             futureReturnPeriod = 1 / (1 - sps.erf(futureSigmaRange /
220                                                   math.sqrt(2)))
221
222             # Equation 3.25
223             futureReturnPeriod_year = futureReturnPeriod /
224                                       hotPeriodNumberOfDays_Future
```

```
225             returnPeriodHolder.extend([futureReturnPeriod_year])
226
227         df = pd.DataFrame([returnPeriodHolder], columns=excelColumns)
228         excelHolder = excelHolder.append(df)
229
230         # PLOT THE GRAPH
231         ax.set_title(cityname.capitalize() + ' (' + model + '-ESM-MR RCP' +
232                      scenario[0] + '.'+ scenario[1] + ', ' +
233                      str(pastStart) + '-' + str(pastEnd) + ' vs. ' +
234                      str(futureStart) + '-' + str(futureEnd) + ')',
235                      fontdict=titlefont)
236         plt.xlim(min(gmmPast_x)-5, max(gmmFuture_x)+5)
237
238         # Draw legend
239         plt.legend(fontsize=10, loc=0)
240
241         # SAVE FIG
242         plt.savefig(outputGraphFolder + '\\' + key + '\\' +
243                     cityname + '_' + model + '_' + scenario + '_' +
244                     value.replace(' ', '_') + '.png')
245         plt.close()
246 excelHolder.to_excel(outputGraphFolder + '\\' + 'yearevents.xlsx',
247                      index=False)
```